Université du Québec
Institut national de la recherche scientifique
Centre Énergie Matériaux Télécommunications

PERFORMANCE ANALYSIS of MIXED FREE-SPACE OPTICS/RADIO FREQUENCY AMPLIFY-AND-FORWARD SYSTEMS WITH POINTING ERRORS

Par

Nesrine Cherif

Mémoire présenté pour l'obtention du grade de
Maître es Sciences, M.Sc.
en télécommunications

Jury d'évaluation

Examinateur externe	Halim Yanikomeroglu Carleton University
Examinateur interne	Tarek Djerafi EMT-INRS
Directeur de recherche	Sofiène Affes EMT-INRS

Abstract

Driven by the high data rates demand and the exponential growth of wireless devices, free-space optics FSO is presented as a strong and reliable candidate for the next generation mobile cellular networks. In addition to securing a high throughput and high-speed data services, FSO technology is an easily deployable cost-effective approach that offers a strong immunity to interference. Despite these advantages, FSO transmission is hampered by atmospheric turbulence-induced fading and pointing errors. These constraints shorten the FSO transmission to small distance. To widen the coverage and ensure the reliability of the FSO link for next generation cellular backhaul networks, relay-assisted mixed FSO/RF systems have gained such a great interest in recent times. The main objective of this work is to investigate the performance of relay-assisted mixed FSO/RF system. Toward this end, we derive closed-form expressions for the ergodic capacity and the outage probability that unify almost all turbulence/fading linear distributions discovered until present while accounting for heterodyne and intensity modulation/direct detection (IM/DD) techniques. The originality of this work relies on the consolidation of two generalized channel models for the FSO and RF links. Furthermore, the derived closed-form expressions, all in terms of Fox-H function (FHF) and bivariate FHF, are exact and accurate since no approximations were employed. Moreover, we extend our analysis to a mixed FSO/RF design where the co-channel interference (CCI) at the mobile user is presumed. In this system model, we derive closed-form expressions of the end-to-end performance metrics, i.e., the outage probability, the average bit-error rate (BER),

and the ergodic capacity, all in terms of bivariate FHF. The completeness of our work is emphasized through the investigation of fixed-gain and channel-state information (CSI)-assisted relaying schemes and the association of both heterodyne and IM/DD detection techniques. Motivated by the obtained results, we conduct a further study to investigate the effect of spatial diversity on the system performance by considering multi-aperture/multiuser system, where we also study the large scale regime. The spacial diversity resulting from the use of the maximum ratio transmission (MRT) at the multi-aperture FSO link and the user scheduling for the multiuser RF link further enhanced the performance by mitigating the effects of the turbulence, the pointing errors, and the fading in the mixed FSO/RF system.

Dedicated to my parents Mohamed & Zahra

List of Publications

Journal Papers

- Imène Trigui, **Nesrine Cherif**, and Sofiène Affes, "Relay-assisted mixed FSO/RF systems over Málaga-$\mathcal{M}$ and κ-μ shadowed fading channels", *IEEE Wireless Communications Letters*, vol.PP, no.99, pp.1-1.

- **Nesrine Cherif**, Imène Trigui, and Sofiène Affes, "Interference-limited mixed FSO/RF AF relay systems over Málaga-$\mathcal{M}$ and generalized-$\mathcal{K}$ fading", in preparation for submission to *IEEE Transactions on Wireless Communications*.

- **Nesrine Cherif**, Imène Trigui, and Sofiène Affes, "Mixed multi-aperture multiuser FSO/RF interference-limited AF relay systems over Málaga $\mathcal{M}$-turbulence channels with pointing errors", in preparation for submission to *IEEE Transactions on Wireless Communications*.

Conference Papers

- **Nesrine Cherif**, Imène Trigui, and Sofiène Affes, "On the performance analysis of mixed multi-aperture FSO/multiuser RF relay systems with interference", *IEEE 18th International Workshop on Signal Processing Advances in Wireless Communications (SPAWC)* 2017, 3-6 July 2017, Sapporo, Japan.

- Imène Trigui, **Nesrine Cherif**, Sofiène Affes, Xianbin Wang,Victor Leung, and Alex Stéphenne, "Interference-limited mixed Málaga-$\mathcal{M}$ and generalized-$\mathcal{K}$ dual-hop FSO/RF systems", *28th Annual IEEE International Symposium on Personal, Indoor and Mobile Radio Communications (PIMRC)* 2017, 08-13 October 2017, Montreal, QC, Canada.

- **Nesrine Cherif**, Imène Trigui, and Sofiène Affes, "Dual-hop Málaga-$\mathcal{M}$ FSO systems with pointing errors", *28th Annual IEEE International Symposium on Personal, Indoor and Mobile Radio Communications (PIMRC)* 2017, 08-13 October 2017, Montreal, QC, Canada.

Acknowledgments

First and foremost praise is to Allah, the most Gracious and the most Merciful, on whom ultimately we depend for sustenance and guidance. I am grateful to Allah for giving me strength and determination to complete my research.

This thesis has been seen through to completion with the continuous support of numerous people including my family, friends, colleagues and various institutions.

First of all, I would like to thank and express my sincere gratitude to my supervisor Professor Sofiène Affes for providing necessary resources and guidance throughout my research.

My sincere gratitude goes also to Dr. Imène Trigui, on whom I learned the straight steps in academic research. Her expertise and insightful comments were the reason behind my performance in this thesis. Indeed, her quick feedback and constructive comments were really valuable and helpful. This work would not been possible without her guidance and encouragement. I deeply hope she is satisfied by what I accomplished during my master research. I am sure that I will never have a competent mentor as she was for me.

I would like also to express my gratitude to the Tunisian ministry of higher education and scientific research and the university mission of Tunisia in north America 'MUTAN' for giving me the opportunity to pursue my graduate studies in Canada. Indeed, I appreciate their support for all the things that facilitated my stay in Montreal and my research work.

Besides my research work at INRS, I enjoyed my time with my friends and colleagues. I am also grateful to my friends back home for supporting me throughout my master. Finally, I would like to thank my family. They have been always encouraging me with their best wishes and prayers. I hope I have made them proud of me as I am proud of them.

Table of Contents

List of Figures

List of Tables

Glossary of Acronyms

The following acronyms and terms are used within this report.

AF	Amplify-and-Forward
BER	Bit-Error Probability
CCDF	Complementary Cumulative Distribution Function
CDF	Cumulative Distribution Function
CCI	Co-Channel Interference
CMGF	Complementary Moment Generation Function
CSI	Channel-State Information
FSO	Free-Space Optics
IM/DD	Intensity Modulation/ Direct Detection
MGF	Moment Generation Function
SIR	Signal-to-Interference Ratio
SINR	Signal-to-interference-and-Noise Ratio
SNR	Signal-to-Noise Ratio
PDF	Probability Distribution Function
RF	Radio Frequency

Chapter 1

Introduction

1.1 Background

The proliferation of wireless services and devices marks the most changing phenomena in the history of technology. The exponential growth of mobile users in the very recent years jointly with the high data throughput demand present a challenging tasks for the existing architecture of wireless communications where the cellular backhaul is required to provide a reliable link with high-speed data services [1]. More specifically, cellular backhaul link consists of base stations, radio network controller, and base station controllers [1], [2].Furthermore, the cellular backhaul is the most costly component in the network architecture with almost half of the total network deployment cost [1]. Thus, it is an urgent need and a key enabler for the next generation of wireless communication to reduce the cellular backhaul deployment cost while offering a high throughput and high-speed data services [2].

The majority of traditional cellular backhaul networks nowadays relies on copper mediums which can be explained by the fact that operators try to maintain the existing architecture to save the cost of deployment of a new architecture [2]. Optical fiber-based cellular backhaul has been rarely used in the current network architecture due to the high cost of initial investment to substitute the copper links by its optical fiber counterparts especially over deep oceans and difficult lands [2]. Recently, a new wireless-based cellular backhaul, free-space optics (FSO), has been introduced as a strong candidate for the next generation cellular networks to provide high data throughput while being a cost-effective architecture [3–9].

Free-space optics refers to the transmission of laser beams through optical carriers, i.e., infrared (IR) and ultraviolet (UV) bands [10]. Since FSO transmission requires a line-of-sight between the optical transmitter and the optical receiver, it as-

sesses high security and immunity to interference at the unlicensed spectrum (beyond 300 Thz) compared to traditional radio frequency (RF) transmission [10]. Based on narrow laser beams transmission, FSO technology allows high degrees of frequency reuse in unregulated spectrum. Another attractive feature of FSO technology is its cost-effectiveness from the fact that its deployment does not require any regulation of licensing fees from the frequency government agencies [10]. Furthermore, wireless property of the FSO link makes its deployment easy conversely to copper or optical fibers based links that require more time for their implementation [4]. FSO is considered as a revolutionary technology from its capability of enabling a wireless end-to-end cellular transmission [5].

Contrary to RF transmission, FSO link provides a very high data rates and a strong immunity to interference in the Terahertz bandwidth among others [7], [8], [11]. However, although all the advantages that FSO technology presents, FSO transmission is inhibited by the poor link reliability especially in long distances due to atmospheric turbulence-induced fading and its high sensitivity to weather conditions [12–15]. More specifically, rain, fog and temperature fluctuations directly affect FSO transmission and result a less reliable link, and consequently, a severe performance degradation. In addition, beam deviation from its original path caused by natural disasters results a further performance deterioration of the FSO link [16]. This misalignment is widely refereed in the literature as pointing errors [16]. These main weaknesses of the FSO link, i.e., atmospheric turbulence-induced fading and pointing errors, severely affect the FSO link's quality [10].

Th atmospheric turbulence-induced fading channel modeling is widely investigated in the literature [15], [17], where lognormal and Gamma-Gamma are presented as the most common distributions for the FSO link [15]. The lognormal distribution is an effective channel model only under weak turbulence conditions. However, the Gamma-Gamma model is suitable for small and large scale atmospheric fluctuations. Recently, Navas *et al* [18], derived a new generalized statistical model for wireless optical communications, i.e., the Málaga-$\mathcal{M}$ distribution, that unifies almost all the existing FSO channel models in the literature discovered so far. The Málaga-$\mathcal{M}$ statistical distribution is a versatile model with its ability to reflect a wide range of optical fluctuations and offers an attractive mathematical tractability for performance analysis [18], [19].

1.2 Mixed FSO/RF in the Literature

The short distance coverage, the turbulence-induced fading and the pointing errors can seriously cause FSO link outage and failure. In an attempt to overpass all listed constraints, relay-assisted mixed FSO/RF communication system, where one hop operates over FSO link whether the other hop experiences RF transmission, has gained a prominent interest in the very recent few years [20–23]. Mixed FSO/RF relay system is an efficient solution to broaden the FSO coverage, to improve the system performance when the FSO link becomes inoperative [24], [25] and to fill the gap connectivity between the cellular backhaul (FSO) and the RF access network. Many attempts have been made to study the overall performance of mixed FSO/RF relay systems assuming variety of FSO and RF channel distributions and under both heterodyne and intensity modulation/direct detection (IM/DD) techniques employing either decode-and-forward (DF) or amplify-and-forward (AF) relaying schemes [24], [25]. Interestingly, fixed-gain and channel-state information (CSI) relaying schemes have been widely considered in the mixed FSO/RF research line. All previous works in this field always assume restrictive turbulence and fading channel models [20–25]. For example, Gamma-Gamma and Nakagami-m are the most considered distributions for the FSO and RF links, respectively, on relay-assisted mixed FSO/RF systems [24], [25] (and references therein).

1.3 Contributions

The main contributions of this work compared to existing efforts in the literature can be summarized as follows:

- We were able to provide closed-form expressions of some performance measures (outage probability and ergodic capacity) of mixed FSO/RF under the most generalized FSO and RF channel models, i.e., Málaga-$\mathcal{M}$ and shadowed κ-μ fading, respectively, under both heterodyne and IM/DD detection techniques. The performance analysis is valid for any restrictive distribution of the Málaga-$\mathcal{M}$ and shadowed κ-μ fading. None of the existing works have assumed such a generalized distributions to study the systems's end-to-end performance. The majority of the attempts in this research line have considered Gamma-Gamma for the FSO link and either Nakagami-m or Rayleigh distributions for the RF link.

- Assuming a practical wireless communication scenario, where the co-channel interference (CCI) is presumed at the RF user and the RF channel is hampered not only by small scale variations, i.e., fading, but also by large scale variations, i.e., shadowing, we have elaborated a complete and a unified mathematical formulation of the outage probability, the average bit-error rate (BER), and the ergodic capacity for interference-limited mixed FSO/RF systems experiencing Málaga-$\mathcal{M}$ and generalized-K distributions under both heterodyne and detection techniques and assuming fixed-gain and CSI-assisted relaying schemes, all in terms of bivariate Fox's H function (FHF).

- Motivated by the promises of MIMO systems in the traditional RF wireless communication networks, we emphasize the utility of spatial diversity resulted from MIMO setups to reduce the turbulence-induced fading and to improve the FSO link reliability. Firstly, we provide some interesting results of the ergodic capacity and the average BER in finite-count multi-aperture/multiuser network. Driven by the obtained results, we investigate the system performance analysis in large scale apertures and users.

1.4 Report Outline

The remainder of this thesis is organized as follows: Chapter 2 presents the end-to-end ergodic capacity and outage probability analysis of amplify-and-forward (AF) CSI-assisted relay mixed Málaga/shadowed κ-μ fading under both heterodyne and IM/DD techniques in terms of FHF and bivariate FHF. Some asymptotic results are presented in high SNR regime as an alternative of the cumbersome closed-form expressions. In Chapter 3, we investigate the CCI and the composite fading shadowing effects on the outage probability, the average BER, and the ergodic capacity of mixed FSO/RF systems under both detection techniques and assuming the two relaying schemes, i.e., fixed-gain and CSI-assisted relaying. Motivated by the results obtained in Chapters 2 and 3, we derive in Chapter 4 the ergodic capacity and the average BER of multi-apertures/multiuser network where the maximum ratio transmission (MRT) scheme is employed at the FSO link and the opportunistic scheduling scheme is applied in the RF link. Further, some large-scale analysis has been presented. Finally, we provide conclusion in Chapter 5.

Chapter 2

Relay-Assisted Mixed FSO/RF Systems over Málaga-$\mathcal{M}$ and κ-μ Shadowed Fading Channels

2.1 Introduction

Recently, free-space optical (FSO) communications have gained a significant attention due to their advantages of higher bandwidth in unlicensed spectrum and higher throughput compared to their RF counterparts [26]. Hence, the gathering of both FSO and RF technologies arises as a promising solution for securing connectivity between the RF access network and the fiber-optic-based backbone network. As such, there has been prominent interest in mixed FSO/RF systems where RF transmission is used at one hop and FSO transmission at the other [16], [25]. Most contributions within this research line consider restrictive irradiance and channel gain probability density function (PDF) models for the FSO and RF links, respectively. The most commonly utilized models for the irradiance in FSO links are the lognormal and the Gamma-Gamma ($\mathcal{G}$-$\mathcal{G}$) [16], [25]. Recently, a new generalized statistical model, the Málaga-$\mathcal{M}$ distribution, was proposed in [18] to model the irradiance fluctuation of an unbounded optical wavefront (plane or spherical waves) propagating through a turbulent medium under all irradiance conditions in homogeneous and isotropic turbulence. The Málaga-$\mathcal{M}$ distribution is a generalized distribution that unifies most statistical models proposed so far with its ability to better reflect a wider range of turbulence conditions [18], [27]. It can be described also as a mixture of Generalized-

This work has been accepted for publication in *IEEE Wireless Communications Letters*

K distribution and a discrete Binomial distribution [19]. On the RF side, previous works typically assume either Rayleigh or Nakagami-m fading [24], [25], thereby lacking the flexibility to account for disparate signal propagation mechanisms as those characterized in 5G communications which will accommodate a wide range of usage scenarios with diverse link requirements. To bridge this gap in the literature, the κ-μ shadowed fading model, recently derived in [28], is an attractive proposition. In addition to presenting an excellent fit to the fading observed in a range of real-world applications (e.g. device-to-device, and body-centric fading channels [29]), the κ-μ shadowed fading encompasses several RF channel models such as Nakagami-m, Rayleigh, Rice, κ-μ and shadowed Rician fading distributions. This new channel fading model offers far better and much more flexible representations of practical fading LOS (line of sight), NLOS (non-LOS), and shadowed channels than the Rayleigh and Nakagami-m distributions. Under the assumption of AF relaying and taking into account the effect of pointing errors while considering both heterodyne and intensity modulation/direct detection techniques, we derive closed-form expressions for ergodic capacity and outage probability of mixed RF/FSO systems. We further pursue high signal-to-noise ratio (SNR) analysis to derive the diversity order.

2.2 Channel and System Models

We consider a relay-assisted mixed FSO/RF transmission composed of both Málaga-$\mathcal{M}$ with pointing errors and κ-μ shadowed fading environments. The source communicates with the destination through an intermediate relay, able to activate both heterodyne and IM/DD detection techniques at the reception of the optical beam.

The FSO (S-R) link irradiance is assumed to follow a Málaga-$\mathcal{M}$ distribution with pointing errors impairments for which the PDF of the irradiance, I, is given by [27, Eq.(5)]

$$f_I(x) = \frac{\xi^2 A}{x\Gamma(\alpha)} \sum_{k=1}^{\beta} \frac{b_k}{\Gamma(k)} \mathrm{G}_{1,3}^{3,0}\left[\frac{\alpha\beta}{g\beta+\Omega}\frac{x}{A_0} \middle| \begin{matrix} \xi^2+1 \\ \xi^2, \alpha, k \end{matrix} \right], \tag{2.1}$$

where ξ is the ratio between the equivalent beam radius and the pointing error displacement standard deviation (i.e., jitter) at the relay (for negligible pointing errors $\xi \to \infty$), A_0 defines the pointing loss [16], $A = \alpha^{\frac{\alpha}{2}} \left[g\beta/(g\beta+\Omega)\right]^{\beta+\frac{\alpha}{2}} g^{-1-\frac{\alpha}{2}}$ and $b_k = \binom{\beta-1}{k-1}(g\beta+\Omega)^{1-\frac{k}{2}} \left[(g\beta+\Omega)/\alpha\beta\right]^{\frac{\alpha+k}{2}} (\Omega/g)^{k-1} (\alpha/\beta)^{\frac{k}{2}}$, where α, β, g and Ω are the fading parameters related to the atmospheric turbulence conditions [18], [27]. Moreover in (2.1), $\mathrm{G}_{p,q}^{m,n}[\cdot]$ and $\Gamma(\cdot)$ stand for the Meijer-G function [30, Eq.(9.301)] and

the incomplete gamma function [30, Eq.(8.310.1)], respectively.

It is worth highlighting that the $\mathcal{M}$ distribution unifies most of the proposed statistical models characterizing the optical irradiance in homogeneous and isotropic turbulence [18]. Hence both $\mathcal{G}$-$\mathcal{G}$ and $\mathcal{K}$ models are special cases of the Málaga-$\mathcal{M}$ distribution, where they mathematically derives from (2.1) by setting ($g = 0$, $\Omega = 1$) and ($g \neq 0$, $\Omega = 0$ or $\beta = 1$), respectively [18, Table 1].

The RF (R-D) link, experiences the κ-μ shadowed fading with non-negative real shape parameters κ, μ and m, for which the PDF of instantaneous SNR, γ_2, is given by [28, Eq.(4)]

$$f_{\gamma_2}(x) = \frac{\mu^{\mu} m^m (1+\kappa)^{\mu}}{\Gamma(\mu)\bar{\gamma}_2(\mu\kappa + m)^m} \left(\frac{x}{\bar{\gamma}_2}\right)^{\mu-1} e^{-\frac{\mu(1+\kappa)x}{\bar{\gamma}_2}} {}_1F_1\left(m, \mu; \frac{\mu^2\kappa(1+\kappa)}{\mu\kappa + m}\frac{x}{\bar{\gamma}_2}\right), \quad (2.2)$$

where ${}_1F_1(\cdot)$ is the confluent hypergeometric function [30, Eq.(9.210.1)] and $\bar{\gamma}_2 = \mathbb{E}[\gamma_2]$. This fading model jointly includes large-scale and small-scale propagation effects, by considering that only the dominant components (DSCs) are affected by Nakagami-m distributed shadowing [28]. The shadowed κ-μ distribution is an extremely versatile fading model that includes as special cases nearly all linear fading models pertaining to LOS and NLOS scenarios, such as κ-μ ($m \to \infty$), Nakagami-m ($\mu = m$ and $\kappa \to 0$), Rayleigh ($\mu = m = 1$ and $\kappa \to 0$), and Rice ($\mu = 1, \kappa = K$ and $m \to \infty$), to name a few [28, Table I].

Assuming AF relaying with channel state information (CSI), then the end-to end SNR can be expressed as [25, Eq.(7)]

$$\gamma = \frac{\gamma_1\gamma_2}{\gamma_1 + \gamma_2 + 1}, \quad (2.3)$$

where $\gamma_1 = (A_0 h(g+\Omega))^{-r}\mu_r I^r$ is the instantaneous SNR of the FSO link ($S-R$) with r being the parameter that describes the detection technique at the relay (i.e., $r = 1$ is associated with heterodyne detection and $r = 2$ is associated with IM/DD) and, μ_r refers to the electrical SNR of the FSO hop [27] and $h = \xi^2/(\xi^2+1)$. In particular, for $r = 1$, $\mu_1 = \mu_{\text{heterodyne}} = \mathbb{E}[\gamma_1] = \bar{\gamma}_1$ and for $r = 2$, $\mu_2 = \mu_{\text{IM/DD}} = \mu_1\alpha\xi^2(\xi^2+1)^{-2}(\xi^2+2)(g+\Omega)/((\alpha+1)[2g(g+2\Omega) + \Omega^2(1+1/\beta)])$ [27, Eq.(8)].

2.3 Exact Performance Analysis

In this section, a new mathematical framework investigating the average capacity and the outage probability of the mixed FSO/RF transmission composed of both Málaga-

$\mathcal{M}$ with pointing errors and shadowed κ-μ fading environments and accounting for both detection techniques is presented. To the best of the author's knowledge, there are few works that consider these metrics of mixed FSO/RF systems, yet mostly considering the mixed $\mathcal{G}$-$\mathcal{G}$/Nakagami-m fading ([24], [25] and references therein). This work completes and extends the efforts of [24], [25] by unifying the ergodic capacity and the outage probability analysis for any turbulence/fading model under both types of detection techniques.

2.3.1 Ergodic Capacity

Hereafter, we provide capacity formulas for the considered system by using the complementary moment generation function CMGF-based approach [31].

Form [31], the ergodic capacity can be computed as

$$C \triangleq \frac{\mathbb{E}[\ln(1+\gamma)]}{2\ln(2)} = \frac{1}{2\ln(2)}\int_0^\infty s e^{-s} M_{\gamma_1}^{(c)}(s) M_{\gamma_2}^{(c)}(s) ds, \tag{2.4}$$

where $M_X^{(c)}(s) = \int_0^\infty e^{-sx} F_X^{(c)}(x) dx$ stands for the CMGF with $F_X^{(c)}(x)$ denoting the complementary cumulative distribution function (CCDF) of X.

The ergodic capacity of mixed Málaga-$\mathcal{M}$/κ-μ shadowed fading FSO transmission system under heterodyne and IM/DD detection techniques with pointing errors taken into account is given for

- *Integer m, μ, with $m \geqslant \mu$ as*

$$C = \frac{\xi^2 A r \mu_r}{2\ln(2)\Gamma(\alpha) B^r} \sum_{k=1}^{\beta} \frac{b_k}{\Gamma(k)} \sum_{l=1}^{m} \frac{\chi_l}{\Gamma(m)} T(\theta_2, l, m), \tag{2.5}$$

where $B = \alpha\beta h(g+\Omega)/[(g\beta+\Omega)]$, and,

$$\chi_l = \begin{cases} \binom{m}{l}\theta_2^l - \binom{m-\mu}{l}\theta_1^l & \text{for } 1 \leqslant l \leqslant m-\mu, \\ \binom{m}{l}\theta_2^l & \text{for } l > m-\mu, \end{cases}$$

with $\theta_1 = \frac{\bar{\gamma}_2}{\mu(1+\kappa)}$, and, $\theta_2 = \frac{\bar{\gamma}_2(\mu\kappa+m)}{\mu m(1+\kappa)}$.

Moreover in (2.5),

$$T(x,y,z)=\mathrm{H}_{1,0,4,3,1,1}^{0,1,1,4,1,1}\left[\begin{array}{c|c} & (-y,1,1) \\ & - \\ \frac{\mu_r}{B^r} & (\sigma,\Sigma) \\ x & (\phi,\Phi) \\ & (1-z,1) \\ & (0,1) \end{array}\right] \tag{2.6}$$

where H[.] denotes the Fox-H function (FHF) of two variables [32, Eq.(1.1)] also known as the bivariate FHF whose Mathematica implementation may be found in [33, Table I], whereby $(\sigma,\Sigma)=(1-r,r),(1-\xi^2-r,r),(1-\alpha-r,r),(1-k-r,r)$ and $(\phi,\Phi)=(0,1),(-\xi^2-r,r),(-r,r)$. Moreover, it becomes for

- *Integer m, μ, with $m<\mu$ as:*

$$\begin{aligned} C &= \frac{\xi^2 A r \mu_r}{2\ln(2)\Gamma(\alpha)B^r}\sum_{k=1}^{\beta}\frac{b_k}{\Gamma(k)}\sum_{\substack{p=0\\(p,q)\neq(0,0)}}^{m}\sum_{q=0}^{\mu-m}\binom{m}{p}\binom{\mu-m}{q} \\ &\quad \theta_2^p\theta_1^q\Bigg(\sum_{i=1}^{\mu-m}\frac{\Delta_{1i}}{\Gamma(\mu-m-i+1)}T(\theta_1,q+p,\mu-m-i+1) \\ &\quad -\sum_{i=1}^{m}\frac{\Delta_{2i}}{\Gamma(m-i+1)}T(\theta_2,q+p,m-i+1)\Bigg), \end{aligned} \tag{2.7}$$

where $\Delta_{1i}=(-1)^m\binom{m+i-2}{i-1}\left(\frac{m}{\mu\kappa+m}\right)^m\left(\frac{\mu\kappa}{\mu\kappa+m}\right)^{-m-i+1}$ and $\Delta_{2i}=(-1)^{i-1}\binom{\mu-m+i-2}{i-1}\left(\frac{m}{\mu\kappa+m}\right)^{i-1}\left(\frac{\mu\kappa}{\mu\kappa+m}\right)^{m-\mu-i+1}$.

Proof. Capitalizing on (2.4) and recalling the fact that the FSO link's CMGF $M_{\gamma_1}^{(c)}(s)=\mathcal{L}(F_{\gamma_1}^{(c)}(x))$ where $\mathcal{L}$ denotes the Laplace transform operator with the FSO link's CCDF obtained as

$$\begin{aligned} F_{\gamma_1}^{(c)}(x) &= F_I^{(c)}\left(A_0 h(g+\Omega)\left(\frac{x}{\mu_r}\right)^{\frac{1}{r}}\right) \\ &\overset{(a)}{=} \frac{\xi^2 A}{\Gamma(\alpha)}\sum_{k=1}^{\beta}\frac{b_k}{\Gamma(k)}\mathrm{G}_{2,4}^{4,0}\left[B\left(\frac{x}{\mu_r}\right)^{\frac{1}{r}}\middle|\begin{matrix}\xi^2+1,1\\0,\xi^2,\alpha,k\end{matrix}\right], \end{aligned} \tag{2.8}$$

where (a) follows from integrating (2.1) using [30]. Then, expressing the Meijer-G function in (2.8) in terms of Fox-H function by means of [34, Eq.(1.111)] and resorting

to [34, Eq.(2.19)] with some additional manipulations using [34, Eqs.(1.58),(1.59) and (1.60)] yield

$$M_{\gamma_1}^{(c)}(s) = \frac{\xi^2 A r \mu_r}{\Gamma(\alpha) B^r} \sum_{k=1}^{\beta} \frac{b_k}{\Gamma(k)} \mathrm{H}_{4,3}^{1,4}\left[\frac{\mu_r}{B^r} s \middle| \begin{matrix} (\sigma, \Sigma) \\ (\phi, \Phi) \end{matrix} \right], \tag{2.9}$$

where $\mathrm{H}_{p,q}^{m,n}[\cdot]$ is the Fox-H function [34, Eq.(1.2)].

On the RF side, the CMGF of γ_2 under shadowed κ-μ fading is given by

$$M_{\gamma_2}^{(c)}(s) = \frac{1 - M_{\gamma_2}(s)}{s} \overset{(a)}{=} \frac{1}{s} \left(1 - \frac{(\theta_1 s + 1)^{m-\mu}}{(\theta_2 s + 1)^m} \right), \tag{2.10}$$

where (a) follows from the recent result in [28, Eq.(5)]. By assuming integer-valued m and μ, the RF link's CMGF can be rewritten after resorting to the transformation $\Gamma(\alpha)(1+z)^{-\alpha} = \mathrm{H}_{1,1}^{1,1}[z|_{(0,1)}^{(1-\alpha,1)}]$ in [34, Eq.(1.43)] as

- For $\mu \leqslant m$

$$M_{\gamma_2}^{(c)}(s) \overset{(a)}{=} \sum_{l=1}^{m} \frac{\chi_l s^{l-1}}{\Gamma(m)} \mathrm{H}_{1,1}^{1,1}\left[\theta_2 s \middle| \begin{matrix} (1-m, 1) \\ (0, 1) \end{matrix} \right]. \tag{2.11}$$

- For $m < \mu$

$$\begin{aligned} M_{\gamma_2}^{(c)}(s) \overset{(b)}{=} & \sum_{\substack{p=0 \\ (p,q)\neq(0,0)}}^{m} \sum_{q=0}^{\mu-m} \binom{m}{p} \binom{\mu-m}{q} \theta_2^p \theta_1^q s^{p+q-1} \\ & \left(\sum_{i=1}^{\mu-m} \frac{\Delta_{1i}}{\Gamma(\mu - m - i + 1)} \mathrm{H}_{1,1}^{1,1}\left[\theta_1 s \middle| \begin{matrix} (m+i-\mu, 1) \\ (0, 1) \end{matrix} \right] \right. \\ & \left. - \sum_{i=1}^{m} \frac{\Delta_{2i}}{\Gamma(m-i+1)} \mathrm{H}_{1,1}^{1,1}\left[\theta_2 s \middle| \begin{matrix} (i-m, 1) \\ (0, 1) \end{matrix} \right] \right), \end{aligned} \tag{2.12}$$

where (a) and (b) follow after applying the binomial expansion and the partial fraction decomposition [35, Eq.(27)], respectively. Plugging (2.9), (2.11) and (2.12) into (2.4), respectively, yield the exact ergodic capacity expressions as shown in (2.5) and (2.7) after applying [32, Eq.(2.2)] with some algebraic manipulations. □

2.3.2 Outage Probability

The quality of service (QoS) of the considered mixed FSO/RF system is ensured by keeping the instantaneous end-to-end SNR, γ, above a threshold γ_{th}. The probability of outage in the mixed FSO/RF relaying setup is expressed as

$$P_{out} = \Pr[\gamma < \gamma_{th}] = \Pr\left[\frac{\gamma_1 \gamma_2}{\gamma_1 + \gamma_2 + 1} < \gamma_{th} \right]. \tag{2.13}$$

Marginalization over γ_1 and making the change $u = 1 + \gamma/\gamma_{th}$ yield

$$P_{out}(\gamma_{th}) = 1 - \gamma_{th} \int_1^{\infty} F_{\gamma_2}^{(c)} \left(\gamma_{th} + \frac{1+\gamma_{th}}{u-1} \right) f_{\gamma_1}(u\gamma_{th}) du, \tag{2.14}$$

where $F_{\gamma_2}^{(c)}$ is the CCDF of γ_2 and f_{γ_1} is the PDF of the first link SNR obtained from deriving (2.8) with respect to x as

$$f_{\gamma_1}(x) = \frac{\xi^2 A B^r}{\Gamma(\alpha)\mu_r} \sum_{k=1}^{\beta} \frac{b_k}{\Gamma(k)} \mathrm{H}_{1,3}^{3,0} \left[\frac{B^r x}{\mu_r} \middle| \begin{matrix} (\xi^2 + 1 - r, r) \\ (\xi^2 - r, r), (\alpha - r, r), (k - r, r) \end{matrix} \right]. \tag{2.15}$$

Plugging (2.15) and the RF link's CCDF expression for integer m, μ, with $m \geqslant \mu$ recently derived in [35, Eq.(10)] into the above integral and making a Taylor expansion of exponential and power terms, we infer that

$$P_{out}(\gamma_{th}) = 1 - \frac{\xi^2 A B^r \gamma_{th} e^{-\frac{\gamma_{th}}{\theta_2}}}{\Gamma(\alpha)\mu_r} \sum_{k=1}^{\beta} \sum_{i=0}^{m-\mu} \sum_{j=0}^{m-i-1} \sum_{p=0}^{j} \frac{\binom{j}{p} b_k \Upsilon_i}{j! \Gamma(k) \theta_2^j} \gamma_{th}^{j-p} (\gamma_{th} + 1)^p \times \mathcal{I}, \tag{2.16}$$

with the term $\mathcal{I}$ given by

$$\begin{aligned} \mathcal{I} &= \sum_{q=0}^{\infty} \sum_{l=0}^{\infty} \frac{(-1)^q (p+q)_l}{q! l! \theta_2^q} (\gamma_{th} + 1)^q \\ &\quad \int_1^{\infty} u^{-p-q-l} \mathrm{H}_{1,3}^{3,0} \left[\frac{B^r \gamma_{th}}{\mu_r} u \middle| \begin{matrix} (\xi^2 + 1 - r, r) \\ (\xi^2 - r, r), (\alpha - r, r), (k - r, r) \end{matrix} \right] du. \end{aligned} \tag{2.17}$$

Substituting (2.3) into (2.16) after resorting to [34, Eq.(2.54)], yield the outage probability of mixed FSO/RF in Málaga-$\mathcal{M}/\kappa$-μ shadowed fading ($\mu \leqslant m$) environments with pointing errors under both detection techniques as

$$P_{out}(\gamma_{th}) = 1 - \frac{\xi^2 A B^r \gamma_{th}}{\Gamma(\alpha) e^{\frac{\gamma_{th}}{\theta_2}} \mu_r} \sum_{k=1}^{\beta} \frac{b_k}{\Gamma(k)} \sum_{i=0}^{m-\mu} \sum_{j=0}^{m-i-1} \Upsilon_i \;\; \Xi(\theta_2), \tag{2.18}$$

where $\Upsilon_i = \binom{m-\mu}{i} \left(\frac{m}{\mu\kappa + m} \right)^i \left(\frac{\mu\kappa}{\mu\kappa + m} \right)^{m-\mu-i}$, and,

$$\Xi(x) = \sum_{p=0}^{j} \sum_{q=0}^{\infty} \sum_{l=0}^{\infty} \frac{(-1)^q (p+q)_l \binom{j}{p} \Upsilon_i \gamma_{th}^{j-p}}{j! q! l! x^{j+q} (\gamma_{th} + 1)^{-p-q}} \mathrm{H}_{2,4}^{4,0} \left[\frac{B^r \gamma_{th}}{\mu_r} \middle| \begin{matrix} (\sigma_1, \Sigma_1) \\ (\phi_1, \Phi_1) \end{matrix} \right], \tag{2.19}$$

with $(a)_n$ stands for the Pochhammer symbol [30], and $(\sigma_1, \Sigma_1) = (\xi^2 + 1 - r, r), (l + p + q, 1)$ and $(\phi_1, \Phi_1) = (l + p + q - 1, 1), (\xi^2 - r, r), (\alpha - r, r), (k - r, r)$.

Similar to (2.18), the outage probability of the considered mixed FSO Málaga/RF

shadowed κ-μ fading with $m < \mu$ is obtained by resorting to [35, Eq.(9)] as

$$P_{out}(\gamma_{th}) = 1 - \frac{\xi^2 A B^r \gamma_{th}}{\Gamma(\alpha)\mu_r} \sum_{k=1}^{\beta} \frac{b_k}{\Gamma(k)} \left(e^{-\frac{\gamma_{th}}{\theta_1}} \sum_{i=1}^{\mu-m} \sum_{j=0}^{\mu-m-i} \Delta_{1i} \Xi(\theta_1) + e^{-\frac{\gamma_{th}}{\theta_2}} \sum_{i=1}^{m} \sum_{j=0}^{m-i} \Delta_{2i} \Xi(\theta_2) \right). \tag{2.20}$$

2.4 Asymptotic Analysis

To gain more insights into the effect of turbulence/fading parameters on both the ergodic capacity and the outage probability, we study hereafter their asymptotic behaviors. To this end we invoke asymptotic expansions of The Fox-H function [36, Theorems 1.7 and 1.11] and the Mellin-Barnes integrals involving the bivariate Fox-H function [34, Eq.(2.56)].

2.4.1 Asymptotic Ergodic Capacity

High RF link's SNR: Based on (2.5), the asymptotic behavior of the ergodic capacity is derived for $\bar{\gamma}_2 \to +\infty$ as

$$\begin{aligned} C^{\infty} \;=\; & \frac{\xi^2 A r \mu_r}{2\ln(2)\Gamma(\alpha) B^r} \sum_{k=1}^{\beta} \sum_{l=1}^{m} \frac{b_k \chi_l}{\Gamma(k)} \left(\frac{\theta_2^{-1-l}}{\Gamma(m)} \mathrm{H}_{5,4}^{2,5} \left[\frac{\mu_r}{B^r \theta_2} \middle| \begin{matrix} (-l,1),(\sigma,\Sigma) \\ (m-1-l,1),(\phi,\Phi) \end{matrix} \right] \right. \\ & \left. + \theta_2^{-m} \mathrm{H}_{5,3}^{1,5} \left[\frac{\mu_r}{B^r} \middle| \begin{matrix} (m-l,1),(\sigma,\Sigma) \\ (\phi,\Phi) \end{matrix} \right] \right). \end{aligned} \tag{2.21}$$

Proof. See Appendix A. □

High FSO link's SNR: The asymptotic behavior when $\mu_r \to +\infty$ is inferred by computing the residue of the integrand of the bivariate FHF in (2.5) at the highest pole, i.e., -1, as

$$C^{\infty} = \frac{A}{2\ln(2)\Gamma(m)} \sum_{k=1}^{\beta} \sum_{l=1}^{m} \mathrm{G}_{2,1}^{1,2} \left[\theta_2 \middle| \begin{matrix} 1-m, 1-l \\ 0 \end{matrix} \right]. \tag{2.22}$$

Notice that the ergodic capacity asymptotic behavior when $m < \mu$ is assessed using the same approach.

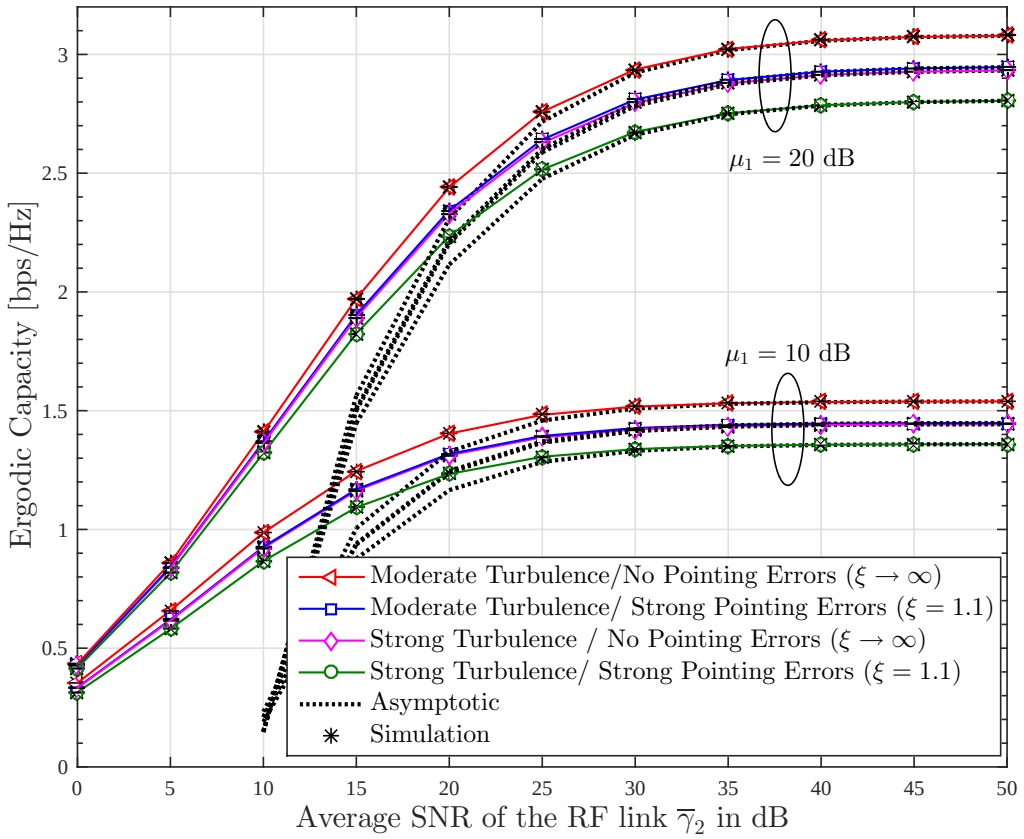

Fig. 2.1: Ergodic Capacity of relay-assisted mixed Málaga/κ-μ shadowed fading with heterodyne detection.

2.4.2 Asymptotic Outage Probability

At high SNR values, the outage probability of the mixed FSO/RF relaying system can be expressed as $P_{out} \simeq (G_c SNR)^{-G_d}$, where G_c and G_d denote the coding gain and the diversity order of the system, respectively. Hence, as $\mu_r \to +\infty$ while keeping the low-order terms in (2.19), i.e., $q + l < 1$, and then applying [36, Eq.(1.8.5)] yield the asymptotic CDF when $m \geqslant \mu$ as

$$P_{\text{out}}^{\infty} = 1 - \frac{\xi^2 A e^{-\frac{\gamma_{th}}{\theta_2}}}{\Gamma(\alpha)} \sum_{k=1}^{\beta} \frac{b_k}{\Gamma(k)} \sum_{i=0}^{m-\mu} \sum_{j=0}^{m-i-1} \sum_{p=0}^{j} \frac{\binom{j}{p} \Upsilon_i \gamma_{th}^{j-p} \theta_2^{-j}}{j! (\gamma_{th}+1)^{-p}}$$
$$\sum_{t=1}^{4} \frac{1}{\Phi_{1t}} \frac{\prod_{\substack{s=1 \\ s \neq t}}^{4} \Gamma(\phi_{1s} - \phi_{1t} \frac{\Phi_{1s}}{\Phi_{1t}})}{\prod_{s=1}^{2} \Gamma(\sigma_{1s} - \phi_{1t} \frac{\Sigma_{1s}}{\Phi_{1t}})} \left(\frac{B^r \gamma_{th}}{\mu_r} \right)^{\frac{\phi_{1t}}{\Phi_{1t}}+1}. \tag{2.23}$$

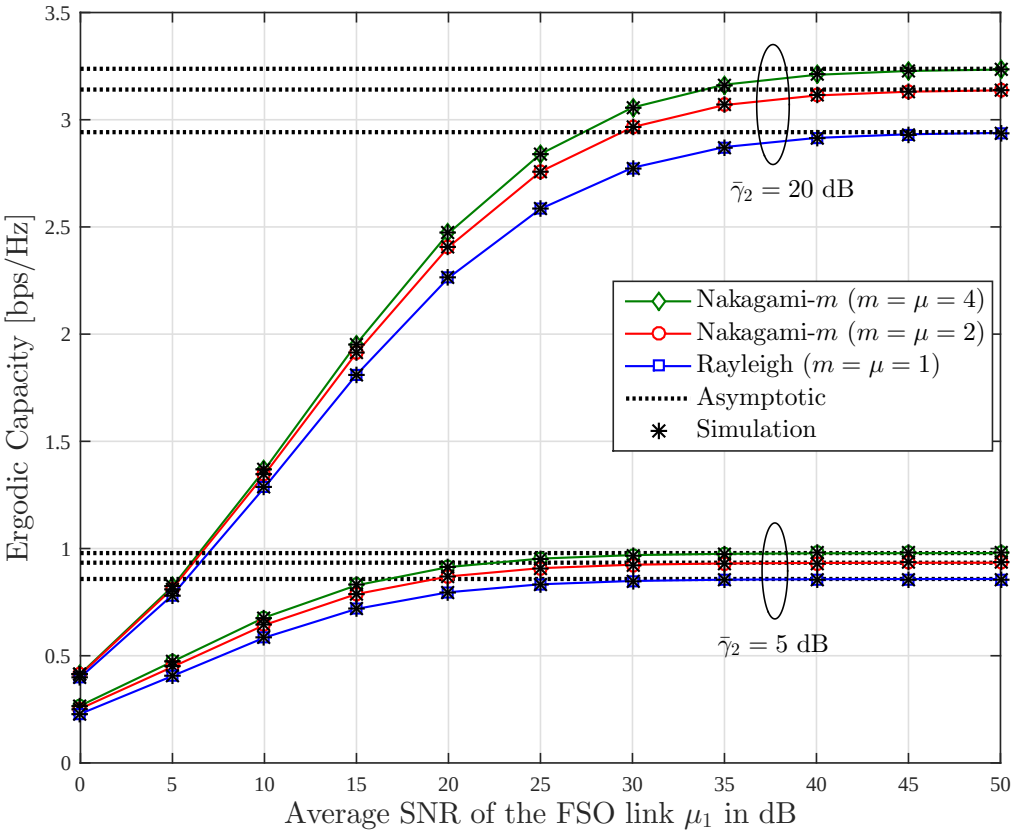

Fig. 2.2: Ergodic Capacity of relay-assisted mixed Málaga/Nakagami-m fading with heterodyne detection.

Compared to (2.19) which is expressed in terms of Fox-H function, (2.23) includes only finite summations of elementary functions. The diversity gain of the studied system over atmospheric turbulence conditions is inferred after applying $e^{-\frac{\gamma_{th}}{\theta_2}} \underset{\bar{\gamma}_2>>1}{\approx} 1 - \frac{\gamma_{th}}{\theta_2}$ to (2.23) as $G_d = \min\{\mu, \frac{\xi^2}{r}, \frac{\alpha}{r}, \frac{\beta}{r}\}$.

Special case: setting $m = \mu, \kappa \to 0$, $g = 0$ and $\Omega = 1$ in (2.23) yield P_{out}^{∞} for mixed $\mathcal{G}$-$\mathcal{G}$/Nakagami-m as

$$P_{\text{out}}^{\infty} = 1 - \frac{\xi^2 e^{-\frac{m\gamma_{th}}{\bar{\gamma}_2}}}{\Gamma(\alpha)\Gamma(\beta)} \sum_{j=0}^{m-1} \sum_{p=0}^{j} \sum_{t=1}^{4} \frac{\binom{j}{p} m^j \gamma_{th}^{-p} (\alpha\beta h)^{r(\frac{\phi_{1t}}{\Phi_{1t}}+1)}}{j! \Phi_{1t} (\gamma_{th}+1)^{-p}} \frac{\prod_{\substack{s=1 \\ s\neq t}}^{4} \Gamma(\phi_{1s} - \phi_{1t}\frac{\Phi_{1s}}{\Phi_{1t}})}{\prod_{s=1}^{2} \Gamma(\sigma_{1s} - \phi_{1t}\frac{\Sigma_{1s}}{\Phi_{1t}})} \left(\frac{\gamma_{th}}{\mu_r}\right)^{\frac{\phi_{1t}}{\Phi_{1t}}+1} \left(\frac{\gamma_{th}}{\bar{\gamma}_2}\right)^{j}, \tag{2.24}$$

thereby inferring [25, Eq.(29)], i.e., $G_d = \min\{m, \frac{\xi^2}{r}, \frac{\alpha}{r}, \frac{\beta}{r}\}$.

Similar to (2.23) while considering (2.20), the asymptotic outage probability can

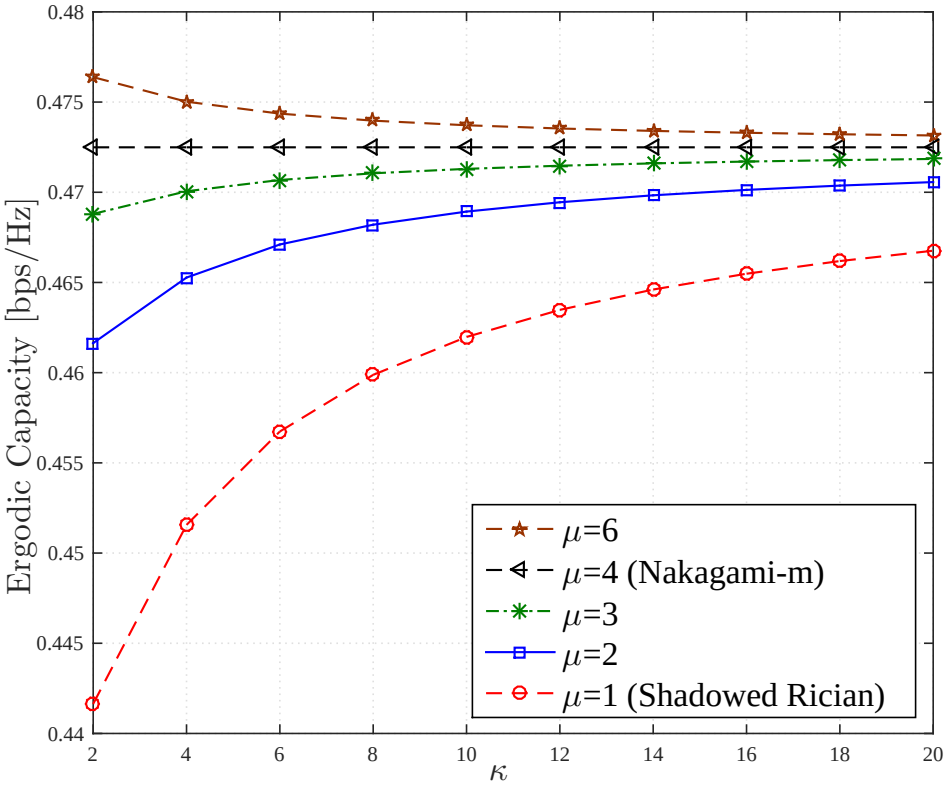

Fig. 2.3: Ergodic Capacity versus κ for $m = 4$. Setup: $\alpha = 5, \beta = 2, g = 0.17, \xi = 1.1, \mu_1 = 30$ dB and $\bar{\gamma}_2 = 0$ dB.

be derived in closed form when $m < \mu$.

2.5 Numerical Results

Fig.2.1 investigates the impacts of the turbulence-induced fading and pointing errors on the system performance when the RF link is subject to Rician shadowed fading distribution ($\kappa = 5$, $\mu = 1$, $m = 2$). As expected, the ergodic capacity deteriorates by decreasing the pointing error displacement standard deviation, i.e., for smaller ξ, or decreasing the turbulence fading parameter, i.e., smaller α and β, where we associate the strong turbulence to $(\alpha, \beta) = (2.29, 2)$ and the moderate turbulence to $(\alpha, \beta) = (4.2, 3)$. At high SNR, the asymptotic expansion match very well its exact counterpart, which confirms the validity of our mathematical analysis for different parameter settings.

Fig.2.2 illustrates the impacts of the fading parameter m on the system performance when the FSO link is subject to Málaga-$\mathcal{M}$ ($\alpha = 2.296$, $\beta = 2$, $g = 0.17$, $\Omega = 0.71$, and $\xi = 15.1$). The result is in perfect agreement with what observed

in [24], where the performance increases when the fading is less severe, i.e, higher m. It can be seen also that the asymptotic ergodic capacity in high SNR region at the FSO link in (2.22) is a very good approximation and it presents an attractive alternative to the cumbersome expression of (2.5).

Fig.2.3 plots the ergodic capacity of mixed FSO/RF relay systems over Málaga-$\mathcal{M}$/shadowed κ-μ fading channels versus κ. We observe that larger κ improves the ergodic capacity when $m > \mu$. However, when $m < \mu$, increasing the parameter κ is detrimental for capacity. When $m = \mu$ the shadowed κ-μ distribution boils down to the Nakagami-m distribution, [35], whence the ergodic capacity's independency of κ. Fig.2.3 also shows that increasing μ, which denotes the number of multipath clusters [28], reduces the fading severity of the small-scale propagation effects thereby improving the ergodic capacity.

Fig.2.4 depicts the outage probability of mixed FSO/RF relay systems in Málaga-$\mathcal{M}$ and shadowed κ-μ fading channels for both heterodyne and IM/DD detection at the relay. Throughout our numerical experiments, we found out that regardless of

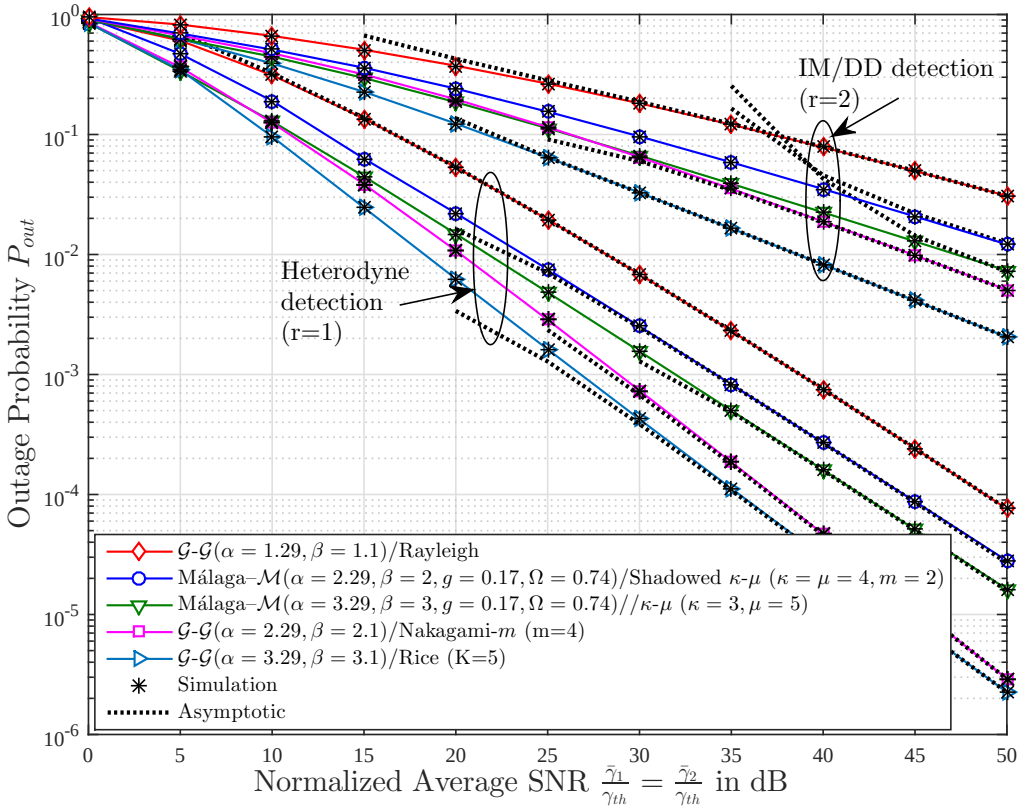

Fig. 2.4: Outage Probability of relay-assisted mixed Málaga/κ-μ shadowed fading for $\xi = 1.1$.

the average SNRs and turbulence/fading settings, accurate analytical curves can be obtained by truncating the infinite sums at $q = 50$ and $l = 5$ terms. In the legend, please note that we have identified some particular turbulence and fading distribution cases that simply stem from the general Málaga amd κ-μ shadowed fading scenarios, respectively. The exact match with Monte-Carlo simulation results confirms the precision of the theoretical analysis of section 2.4. Moreover, we notice that the exact and asymptotic expansions (2.23) agree very well at high SNRs.

2.6 Summary

We have presented a unified analytical framework for relay-assisted mixed FSO/RF systems that remarkably accommodates generic turbulence/fading models including Málaga-$\mathcal{M}$ with pointing errors and shadowed κ-μ distribution that account for shadowed LOS and NLOS scenarios. The results demonstrate the unification of various FSO turbulent/RF fading scenarios into a single closed-form expression for the ergodic capacity and the outage probability while accounting for both IM/DD and heterodyne detection techniques at the relay.

Chapter 3

Interference-Limited Mixed Málaga-$\mathcal{M}$ and Generalized-$\mathcal{K}$ Dual-Hop FSO/RF Systems

3.1 Introduction

The performance of mixed FSO/RF relaying networks was investigated in [20, 22–25, 37] assuming restrictive irradiance probability density function (PDF) models for the FSO link and restrictive statistical characterization for the RF link. For instance, on the RF side, previous works typically assume either Nakagami-m [24, 25] or Rayleigh [37, 38] fading, thereby lacking the flexibility to account for disparate signal propagation mechanisms as those characterized in 5G communications which will accommodate a wide range of usage scenarios with diverse link requirements. In fact, in 5G communications design, the combined effect of small-scale and shadowed fading needs to be properly addressed. Shadowing, which is due to obstacles in the local environment or human body (user equipments) movements, can impact link performance by causing fluctuations in the received signal. For example, the shadowing effect comes to prominence in millimeter wave (mmWave) communications due to the higher carrier frequency. In this respect, the generalized-K ($\mathcal{GK}$) model was proposed by combining Nakagami-m multipath fading and Gamma-Gamma distributed shadowing [39, 40].

Results from this work has been accepted for publication in *28th Annual IEEE International Symposium on Personal, Indoor and Mobile Radio Communications (PIMRC)*.
The entire work conducted in this chapter is in preparation for submission in *IEEE Transactions on Wireless Communications*.

While FSO transmissions are robust to RF interference, mixed FSO/RF systems are inherently vulnerable to the harmful effect of co-channel interference (CCI) through the RF link (cf. [31] and references therein). Previous contributions pertaining to FSO relay-assisted communications [20, 22–25, 37] relied on the absence of CCI. Recently, the recognition of the interference-limited nature of emerging communication systems has motivated [41] to account for CCI in mixed decode-and-forward RF/FSO systems performance analysis. Besides ignoring the shadowing effect on the RF link, [41] assumes restrictive Gamma-Gamma model on the FSO link. In this chapter, motivated by the aforementioned challenges, we assess the impact of RF CCI on the performance of dual-hop AF mixed FSO/RF system operating over Málaga-$\mathcal{M}$ and composite fading shadowing generalized-K ($\mathcal{GK}$) channels, respectively. Assuming fixed-gain relaying as well as CSI-assisted relaying and taking into account the effect of pointing errors while considering both heterodyne and IM/DD detection techniques, we present a comprehensive performance analysis by exploiting seminal results form the H-transform theory [34, 36].

3.2 Channel and System Models

We consider a downlink of an AF half-duplex relay network featuring a mixed FSO/RF communication. We assume that the optical source communicates with the destination in a dual-hop fashion through a multiple antenna AF relay using an orthogonal multiple access scheme within the cell so that a single user per cell is supported in any given spectral resource slot (time slot, frequency slot, code slot, etc.). We assume that the destination (user) is subject to inter-cell interference brought by L co-channel RF sources in the network (See Fig.3.1).

The optical channel follows a Málaga-$\mathcal{M}$ distribution for which the CCDF of the instantaneous SNR γ_1 in the presence of pointing errors is given by (2.8).

The RF (R-D) and (I-D) links experience the Generalized-$\mathcal{K}$ distribution, for which the instantaneous SNR, γ_{XD}, $X \in (R, I)$, follows a generalized-$\mathcal{K}$ statistical model for which its probability density function (PDF) is given by [39, Eq.(5)]

$$f_{\gamma_{XD}}(x) = \frac{2\left(\frac{m_X \kappa_X}{\bar{\gamma}_{XD}}\right)^{\frac{\kappa_X+\delta_X m_X}{2}} x^{\frac{\kappa_X+\delta_X m_X}{2}-1}}{\Gamma(\delta_X m_X)\Gamma(\kappa_X)} K_{\kappa_X-\delta_X m_X}\left(2\sqrt{\frac{\kappa_X m_X x}{\bar{\gamma}_{XD}}}\right), \quad (3.1)$$

where $X \in \{R, I\}$ and $K_\nu(\cdot)$ stands for the Bessel function of second order [30, Eq.(8.407.1)]. Moreover, $m_X \geqslant 0.5$ and $\kappa_X \geqslant 0$ denote the multipath fading and

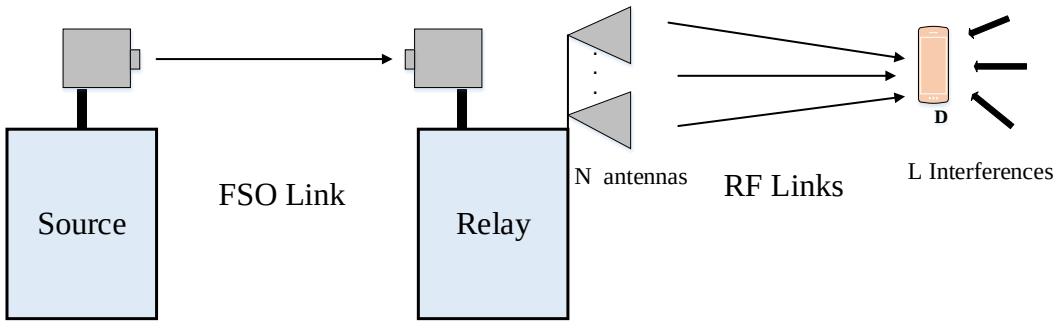

Fig. 3.1: Two-hop interfere-limited mixed FSO/RF AF relay network.

shadowing severity of the X-Dth channel coefficient, respectively. Moreover, $\delta_X = \{N, L\}$ for $X \in \{R, I\}$ follows form the conservation property under the summation of N and L i.i.d generalized-$\mathcal{K}$ random variables. Using [30, Eq.(9.34.3)], the PDF of the generalized-$\mathcal{K}$ distribution can be represented in terms of the Meijer's G function as in (3.2)

$$f_{\gamma_{XD}}(x)=\frac{\frac{m_X\kappa_X}{\bar{\gamma}_{XD}}}{\Gamma(\delta_X m_X)\Gamma(\kappa_X)}\mathrm{G}_{0,2}^{2,0}\left[\frac{\kappa_X m_X}{\bar{\gamma}_{XD}}x\middle|\begin{matrix}-\\ \delta_X m_X-1,\kappa_X-1\end{matrix}\right]. \tag{3.2}$$

The CDF of the signal-to-interference-ratio (SIR) $\gamma_2 = \gamma_{RD}/\gamma_{ID}$ under generalized-$\mathcal{K}$ fading can be derived from a recent result in [40, Lemma 1] as

$$F_{\gamma_2}(x) = 1 - \frac{1}{\Gamma(Nm)\Gamma(\kappa)\Gamma(Lm_I)\Gamma(\kappa_I)}\mathrm{G}_{3,3}^{3,2}\left[\frac{\kappa m}{\kappa_I m_I \bar{\gamma}_2}x\middle|\begin{matrix}1-\kappa_I, 1-Lm_I, 1\\ 0, \kappa, Nm\end{matrix}\right], \tag{3.3}$$

where $\bar{\gamma}_2 = \bar{\gamma}_{RD}/\bar{\gamma}_{ID}$ is the average SIR of the RF link where, for consistency, we have dropped the subscript R from the parameters m_R and κ_R.

It may be useful to notice that (3.3) includes the distribution of the SIR under Nakagami-m fading when ($\kappa_X \to \infty$) by means of

$$\lim_{b_1\to+\infty}\frac{1}{\Gamma(b_1)}\mathrm{G}_{p,q}^{m,n}\left[b_1 z\middle|\begin{matrix}a_1,\ldots,a_p\\ b_1,\ldots,b_q\end{matrix}\right] = \mathrm{G}_{p,q-1}^{m-1,n}\left[z\middle|\begin{matrix}a_1,\ldots,a_p\\ b_2,\ldots,b_q\end{matrix}\right]. \tag{3.4}$$

With fixed-gain relaying scheme, the end-to-end SINR can derived under the as-

sumption of negligible saturation as [42, Eq.(2)]

$$\gamma = \frac{\gamma_1 \gamma_2}{\gamma_2 + \mathrm{C}}, \tag{3.5}$$

where C stands for the fixed gain of the relay.

The end-to-end SNR with CSI-assisted relaying scheme is given in (2.3).

3.3 End-to-End Statistics

3.3.1 Fixed-gain Relaying

3.3.1.1 Cumulative Distribution Function

The CDF of the end-to-end SNR of interference-limited dual-hop FSO/ RF systems using fixed-gain relays in Málaga-$\mathcal{M}/\mathcal{GK}$ fading under both heterodyne detection and IM/DD is given by

$$F_\gamma(x) = \frac{\xi^2 A \kappa m \mathrm{C}}{\Gamma(\alpha)\Gamma(Nm)\Gamma(\kappa)\Gamma(Lm_I)\Gamma(\kappa_I)\kappa_I m_I \bar{\gamma}_2} \sum_{k=1}^{\beta} \frac{b_k}{\Gamma(k)} \mathrm{H}_{1,0:3,2:4,5}^{0,1:0,3:4,3}\left[\begin{matrix} \frac{\mu_r}{B^r x} \\ \frac{\kappa m \mathrm{C}}{\kappa_I m_I \bar{\gamma}_2} \end{matrix} \middle| \begin{matrix} (0,1,1) \\ - \\ (1-\xi^2, r), (1-\alpha, r), (1-k, r) \\ (0,1), (-\xi^2, r) \\ (-1,1), (-\kappa_I, 1), (-Lm_I, 1), (0,1) \\ (-1,1), (-1,1), (\kappa-1), (Nm-1), (0,1) \end{matrix} \right]. \tag{3.6}$$

Proof. See Appendix B. □

3.3.1.2 Probability Distribution Function

The PDF of γ may be obtained by taking the derivative of (3.6) as

$$f_{\gamma}(x) = \frac{-\xi^2 A\kappa m \mathrm{C} x^{-1}}{\Gamma(\alpha)\Gamma(Nm)\Gamma(\kappa)\Gamma(Lm_I)\Gamma(\kappa_I)\kappa_I m_I \bar{\gamma}_2} \sum_{k=1}^{\beta} \frac{b_k}{\Gamma(k)} \mathrm{H}_{1,0:3,2:4,5}^{0,1:0,3:4,3}\left[\begin{array}{c|c} \frac{\mu_r}{B^r x} & (0,1,1) \\ & - \\ \frac{\kappa m \mathrm{C}}{\kappa_I m_I \bar{\gamma}_2} & (1-\xi^2, r), (1-\alpha, r), (1-k, r) \\ & (1,1), (-\xi^2, r) \\ & (-1,1), (-\kappa_I, 1), (-Lm_I, 1), (0,1) \\ & (-1,1), (-1,1), (\kappa-1), (Nm-1), (0,1) \end{array} \right]. \quad (3.7)$$

Proof. The PDF of the end-to-end SNR in mixed Málaga-$\mathcal{M}/\mathcal{GK}$ is obtained after differentiation of the Mellin-Barnes integral form of (3.6) over x using $\frac{dx^{-s}}{dx} = -sx^{-s-1}$ with $\Gamma(s+1) = s\Gamma(s)$. □

3.3.2 CSI-assisted Relaying

CDF

Due to the intractability of the end-to-end signalto-interference-and-noise ratio (SINR) in (2.3), we resort to an upper bound given by [38, Eq.(20)] as $\gamma = \min(\gamma_1, \gamma_2) > \gamma_1\gamma_2/(\gamma_1+\gamma_2+1)$, whose CDF can be expressed as $F_{\gamma}(x) = 1 - F_{\gamma_1}^{(c)}(x)F_{\gamma_2}^{(c)}(x)$, where $F_{\gamma_1}^{(c)}$ and $F_{\gamma_2}^{(c)}$ stand for the complementary CDF of γ_1 and γ_2, respectively. Hence, using (2.8) and (3.3), the CDF of dual-hop FSO/RF systems employing CSI-assisted relay can be obtained as

$$F_{\gamma}(x) = 1 - \frac{\xi^2 A}{\Gamma(\alpha)\Gamma(Nm)\Gamma(\kappa)\Gamma(Lm_I)\Gamma(\kappa_I)} \sum_{k=1}^{\beta} \frac{b_k}{\Gamma(k)} \mathrm{G}_{2,4}^{4,0}\left[B\left(\frac{x}{\mu_r}\right)^{\frac{1}{r}} \middle| \begin{array}{c} \xi^2+1, 1 \\ 0, \xi^2, \alpha, k \end{array} \right] \mathrm{G}_{3,3}^{3,2}\left[\frac{\kappa m x}{\kappa_I m_I \bar{\gamma}_2} \middle| \begin{array}{c} 1-\kappa_I, 1-Lm_I, 1 \\ 0, \kappa, Nm \end{array} \right]. \quad (3.8)$$

3.4 Performance Analysis of Fixed-gain Relaying

3.4.1 Outage Probability

Proposition 1. The outage probability of a communication system is a performance measure that defines the probability that the end-to-end SINR, γ, falls below a predetermined threshold γ_{th}. More specifically, the outage probability of interference-limited mixed FSO/RF system operating under both heterodyne and IM/DD techniques can be easily obtained from (3.6) as

$$P_{out} = F_{\gamma}(\gamma_{th}). \tag{3.9}$$

Corollary 1 (Asymptotic Outage Probability)**.** At high normalized average SNR in the FSO link ($\frac{\mu_r}{\gamma_{th}} \to +\infty$), the outage probability of the system under consideration can be rewritten as a sum of single FHF and Meijer's G functions instead of a bivariate FHF as

$$\begin{aligned}
P_{out}^{\infty} = & \frac{\xi^2 A \kappa m \mathrm{C}}{\Gamma(\alpha)\Gamma(Nm)\Gamma(\kappa)\Gamma(Lm_I)\Gamma(\kappa_I)\kappa_I m_I \bar{\gamma}_2} \sum_{k=1}^{\beta} \frac{b_k}{\Gamma(k)} \\
& \left[\frac{\Gamma(\alpha-\xi^2)\Gamma(k-\xi^2)}{r\Gamma(1-\frac{\xi^2}{r})} \left(\frac{B^r \gamma_{th}}{\mu_r} \right)^{\frac{\xi^2}{r}} \mathrm{G}_{5,5}^{4,4}\left[\frac{\kappa m \mathrm{C}}{\kappa_I m_I \bar{\gamma}_2} \middle| \begin{matrix} -\kappa_I, -Lm_I, -1, \frac{\xi^2}{r}, 0 \\ \kappa-1, Nm-1, -1, -1, 0 \end{matrix} \right] \right. \\
& + \frac{\Gamma(\xi^2-\alpha)\Gamma(k-\alpha)}{r\Gamma(1-\frac{\alpha}{r})\Gamma(1+\xi^2-\alpha)} \left(\frac{B^r \gamma_{th}}{\mu_r} \right)^{\frac{\alpha}{r}} \mathrm{G}_{5,5}^{4,4}\left[\frac{\kappa m \mathrm{C}}{\kappa_I m_I \bar{\gamma}_2} \middle| \begin{matrix} -\kappa_I, -Lm_I, -1, \frac{\alpha}{r}, 0 \\ \kappa-1, Nm-1, -1, -1, 0 \end{matrix} \right] \\
& + \frac{\Gamma(\xi^2-k)\Gamma(\alpha-k)}{r\Gamma(1-\frac{k}{r})\Gamma(1+\xi^2-k)} \left(\frac{B^r \gamma_{th}}{\mu_r} \right)^{\frac{k}{r}} \mathrm{G}_{5,5}^{4,4}\left[\frac{\kappa m \mathrm{C}}{\kappa_I m_I \bar{\gamma}_2} \middle| \begin{matrix} -\kappa_I, -Lm_I, -1, \frac{k}{r}, 0 \\ \kappa-1, Nm-1, -1, -1, 0 \end{matrix} \right] \\
& \left. + \frac{B^r \gamma_{th}}{\mu_r} \mathrm{H}_{6,8}^{7,3}\left[\frac{\kappa m \mathrm{C} B^r \gamma_{th}}{\kappa_I m_I \bar{\gamma}_2 \mu_r} \right. \right. \\
& \left. \left. \middle| \begin{matrix} (-\kappa_I, 1), (-Lm_I, 1), (-1, 1), (0, 1), (1+\xi^2-r, r), (0, 1) \\ (\xi^2-r, r), (\alpha-r, r), (k-r, r), (\kappa-1, 1), (Nm-1, 1), (-1, 1), (-1, 1), (0, 1) \end{matrix} \right] \right].
\end{aligned} \tag{3.10}$$

Proof. (3.10)is assessed by following the same steps in Appendix A. □

Corollary 2. At high SNR values, the outage probability of the mixed FSO/RF relaying system can be expressed as $P_{out}^{\infty} = (c\mathrm{SINR})^{-d}$, where c and d denote the coding gain and the diversity order of the system, respectively. When $\bar{\gamma}_2 \to +\infty$,

then by applying [36, Theorem 1.11] to (3.10) while only keeping the dominant term, it follows that, for a fixed CCI power, the diversity order of mixed FSO/RF systems with pointing errors over Málaga- $\mathcal{M}/\mathcal{GK}$ fading conditions is shown to be given by

$$d = \min\left\{Nm, \kappa, \frac{\xi^2}{r}, \frac{\alpha}{r}, \frac{k}{r}\right\}. \tag{3.11}$$

In particular, for Nakgami-m fading ($\kappa \to +\infty$) $d = \min\left\{Nm, \frac{\xi^2}{r}, \frac{\alpha}{r}, \frac{k}{r}\right\}$, while it becomes $d = \min\left\{Nm, \frac{\xi^2}{r}, \frac{\alpha}{r}, \frac{\beta}{r}\right\}$ for mixed FSO/RF under Gamma-Gamma turbulence-induced fading.

3.4.2 Average Bit-Error Rate

The average BER of a variety of modulation schemes may be written as [43, Eq.(19)]

$$\overline{P}_e = \frac{\delta}{2\Gamma(p)} \sum_{j=1}^{n} \int_0^{\infty} \Gamma(p, q_j x) f_\gamma(x) \mathrm{d}x, \tag{3.12}$$

where $\Gamma(\cdot,\cdot)$ stands for the incomplete Gamma function [30, Eq.(8.350.2)] and the parameters δ, n, p and q_j account for different modulations schemes (See [43, Table I]).

Proposition 2. The average BER of interference-limited mixed Málaga-$\mathcal{M}/\mathcal{GK}$ FSO transmission system operating under both IM/DD and heterodyne detection with pointing errors taken into account is given by

$$\overline{P}_e = \frac{\xi^2 A \delta \kappa m \mathrm{C}}{2\Gamma(\alpha)\Gamma(p)\Gamma(Nm)\Gamma(\kappa)\Gamma(Lm_I)\Gamma(\kappa_I)\kappa_I m_I \bar{\gamma}_2} \sum_{j=1}^{n} \sum_{k=1}^{\beta} \frac{b_k}{\Gamma(k)} \mathrm{H}_{1,0:3,3:4,5}^{0,1:1,3:4,3}\left[\begin{array}{c|c} \frac{\mu_r q_j}{B^r} & (0,1,1) \\ & - \\ \frac{\kappa m \mathrm{C}}{\kappa_I m_I \bar{\gamma}_2} & (1-\xi^2, r), (1-\alpha, r), (1-k, r) \\ & (p,1), (0,1), (-\xi^2, r) \\ & (-1,1), (-\kappa_I, 1), (-Lm_I, 1), (0,1) \\ & (-1,1), (-1,1), (\kappa-1), (Nm-1), (0,1) \end{array}\right]. \tag{3.13}$$

Proof. See Appendix C. □

Corollary 3. It should be mentioned that, substituting $g = 0$, $\Omega = 1$ and, $r = 1$ into (3.13) yields the BER for dual-hop FSO/RF systems where the RF link and the

FSO link respectively experience $\mathcal{GK}$ and Gamma-Gamma fading under heterodyne detection given as

$$\overline{P}_e = \frac{\xi^2 A \delta \kappa m \mathrm{C}}{2\Gamma(\alpha)\Gamma(p)\Gamma(Nm)\Gamma(\kappa)\Gamma(Lm_I)\Gamma(\kappa_I)\kappa_I m_I \bar{\gamma}_2} \sum_{j=1}^{n} \sum_{k=1}^{\beta} \frac{b_k}{\Gamma(k)} \\ \mathrm{G}_{1,0:3,3:4,5}^{1,0:1,3:4,3}\left[\frac{\mu_1 q_j}{B}; \frac{\kappa m \mathrm{C}}{\kappa_I m_I \bar{\gamma}_2} \middle| 1 \middle| \begin{matrix} 1-\xi^2, 1-\alpha, 1-\beta \\ p, 0, -\xi^2 \end{matrix} \middle| \begin{matrix} -1, -\kappa_I, -Lm_I, 0 \\ -1, -1, \kappa-1, Nm-1, 0 \end{matrix} \right] \tag{3.14}$$

where $G[\cdot,\cdot]$ denotes the generalized bivariate Meijer's function [30].

Corollary 4. At high SNR regime (i.e. $\mu_r \to \infty$), the asymptotic average BER in interference-limited mixed FSO/RF is given by

$$\begin{aligned} \overline{P}_e^{\infty} \underset{\mu_r \to \infty}{\sim} & \frac{\xi^2 A \delta \kappa m \mathrm{C}}{2\Gamma(\alpha)\Gamma(p)\Gamma(Nm)\Gamma(\kappa)\Gamma(Lm_I)\Gamma(\kappa_I)\kappa_I m_I \bar{\gamma}_2} \sum_{j=1}^{n} \sum_{k=1}^{\beta} \frac{b_k}{\Gamma(k)} \\ & \left[\frac{\Gamma(\alpha-\xi^2)\Gamma(k-\xi^2)\Gamma(p+\frac{\xi^2}{r})}{r\Gamma(1-\frac{\xi^2}{r})} \left(\frac{B^r}{\mu_r q_j} \right)^{\frac{\xi^2}{r}} \mathrm{G}_{5,5}^{4,4}\left[\frac{\kappa m \mathrm{C}}{\kappa_I m_I \bar{\gamma}_2} \middle| \begin{matrix} -\kappa_I, -Lm_I, -1, \frac{\xi^2}{r}, 0 \\ \kappa-1, Nm-1, -1, -1, 0 \end{matrix} \right] \right. \\ & + \frac{\Gamma(\xi^2-\alpha)\Gamma(k-\alpha)\Gamma(p+\frac{\alpha}{r})}{r\Gamma(1-\frac{\alpha}{r})\Gamma(1+\xi^2-\alpha)} \left(\frac{B^r}{\mu_r q_j} \right)^{\frac{\alpha}{r}} \mathrm{G}_{5,5}^{4,4}\left[\frac{\kappa m \mathrm{C}}{\kappa_I m_I \bar{\gamma}_2} \middle| \begin{matrix} -\kappa_I, -Lm_I, -1, \frac{\alpha}{r}, 0 \\ \kappa-1, Nm-1, -1, -1, 0 \end{matrix} \right] \\ & + \frac{\Gamma(\xi^2-k)\Gamma(\alpha-k)\Gamma(p+\frac{k}{r})}{r\Gamma(1-\frac{k}{r})\Gamma(1+\xi^2-k)} \left(\frac{B^r}{\mu_r q_j} \right)^{\frac{k}{r}} \mathrm{G}_{5,5}^{4,4}\left[\frac{\kappa m \mathrm{C}}{\kappa_I m_I \bar{\gamma}_2} \middle| \begin{matrix} -\kappa_I, -Lm_I, -1, \frac{k}{r}, 0 \\ \kappa-1, Nm-1, -1, -1, 0 \end{matrix} \right] \\ & + \frac{B^r}{\mu_r q_j} \mathrm{H}_{7,8}^{7,4}\left[\frac{\kappa m \mathrm{C} B^r}{\kappa_I m_I \bar{\gamma}_2 \mu_r q_j} \right. \\ & \left. \left. \middle| \begin{matrix} (-\kappa_I, 1), (-Lm_I, 1), (-1, 1), (-p, 1), (0, 1), (1+\xi^2-r, r), (0, 1) \\ (\xi^2-r, r), (\alpha-r, r), (k-r, r), (\kappa-1, 1), (Nm-1, 1), (-1, 1), (-1, 1), (0, 1) \end{matrix} \right] \right]. \end{aligned} \tag{3.15}$$

3.4.3 Ergodic Capacity

The ergodic capacity of mixed FSO/RF communication system can be bounded by

$$\overline{C} = \frac{1}{2}\mathbb{E}\left[\ln_2(1+\gamma)\right] = \frac{1}{2\ln(2)} \int_0^{\infty} \ln(1+x) f_{\gamma}(x) dx, \tag{3.16}$$

where the factor $\frac{1}{2}$ penalty in the multiplexing gain comes from the fact that the communication takes place over two time slots (i.e., half-duplex protocol).

Proposition 3. The ergodic capacity of mixed Málaga-$\mathcal{M}/\mathcal{GK}$ FSO transmission

system with interference under both detection techniques with pointing errors taken into account is obtained as

$$\overline{C}= \frac{\xi^2 A\kappa m\mathrm{C}}{2\ln(2)\Gamma(\alpha)\Gamma(Nm)\Gamma(\kappa)\Gamma(Lm_I)\Gamma(\kappa_I)\kappa_I m_I\bar{\gamma}_2}\sum_{k=1}^{\beta}\frac{b_k}{\Gamma(k)}$$
$$\mathrm{H}_{1,0:4,3:4,5}^{0,1:1,4:4,3}\left[\begin{array}{c|c} \frac{\mu_r}{B^r} & (0,1,1) \\ & - \\ \frac{\kappa m\mathrm{C}}{\kappa_I m_I\bar{\gamma}_2} & (1-\xi^2,r),(1-\alpha,r),(1-k,r),(1,1) \\ & (0,1),(1,1),(-\xi^2,r) \\ & (-1,1),(-\kappa_I,1),(-Lm_I,1),(0,1) \\ & (-1,1),(-1,1),(\kappa-1),(Nm-1),(0,1) \end{array}\right]. \tag{3.17}$$

Proof. Plugging (3.7) into (3.16) after applying the identity $\ln(1+x)=\mathrm{G}_{2,2}^{1,2}[x|\,{}^{1,1}_{1,0}]$ yield the result after resorting to [32, Eq.(1.1)] and [30, Eq.(7.811.4)] along some additional algebraic manipulations. □

Corollary 5. In the special case when $\kappa_X \to \infty$ and $r=1$, (3.17) reduces to the ergodic capacity of a dual-hop Gamma-Gamma/Nakagami-m FSO transmission system under heterodyne detection given by

$$\overline{C}=\frac{\xi^2}{2\ln(2)\Gamma(Nm)\Gamma(Lm_I)\Gamma(\alpha)\Gamma(\beta)}$$
$$\mathrm{G}_{1,0:4,3:3,4}^{1,0:1,4:3,2}\left[\frac{\mu_1}{\alpha\beta h};\frac{m\mathrm{C}}{m_I\bar{\gamma}_2}\left|\begin{array}{c} 1 \\ - \end{array}\right|\begin{array}{c|c} 1-\xi^2,1-\alpha,1-\beta,1 & 0,1-Lm_I,1 \\ 0,1,-\xi^2 & 0,0,Nm,1 \end{array}\right]. \tag{3.18}$$

3.5 Performance Analysis of CSI-assisted Relaying

3.5.1 Outage Probability

Based on (3.8), and resorting to the outage probability of CSI-assisted mixed Málaga-$\mathcal{M}$ turbulent/$\mathcal{GK}$ systems can be lower bounded by

$$P_{out} = 1-\frac{\xi^2 A}{\Gamma(\alpha)\Gamma(Nm)\Gamma(\kappa)\Gamma(Lm_I)\Gamma(\kappa_I)}\sum_{k=1}^{\beta}\frac{b_k}{\Gamma(k)}$$
$$\mathrm{G}_{0,0:2,4:3,3}^{0,0:4,0:3,2}\left[B\left(\frac{\gamma_{th}}{\mu_r}\right)^{\frac{1}{r}};\frac{\kappa m\gamma_{th}}{\kappa_I m_I\bar{\gamma}_2}\left|\begin{array}{c} - \\ - \end{array}\right|\begin{array}{c|c} \xi^2+1,1 & 1-\kappa_I,1-Lm_I,1 \\ 0,\xi^2,\alpha,k & 0,\kappa,Nm \end{array}\right]. \tag{3.19}$$

Corollary 6 (Asymptotic outage probability)**.** At high average normalized SINR $\frac{\mu_r}{\gamma_{th}} = \frac{\bar{\gamma}_2}{\gamma_{th}} \to +\infty$ can be rewritten by applying the asymptotic expansion of the Meijer-G function to (2.8) and (3.3) in (3.8) as

$$P_{out}^{\infty} = \frac{\xi^2 A}{\Gamma(\alpha)\Gamma(Nm)\Gamma(\kappa)\Gamma(Lm_I)\Gamma(\kappa_I)} \sum_{k=1}^{\beta} \frac{b_k}{\Gamma(k)} \sum_{j=1}^{5} \zeta_j \left(\frac{\gamma_{th}}{\bar{\gamma}}\right)^{\Phi_j}, \tag{3.20}$$

where

$$\begin{aligned}
\zeta_1 &= -\frac{\Gamma(Nm-\kappa)\Gamma(\kappa_I+\kappa)\Gamma(Lm_I+\kappa)}{\kappa} \left(\frac{m\kappa}{m_I\kappa_I}\right)^{\kappa}, \\
\zeta_2 &= -\frac{\Gamma(\kappa Nm)\Gamma(\kappa_I+Nm)\Gamma(Lm_I+Nm)}{Nm} \left(\frac{m\kappa}{m_I\kappa_I}\right)^{Nm}, \\
\zeta_3 &= -\frac{\Gamma(\alpha-\xi^2)\Gamma(k-\xi^2)}{\xi^2} B^{\xi^2}, \\
\zeta_4 &= -\frac{\Gamma(k-\alpha)}{\alpha(\xi^2-\alpha)} B^{\alpha}, \\
\zeta_5 &= -\frac{\Gamma(\alpha-k)}{k(\xi^2-k)} B^{k},
\end{aligned} \tag{3.21}$$

and, $\Phi = \{\kappa, Nm, \frac{\xi^2}{r}, \frac{\alpha}{r}, \frac{k}{r}\}$, and $\bar{\gamma} = \mu_r = \bar{\gamma}_2$.

Furthermore, the diversity gain follows from (3.20) as

$$d = \min\left\{\kappa, Nm, \frac{\xi^2}{r}, \frac{\alpha}{r}, \frac{k}{r}\right\}. \tag{3.22}$$

This result proves that the performance of the dual-hop mixed FSO/RF system is depending on the weaker link between the FSO and RF links. For strong turbulence and/or pointing errors at the FSO link, and large values of shadowing and multipath and antennas number at the RF link, the performance of the first hop (FSO link) will dominate the end-to-end performance of the system. Furthermore, the effect of the RF parameters (either the shadowing, multipath or antenna's number) will be extremely negligible.

3.5.2 Average Bit-Error Rate

Proposition 4. The average BER of mixed FSO/RF CSI-assited relaying system under Málaga-$\mathcal{M}$ turbulent/$\mathcal{GK}$ fading channels with interference and under heterodyne

and IM/DD detection techniques is obtained as

$$\overline{P_e}=\frac{\delta n}{2}-\frac{\xi^2 Ar\delta}{2\Gamma(p)\Gamma(\alpha)\Gamma(Nm)\Gamma(\kappa)\Gamma(Lm_I)\Gamma(\kappa_I)}\sum_{j=1}^{n}\sum_{k=1}^{\beta}\frac{b_k}{\Gamma(k)}$$
$$\mathrm{H}_{1,0:2,4:3,3}^{0,1:4,0:3,2}\left[\begin{array}{c|c} & (1-p,1,1) \\ & - \\ \frac{B^r}{\mu_r q_j} & (\xi^2+1,r),(1,r) \\ \frac{\kappa m}{\kappa_I m_I \tilde{\gamma}_2 q_j} & (0,r),(\xi^2,r),(\alpha,r),(k,r) \\ & (1-\kappa_I,1),(1-Lm_I,1),(1,1) \\ & (0,1),(\kappa,1),(Nm,1) \end{array}\right]. \tag{3.23}$$

Proof. Substituting (2.3) and (3.3) into (3.12), and resorting to [34, Eq.(1.59)] and [32, Eq.(2.2)] yield the result after some manipulations. □

Corollary 7. The average BER of interference-limited mixed Málaga-$\mathcal{M}/\mathcal{GK}$ system can be asymptotically expressed at high SINR of the FSO and RF links as

$$\overline{P_e}^{\infty}\underset{\mu_r,\tilde{\gamma}_2\gg 1}{\approx}\frac{\delta\xi^2 A\sum_{i=1}^{n}\sum_{k=1}^{\beta}\sum_{j=1}^{5}\frac{b_k}{\Gamma(k)}\zeta_j(q_i\mu_r)^{-\Phi_j}\Gamma(p+\Phi_j)}{2\Gamma(\alpha)\Gamma(p)\Gamma(Nm)\Gamma(\kappa)\Gamma(Lm_I)\Gamma(\kappa_I)}, \tag{3.24}$$

3.5.3 Ergodic Capacity

Proposition 5. The ergodic capacity of mixed FSO/RF CSI-assisted relaying system with interference in Málaga-$\mathcal{M}/\mathcal{GK}$ fading channels under both detection techniques is obtained as

$$\overline{C}=\frac{\xi^2 Ar\mu_r B^{-r}}{2\ln(2)\Gamma(\alpha)\Gamma(Nm)\Gamma(\kappa)\Gamma(Lm_I)\Gamma(\kappa_I)}\sum_{k=1}^{\beta}\frac{b_k}{\Gamma(k)}$$
$$\mathrm{H}_{1,0:4,3:3,4}^{0,1:1,4:3,3}\left[\begin{array}{c|c} & (0,1,1) \\ & - \\ \frac{\mu_r}{B^r} & (1-r,r),(1-\xi^2-r,r),(1-\alpha-r,r),(1-k-r,r) \\ \frac{\kappa_I m_I \tilde{\gamma}_2}{\kappa m} & (0,1),(-\xi^2-r,r),(-r,r) \\ & (1,1),(1-\kappa,1),(1-Nm,1) \\ & (1,1),(\kappa_I,1),(Lm_I,1),(0,1) \end{array}\right]. \tag{3.25}$$

Proof. See Appendix D. □

Corollary 8. When $r=1$, $\kappa_X\to\infty$, (3.25) reduces to the ergodic capacity of mixed FSO/RF systems with heterodyne detection in Málaga/Nakagami-m fading channels

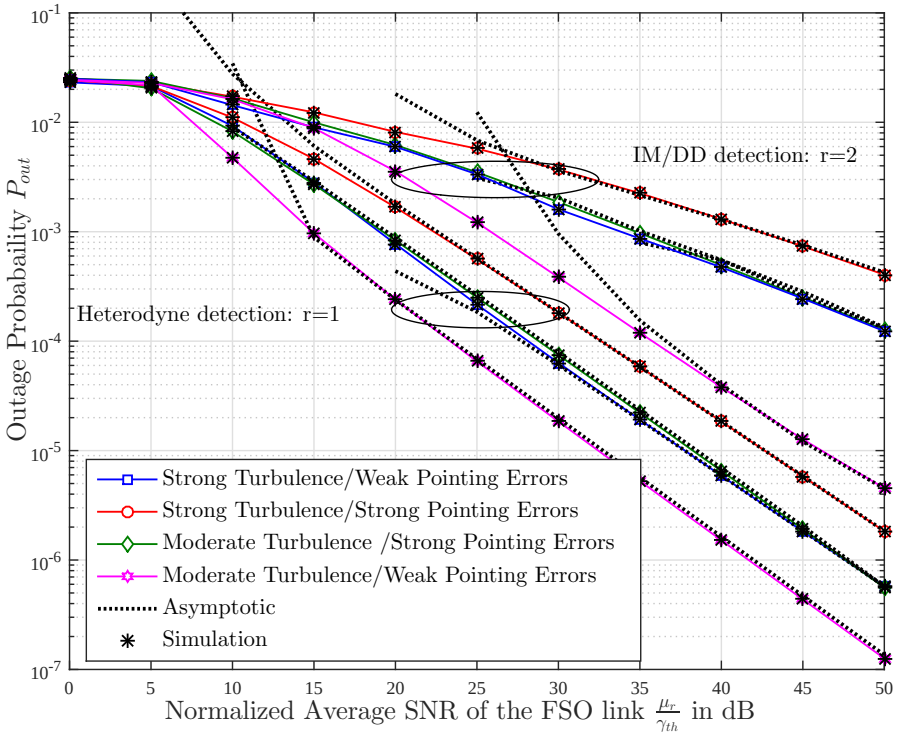

Fig. 3.2: Outage Probability of interference-limited fixed-gain AF mixed FSO/RF under different turbulence and pointing errors severities and detection techniques r.

as given by

$$\overline{C} = \frac{\xi^2 A \mu_1}{2\ln(2) B \Gamma(\alpha)\Gamma(Nm)\Gamma(Lm_I)B} \sum_{k=1}^{\beta} \frac{b_k}{\Gamma(k)} \\ \mathrm{G}_{1,0:4,3:2,3}^{1,0:1,4:2,2}\left[\frac{\mu_1}{B}; \frac{m_I \bar{\gamma}_2}{m} \middle| \begin{matrix} 1 \\ - \end{matrix} \middle| \begin{matrix} 0, -\xi^2, -\alpha, -k \\ 0, -\xi^2 - 1, -1 \end{matrix} \middle| \begin{matrix} 1, 1-Nm \\ 1, Lm_I, 0 \end{matrix}\right]. \tag{3.26}$$

3.6 Numerical Results

In order to prove the correctness of our analytical results, we compare the closed-form expressions against Monte-carlo simulations. Specifically, we demonstrate the performance of interference-limited mixed FSO/RF AF system for different turbulence, fading, interference, and shadowing severities. Moreover, we investigate the impact of pointing errors and detection technique on the overall system performance.

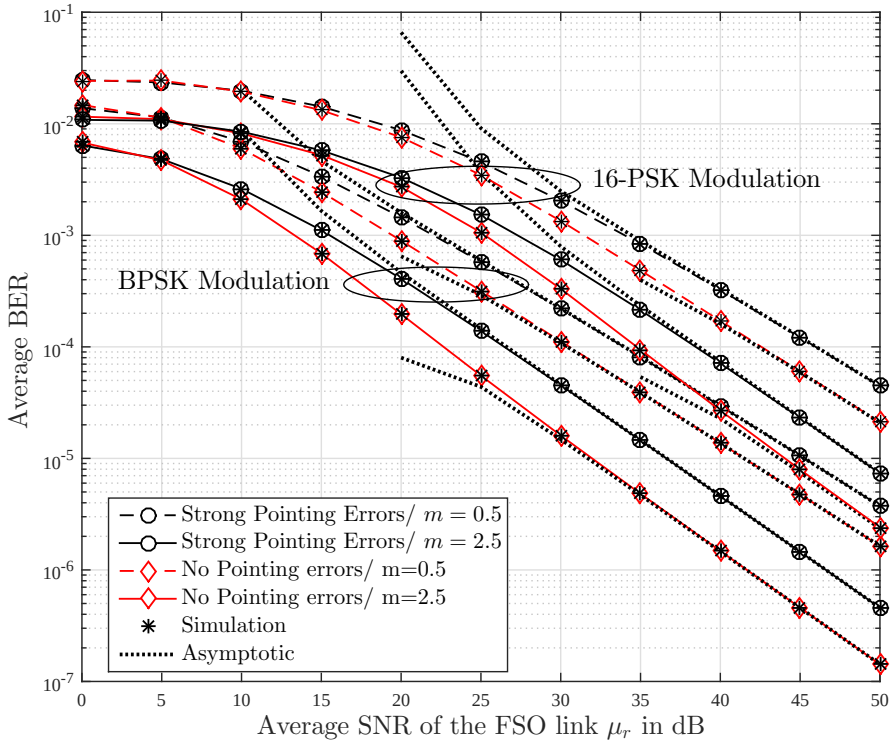

Fig. 3.3: Average BER of interference-limited fixed-gain AF mixed FSO/RF under different pointing errors and fading severities.

3.6.1 Fixed-gain Relaying

In this section, the fixed gain of the relay is equal to C = 1.7. We present two different turbulence severities ($\alpha = 2.4, \beta = 2$) and ($\alpha = 5.4, \beta = 4$) for strong and moderate turbulence, respectively. Furthermore, we assume the following values for pointing errors where it is considered strong for $\xi = 1.1$ and weak of $\xi = 6.8$.

Fig.3.2 illustrates the outage probability of fixed-gain AF mixed FSO/RF systems versus the normalized average SNR of the FSO link. From Fig.3.2, we observe a perfect agreement between the analytical results in(3.9) and their Monte-carlo simulated counterparts. Moreover, it can be noticed that the asymptotic results in (3.10) are very tight approximation especially at high SNR regime. Other outcome is that the heterodyne detection outperforms the IM/DD (a similar behavior seen in [27]) since it overcomes better the turbulence and pointing errors effects which is assessed by complicated coherent receivers. Obviously, the end-to-end performance of interference-limited mixed FSO/RF system is improved under moderate turbulence and weak pointing errors.

In Fig.3.3, The average BER for strong and no pointing errors ($\xi \to +\infty$) scenarios

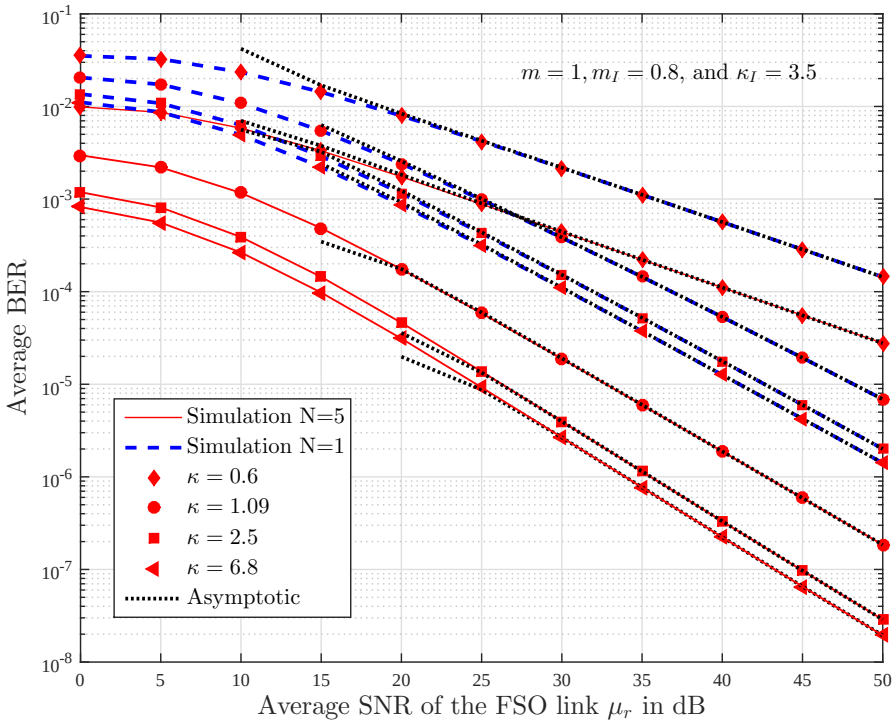

Fig. 3.4: Average BER of an interference-limited fixed-gain mixed FSO/RF network in strong turbulence conditions for different values of κ and antenna number at the relay N.

with different faded RF channel is demonstrated for BSPK and 16-PSK modulation schemes. We highlight again the perfect match between the Monte-carlo simulated results and analytical expression derived in (3.13). The asymptotic result for the average BER in (3.14) is also a very tight approximation when $\mu_r \to +\infty$. It can be noticed from Fig.3.3 that the fading severity in the RF channel is detrimental for the system performance where a severely faded channel ,i.e., $m = 0.5$, leads to a deterioration of the overall performance. Under the same RF link (equal m), the system with no pointing errors, i.e., $\xi \to +\infty$, at the FSO link provides a better performance than its counterpart with strong pointing errors, i.e., $\xi = 1.1$. Expectedly, BPSK binary modulation outperforms 16-PSK modulation scheme independently of the pointing errors/fading severities.

In Fig.3.4, The average BER under BPSK binary modulation scheme for varying RF shadowing severity κ and relay's antennas number N is presented. It can be noticed that, expect for $\kappa = 0.6$, all curves have the same slopes thereby inferring that they have the same diversity order. This is due to the fact that the system diversity order is dependent on $d = \min\left\{Nm, \kappa, \frac{\xi^2}{r}, \frac{\alpha}{r}, \frac{k}{r}\right\}$. For the two curves when

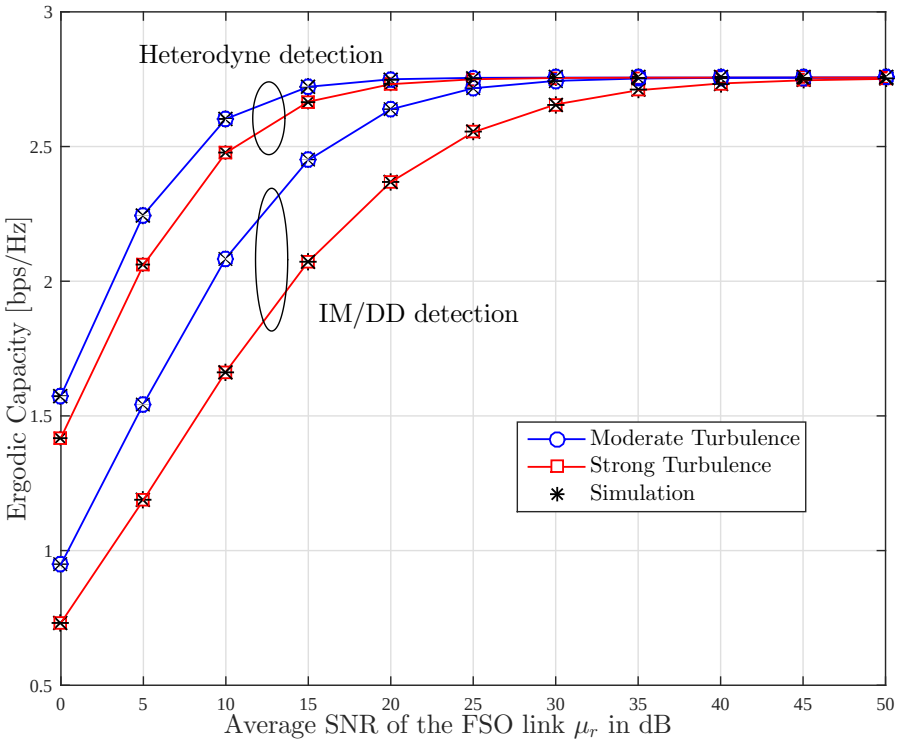

Fig. 3.5: Ergodic Capacity of interference-limited fixed-gain AF mixed FSO/RF for different turbulence severities and detection techniques.

$\kappa = 0.6$, they have the same slope revealing equal diversity order $d = \kappa = 0.6$. Fig.3.4 also shows that the asymptotic expansion in (3.15) agree very well with the simulation results, hence corroborating its usefulness. The impact of the relay antennas number N on the system BER is investigated in Fig.3.4 under several shadowing conditions. As discussed in Corollary 4, spacial diversity resulted from employing higher antennas number N at the relay enhances the overall performance of the system.

The validity of the ergodic capacity's closed-form expression in (3.17) is assessed in Fig.3.5 by Monte-carlo simulations. An expected behavior is observed where moderate turbulence scenario presents a better overall performance of the system independently from the applied detection technique at the relay (either IM/DD or heterodyne detection). In addition, it can be noticed that the degradation of the system performance due to strong turbulence is greater when the IM/DD detection technique is employed.

3.6.2 CSI-assisted Relaying

Fig.3.6 depicts the outage probability under different turbulence conditions at the RF link and interferences at the mobile user. Clearly, the asymptotic expression for the

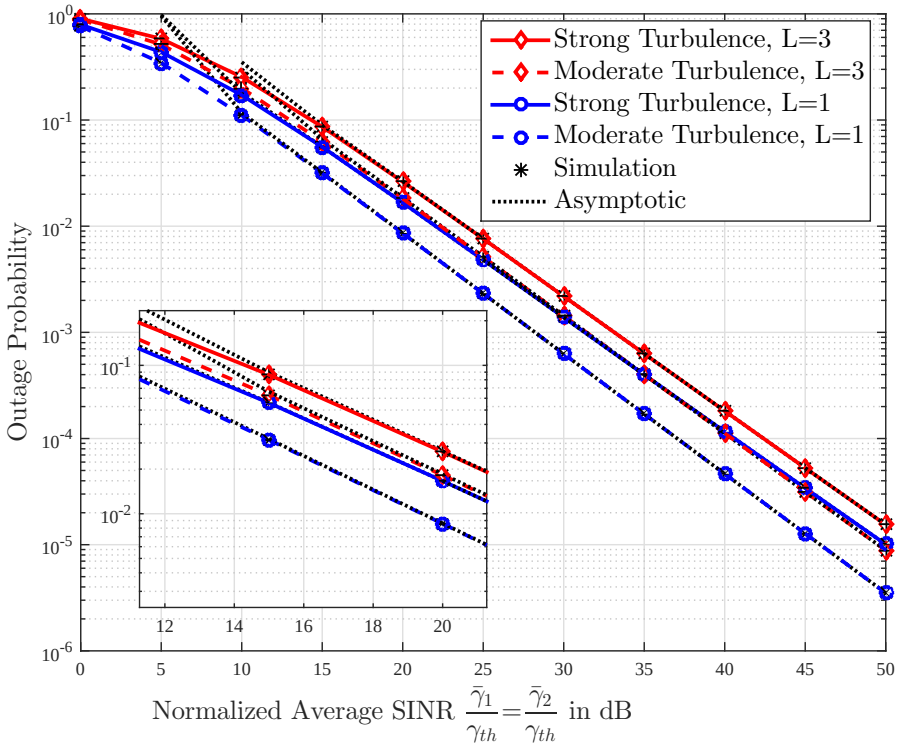

Fig. 3.6: Outage probability of interference-limited CSI-assisted mixed FSO/RF under different turbulence conditions and interference L.

outage probability is close to the analytical results at high SINR regime. As expected increasing L deteriorates the system performance, by increasing the outage probability, while the diversity gain remains unchanged. The figure also demonstrates that the degradation resulted from strong turbulence is much higher when $L = 1$ than for $L = 3$. Fig.3.7 depicts the average BER of mixed FSO/RF relay systems in Málaga-$\mathcal{M}$ and $\mathcal{GK}$ fading channels for different M-PSK and M-QAM modulations. A perfect match between the Monte-carlo curves and their analytical counterparts from (3.23) proves the accuracy of our mathematical framework. Moreover, for the asymptotic analysis, it is observed form Fig. 3.7 that at high SNR regime, the asymptotic expression of the average BER in (3.24) is an accurate approximation for (3.23). Expectedly, under similar turbulence and fading conditions, 16-QAM modulation secures a better performance than 16-PSK modulation. Fig.3.8 illustrates the effect of shadowing severity and co-channel interference on the ergodic capacity in CSI-assisted relaying. The Monte-carlo simulations are in perfect agreement with the analytical expression. A general observation is that shadowing degrades the system's overall performance. Furthermore, more interference (i.e., higher L) at the destination results a lower capacity. A similar behavior has been noticed in [31].

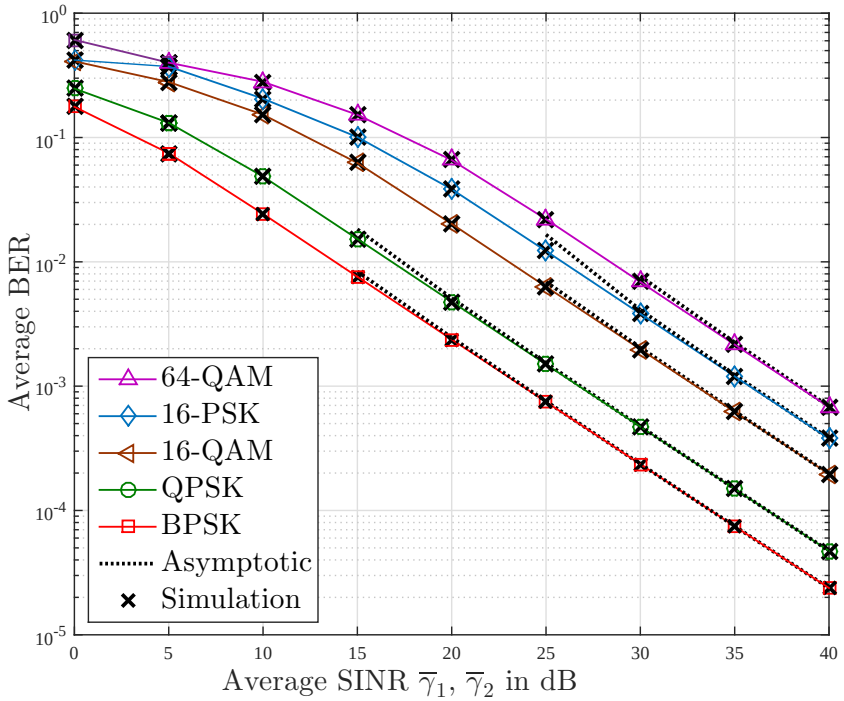

Fig. 3.7: Average BER of interference-limited CSI-assisted mixed FSO/RF different modulations schemes.

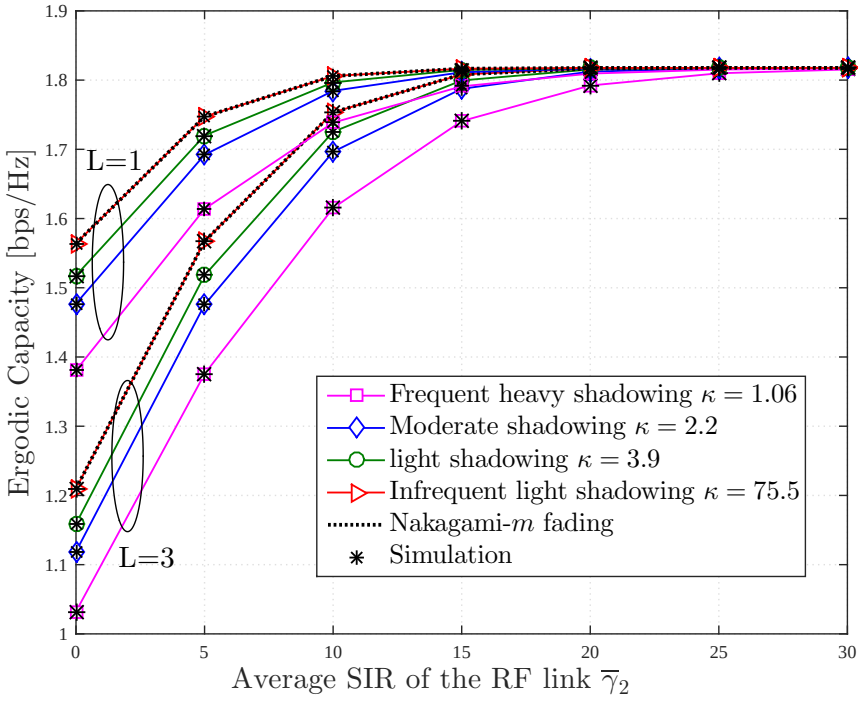

Fig. 3.8: Ergodic Capacity for different κ and L under CSI-assisted relaying

3.7 Summary

In this chapter, we have studied the performance of relay-assisted mixed FSO/RF network with RF interference and two different detection techniques. The H-transform theory is involved into a unified performance analysis framework featuring closed-from expressions for the outage probability, the average BER and the channel capacity assuming Málaga-$\mathcal{M}$/composite fading/shadowing $\mathcal{GK}$ channel models for the FSO/RF links while taking into account pointing errors. Results show that the system diversity order is related to the the minimum value of the atmospheric turbulence, small-scale fading, shadowing and pointing error parameters.

Chapter 4

Mixed Multi-Aperture Multiuser FSO/RF Interference-Limited AF Relay Systems over Málaga $\mathcal{M}$-Turbulence Channels with Pointing Errors

4.1 Introduction

Aiming to further increase the mixed FSO/RF system capacity and reliability, another line of work dedicated to multiuser relay-assisted networks with multi-aperture FSO communications has been longing for understanding such systems [38, 44]. In this context, the Málaga $\mathcal{M}$-distribution was only considered in [38] with Rayleigh distributed user links.

In this chapter, we consider a mixed multi-aperture multiuser FSO/RF system where the FSO and RF links, respectively, experience Málaga $\mathcal{M}$ and Nakagami-m fading. We further take into account the effect of co-channel interference and pointing errors which might be detrimental in RF and FSO links, respectively. This chapter quantifies accurately the capacity of mixed FSO/RF AF relay-assisted networks with opportunistic scheduling among users and transmit selection at the source's apertures.

Under the assumption of transmit aperture selection at the source and oppor-

Results from this work have been accepted for publication in *IEEE SPAWC* 2017.
The entire work conducted in this chapter is in preparation for submission in *IEEE Transactions on Wireless Communications*.

tunistic scheduling at the destination, we derive the exact expression for the ergodic capacity and the average BER in terms of bivariate Meijer's-G function. Additionally, resorting to extreme value theory, we derive closed-form expressions for the asymptotic ergodic capacity and the average BER, all in terms of Meijer's G and elementary functions, whenever the number of apertures at the source and/or users grows large. Finally, we capitalize on these results to investigate the effect of pointing errors on the system performance.

4.2 System Model

We consider a mixed FSO/RF relay system where a multi-aperture source S communicates with multiple users $(D_k, k = 1, \ldots, K)$ via a relay R. It is assumed that L RF co-channel interferers impinge on each user D_k (cf Fig. 4.1). The FSO and RF links are assumed to follow the $\mathcal{M}$ and Nakagami-m distributions, respectively. Assume that the source is equipped with M FSO apertures, then the PDF of the m-th aperture irradiance $I_m, m = 1, \ldots, M$ is given by [18]

$$f_{I_m}(x) = \frac{A}{\Gamma(\alpha)} \sum_{k=1}^{\beta} \frac{b_k}{\Gamma(k)} x^{\frac{\alpha+k}{2}-1} K_{\alpha-k}\left(2\sqrt{\frac{\alpha\beta x}{g\beta+\Omega}}\right), \tag{4.1}$$

where $g = 2b_0(1-\rho)$ with $2b_0$ is the average power of the LOS term and ρ represents the amount of scattering power coupled to the LOS component $(0 \leqslant \rho \leqslant 1)$. Please note that all the parameters involved in (4.1) are described explicitly in below (2.1).

The instantaneous SNR of the m-th FSO link is $\bar{\gamma_1} I_m$, where $\bar{\gamma_1}$ is the average electrical SNR of the FSO link. With transmit selection at the source, the aperture with the highest received channel gain is selected among the M available apertures at the optical transmitter. As a result, the SNR of the selected aperture is given by

$$\gamma^{FSO} = \bar{\gamma_1} \max_{m=1,\ldots,M} (I_m). \tag{4.2}$$

The average SNR of the RF link is $\bar{\gamma}_{RD}$. Moreover, the instantaneous SNR is given by $\gamma_{RD_k} = \bar{\gamma}_{RD}|h_k|^2, k = 1, \ldots, K$, where h_k is the channel fading gain between the relay R and the k-th user. Under the assumption of Nakagami-m distribution, we have $|h_k|^2 \sim \mathfrak{g}(m_1, 1/m_1)$, where $\mathfrak{g}(m, \Omega/m)$ is the Gamma distribution with shape and scale parameters m and Ω, respectively. The PDF of the SNR is given by

$$f_{\gamma_{RD_k}}(x) = \frac{m_1^{m_1}}{\bar{\gamma}_{RD}^{m_1}\Gamma(m_1)} x^{m_1-1} e^{-\frac{m_1}{\bar{\gamma}_{RD}}x}. \tag{4.3}$$

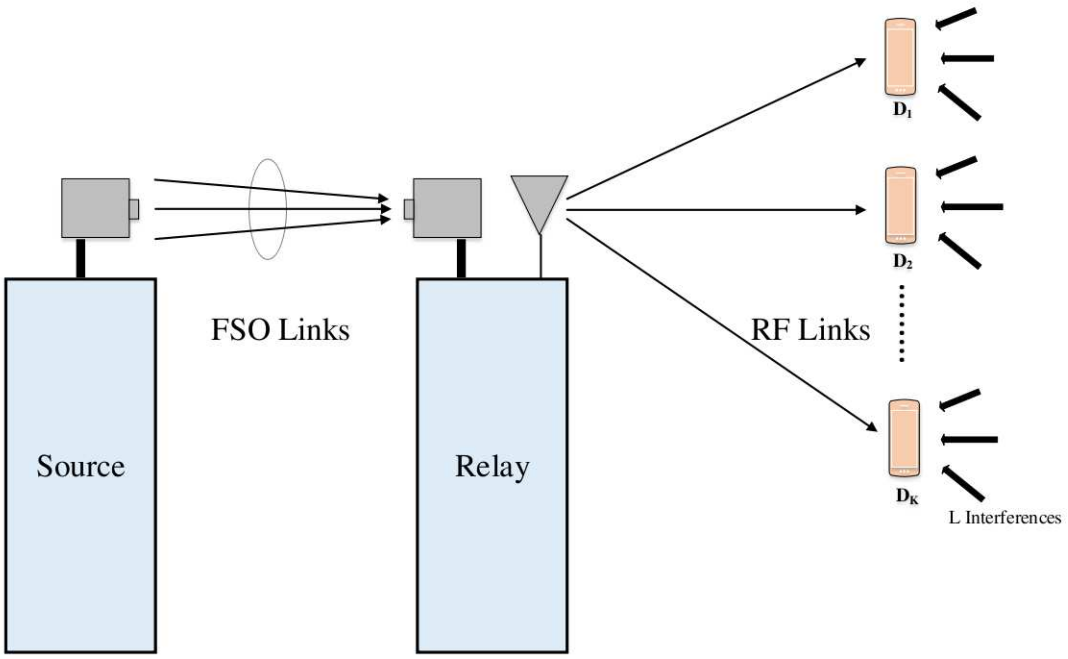

Fig. 4.1: Two-hop multiuser mixed FSO/RF AF relay network. Each RF user is affected by co-channel interference.

On the other hand, the interference-noise-ratio (INR) of the RF link between an interferer $\mathcal{I}_l, l = 1, \ldots, L$ and the destination user D_k is given by $\gamma_{\mathcal{I}_l,D_k} \overset{d}{\sim} \mathfrak{g}(m_2, \bar{\gamma}_{ID}/m_2)$, where $\bar{\gamma}_{ID}$ is the average INR, and m_2 is the Nakagami parameter of the $\mathcal{I}_l - D_k$ link. It is known that the sum of L i.i.d Gamma random variables (RVs) with shape parameter ϱ and scale parameter δ, is also a Gamma RV with parameters $L\varrho$ and δ. By defining $\gamma_{\mathcal{I},D} \overset{\Delta}{=} \sum_{l=1}^{L} \gamma_{\mathcal{I}_l,D}$ as the overall INR, the PDF of $\gamma_{\mathcal{I},D_k}$ can be written as

$$f_{\gamma_{\mathcal{I},D_k}}(x) = \frac{m_2^{Lm_2}}{\bar{\gamma}_{ID}^{Lm_2}\Gamma(Lm_2)} x^{Lm_2-1} e^{-\frac{m_2}{\bar{\gamma}_{ID}}x}. \tag{4.4}$$

With opportunistic scheduling at the relay, the user with the largest signal-to-interference-ratio (SIR) is selected. The SIR of the RF link under consideration can be written as

$$\gamma^{RF} = \bar{\gamma}_2 \max_{k=1,\ldots,K} \left(\frac{\gamma_{RD_k}}{\gamma_{\mathcal{I},D_k}} \right), \tag{4.5}$$

where $\bar{\gamma}_2 = \frac{\bar{\gamma}_{RD}}{\bar{\gamma}_{ID}}$ is the average SIR of the RF link.

Under the assumption of variable-gain relaying, the SINR of the mixed FSO/RF link can be written as [24, Eq.(28)]

$$\gamma^{FSO,RF} = \frac{\gamma^{FSO}\gamma^{RF}}{\gamma^{FSO} + \gamma^{RF} + 1}. \tag{4.6}$$

Next we define the ergodic capacity of the multiuser multi-aperture mixed FSO/RF AF relay system as

$$\begin{aligned} C \quad &\triangleq \frac{1}{2\ln(2)}\mathbb{E}[\ln(1+\gamma^{FSO,RF})], \\ &\overset{(a)}{=} \frac{1}{2\ln(2)}\int_0^\infty s e^{-s} M^{(c)}_{\gamma^{FSO}}(s) M^{(c)}_{\gamma^{RF}}(s) ds, \end{aligned} \tag{4.7}$$

Capitalizing on (4.7), we will analyze the ergodic capacity of the mixed FSO/RF AF system with interference in detail in Sections 4.3 and 4.4.

4.3 Exact Analysis of the Capacity with Finite-Count Apertures and Users

According to (4.7), the exact capacity analysis amounts to studying the CMGF of the SINR in each hop independently. As a result, the analysis will be simplified as shown subsequently.

Lemma 1. Let $\gamma_m^{FSO} = \bar{\gamma}_1 I_m, \quad m = 1, \ldots, M$ be the instantaneous SNR of m-th FSO link following the $\mathcal{M}$-distribution under heterodyne detection [27]. Then the CMGF of $\gamma^{FSO} = \max\limits_{m=1,\ldots,M}(\gamma_m^{FSO})$ is obtained as

$$M^{(c)}_{\gamma^{FSO}}(s) = \sum_{t=1}^{M}\sum_{\Upsilon}\frac{\Theta_t}{s^{\frac{\delta_t}{2}+1}} G^{1,2}_{2,1}\left[\frac{\bar{\gamma}_1(\mu\beta+\Omega)s}{t^2\alpha\beta}\middle| \begin{matrix} 1, \frac{1}{2} \\ \frac{\delta_t}{2}+1 \end{matrix}\right], \tag{4.8}$$

where $\sum_{\Upsilon} = \sum_{\Upsilon_{t_\beta}} \sum_{\Upsilon_{t_{p,\alpha-t_p+\frac{1}{2}}}} \sum_{\Upsilon_{t_{pq}\alpha+t_p-t_{pq}-\frac{1}{2}}}$, with $\Upsilon_{z,l} = \{(z_1, \ldots, z_l) \colon z_i \geqslant 0, \sum_{i=1}^{l} z_i = z\}$; Θ_t is given in (4.9); and $\delta_t = \sum_{l=0}^{\alpha+t_p-t_{pq}-\frac{3}{2}} l t_{p_{q_{l+1}}}$.

Proof. From (4.1) and using [30, Eq 8.468], the PDF of the m-th FSO link I_m can be

$$\Theta_t = \frac{\prod_{r=1}^{\alpha+t-t_p-\frac{1}{2}} \left(\frac{2^{\frac{3}{2}-t_{p_q}} A a_{t_{p_q}} \sqrt{\pi}(\alpha-t_p-\frac{3}{2}+t_{p_q})! g\beta+\Omega^{\frac{\alpha+t_p-t_{p_{q_r}}+1}{2}}}{(4\alpha\beta)^{\frac{\alpha+t-t_{p_{q_r}}+1}{2}}(\alpha-t_p+\frac{1}{2}-t_{p_q})!(t_{p_q}-1)!(t_{p_{q_r}}-1)!} \right)^{t_{p_{q_r}}} \binom{M}{t}(-1)^{t+1} t! t_p! t_{p_q}!}{\sum_{i=1}^{\beta} t_i! \sum_{j=1}^{\alpha-t+\frac{3}{2}} t_{p_j}! \sum_{k=1}^{\alpha+t-t_p-\frac{1}{2}} t_{p_{q_k}}! \sqrt{\pi} \bar{\gamma}_1^{\frac{\delta_t}{2}}}. \tag{4.9}$$

written as

$$f_{I_m}(x) = A\sqrt{\pi} \sum_{k=1}^{\beta} \sum_{j=0}^{\alpha-k+\frac{1}{2}} \frac{\frac{b_k}{\Gamma(k)}(\alpha-k-\frac{1}{2}+j)! x^{\frac{\alpha+k}{2}-\frac{5}{4}-\frac{j}{2}} e^{-2\sqrt{\frac{\alpha\beta x}{(g\beta+\Omega)}}}}{\left(4\sqrt{\frac{\alpha\beta}{(g\beta+\Omega)}}\right)^{j+\frac{1}{2}} (\alpha-k-\frac{1}{2}-j)! j!}. \tag{4.10}$$

Therefore, its CCDF is obtained by resorting to the identity [30, Eq 3.351.2] as

$$F_{I_m}^{(c)}(x) = A\sqrt{\pi} \sum_{k=1}^{\beta} \sum_{j=0}^{\alpha-k+\frac{1}{2}} \frac{\frac{b_k}{\Gamma(k)}(\alpha-k-\frac{1}{2}+j)!}{\left(4\sqrt{\frac{\alpha\beta}{(g\beta+\Omega)}}\right)^{j+\frac{1}{2}} (\alpha-k-\frac{1}{2}-j)! j!} \Gamma\left(\alpha+k-j, 2\sqrt{\frac{\alpha\beta x}{(g\beta+\Omega)}}\right), \tag{4.11}$$

where $\Gamma(\cdot,\cdot)$ is the upper incomplete Gamma function [30, Eq.(8.350.2)]. By substituting the incomplete Gamma function in (4.11) by its series expansion in [30, Eq 8.352.1] and applying the multinomial expansion, the CCDF of $\gamma^{FSO} = \bar{\gamma}_1 \max_{m=1,\ldots,M}(I_m)$ is obtained as

$$F_{\gamma^{FSO}}^{(c)}(x) = \sqrt{\pi} \sum_{t=1}^{M} \sum_{\Upsilon} \Theta_t x^{\frac{\delta_t}{2}} \exp\left(-2t\sqrt{\frac{\alpha\beta}{\bar{\gamma}_1(\mu\beta+\Omega)}x}\right). \tag{4.12}$$

The CMGF of γ^{FSO} is obtained after applying the Laplace transform to (4.12) and resorting to [30, Eq.3.462.1], thereby leading to (4.8) after some manipulations. □

Lemma 2. Let the instantaneous SIR of the k-th RF link be $\gamma_k^{RF} = \bar{\gamma_2}\left(\frac{\gamma_{RD_k}}{\gamma_{\mathcal{I},D_k}}\right), k = 1,\ldots,K$, as the ratio of two Gamma-distributed RVs. The CMGF of $\gamma^{RF} = \max_{k=1,\ldots,K}(\gamma_k^{RF})$

is given by

$$M_{\gamma^{RF}}^{(c)}(s)=\sum_{q=0}^{\Delta-1}\phi_q\Psi\left(q+1,q+2-\Delta,\frac{\bar{\gamma}_2 m_2 s}{m_1}\right)-\sum_{r=1}^{K}\sum_{\Upsilon_{r,Lm_2-1}}\varphi_r$$
$$\Psi\left(\delta_r+2-r(m_1-1),\delta_r+\Delta+r(1-m_1)+1,\frac{\bar{\gamma}_2 m_2 s}{m_1}\right), \tag{4.13}$$

where $\Delta=K(Lm_2+m_1-1)$; $\phi_q=\binom{\Delta}{q}\frac{m_1}{m_2}\Gamma(q+1)\bar{\gamma}_2$; $\Psi(a,b,x)$ is the Triconomi confluent Hypergeometric function [30, Eq.9.211.1]; and $\varphi_r=\frac{\binom{K}{r}m_1 r!\prod_{p=0}^{Lm_2-2}\left(\frac{(1-Lm_2)_p(-1)^p}{(1+m_1)_p}\right)^{r_{p+1}}\bar{\gamma}_2\Gamma(\delta_r+\Delta+1)}{m_2(m_1B(Lm_2,m_1))^r\prod_{m=1}^{Lm_2-1}r_m!}$.

Proof. Let $r_k=\frac{\gamma_{RD_k}}{\gamma_{\mathcal{I},D_k}},k=1,\ldots,K$, then from (4.3) and (4.4) and resorting to [30, Eq.1.194.1], the CCDF of r_k follows as

$$\begin{aligned}F_{r_k}(x)&=\frac{\left(\frac{m_1x}{m_2}\right)^{m_1}{}_2F_1\left(Lm_2+m_1,m_1;m_1+1;-\frac{m_1x}{m_2}\right)}{m_1B(Lm_2,m_1)}\\&\overset{(a)}{=}\frac{\left(1+\frac{m_1x}{m_2}\right)^{1-Lm_2-m_1}}{m_1B(Lm_2,m_1)}\sum_{p=0}^{Lm_2-1}\frac{(1-Lm_2)_p(-1)^p}{(1+m_1)_p}\left(\frac{\frac{m_1x}{m_2}}{\frac{m_1x}{m_2}+1}\right)^{p+m_1},\end{aligned} \tag{4.14}$$

where $B(a,b)$ and ${}_2F_1(a,b;c;x)$ denote the incomplete Beta function and the Gauss Hypergeometric function [30, Eq. 9.100.1], respectively, and (a) follows from substituting the Gauss Hypergeometric function by its finite series expansion [30]. The CCDF of $\gamma^{RF}=\bar{\gamma}_2\max_{k=1,\ldots,K}(r_k)$ is then obtained as

$$\begin{aligned}F_{\gamma^{RF}}^{(c)}(x)&\overset{(b)}{=}\sum_{q=0}^{\Delta-1}\binom{\Delta}{q}\left(\frac{m_1x}{m_2\bar{\gamma}_2}\right)^q\left(1+\frac{m_1x}{m_2\bar{\gamma}_2}\right)^{-\Delta}-\sum_{r=1}^{K}\sum_{\Upsilon_{r,Lm_2-1}}\\&\qquad\frac{\varphi_r m_1\left(\frac{m_1x}{m_2\bar{\gamma}_2}\right)^{\delta_r+\Delta+r(1-Lm_2)}}{m_2\bar{\gamma}_2\Gamma\left(\delta_r+\Delta+1\right)\left(1+\frac{m_1x}{m_2\bar{\gamma}_2}\right)^{\Delta}},\end{aligned} \tag{4.15}$$

where (b) follows from applying the multinomial expansion [30, Eq.(1.111.1)]. The CMGF of γ^{RF} is obtained after applying the Laplace transform to (4.15) and resorting to [30, Eq. 9.211.1], thereby leading to (4.13) after some manipulations. □

Proposition 6 (Closed-form expression of C)**.** The ergodic capacity for arbitrary M and K in mixed FSO/RF AF systems with interference is obtained as in (4.16), where $G_{A,[C,E],B,[D,F]}^{p,q,r,s,t}(\cdot,\cdot)$ stands for the bivariate generalized Meijer-G function [45].

$$C = \frac{1}{2\ln(2)} \sum_{t=1}^{M} \sum_{\Upsilon} \Theta_t \left[\sum_{q=0}^{\Delta-1} \frac{\phi_q}{\Gamma(q+1)\Gamma(\Delta)} G_{1,[1,2],0,[2,1]}^{1,1,2,2,1} \left[\frac{\bar{\gamma}_1(\mu\beta+\Omega)}{t^2\alpha\beta}, \frac{\bar{\gamma}_2 m_2}{m_1} \;\middle|\; \begin{matrix} 1-\frac{\delta_t}{2}; 1, \frac{1}{2}; -q \\ \frac{\delta_t}{2}+1; 0, \Delta-q-1 \end{matrix} \right] \right.$$
$$- \sum_{r=1}^{K} \sum_{\Upsilon_{r,Lm_2-1}} \frac{\varphi_r}{\Gamma(\delta_r+2-r(m_1-1))\Gamma(2-\Delta)}$$
$$\left. G_{1,[1,2],0,[2,1]}^{1,1,2,2,1} \left[\frac{\bar{\gamma}_1(\mu\beta+\Omega)}{t^2\alpha\beta}, \frac{\bar{\gamma}_2 m_2}{m_1} \;\middle|\; \begin{matrix} 1-\frac{\delta_t}{2}; 1, \frac{1}{2}; r(1-m_1)-\delta_r-1 \\ \frac{\delta_t}{2}+1; 0, -\delta_r-\Delta-r(1-m_1) \end{matrix} \right] \right]. \tag{4.16}$$

Proof. Plugging (4.8) and (4.13) into (4.7) reveals that the computation of C requires the resolution of integrals of the form

$$I = \int_0^\infty x^p e^{-x} G_{m,n}^{p,q} \left(yx \;\middle|\; \begin{matrix} (a) \\ (b) \end{matrix} \right) \Psi(a_1, b_1, zx) dx. \tag{4.17}$$

By resorting to the following identity

$$\Psi(a,b,x) = \frac{1}{\Gamma(a)\Gamma(a-b+1)} G_{1,2}^{2,1} \left[x \;\middle|\; \begin{matrix} 1-a \\ 0, 1-b \end{matrix} \right], \tag{4.18}$$

(4.7) can be evaluated by means of the bivariate generalized Meijer-G function, as can be seen from a more general integral formula due to [46, Eq.(2.1)], thereby leading to (4.16) after some manipulations. □

4.4 Large-Scale Analysis of the Capacity

In this section, the ergodic capacity of the mixed FSO/RF relay network with massive aperture selection and/or user scheduling is considered. Thereby, by using extreme value theory, the asymptotic CMGF expressions are derived, for the case in which the numbers of apertures and users grow without bound. The new computed CMGF expressions of the two hops are given by the following lemmas.

Lemma 3. As the number of apertures M at the FSO link grows large, the CMGF expression of γ^{FSO} can be written as

$$M_{\gamma^{FSO}}^{(c)}(s) = \frac{1}{s} \left(1 - e^{-\bar{\gamma}_1 (b_M - c_M) s} \right), \tag{4.19}$$

where b_M and c_M are constants given by

$$F_{I_m}^{(c)}(b_M) = \frac{1}{M}, \quad \text{and} \quad c_M = \frac{F_{I_m}^{(c)}(b_M)}{f_{I_m}(b_M)}, \tag{4.20}$$

with $F_{I_m}^{(c)}$ and f_{I_m} given in (4.11) and (4.1), respectively.

Proof. We denote by the growth function $g_{I_m}(x) = \frac{F_{I_m}^{(c)}(x)}{f_{I_m}(x)}$. Then, by resorting to the Hospital's rule, it follows that

$$\begin{aligned}
\lim_{x\to\infty} g_{I_m}(x) &= \lim_{x\to\infty} \left(-1 - \frac{f'_{I_m}(x)(F_{I_m}^{(c)}(x))}{f_{I_m}^2(x)} \right), \\
&\overset{(a)}{=} -1 - \lim_{x\to\infty} \frac{d(F_{I_m}^{(c)})}{d\left(\frac{f_{I_m}^2(x)}{f'_{I_m}(x)}\right)}, \\
&\overset{(b)}{=} -1 - (-1) = 0,
\end{aligned} \tag{4.21}$$

where in (a), f'_{I_m} is the derivative of f_{I_m} given by

$$\begin{aligned}
f'_{I_m}(x) &= \frac{A}{\Gamma(\alpha)} \sum_{k=1}^{\beta} \left(\frac{b_k}{\Gamma(k)} (k-1) x^{\frac{\alpha+k}{2}-2} K_{\alpha-k}\left(2\sqrt{\frac{\alpha\beta x}{(g\beta+\Omega)}} \right) \right. \\
&\left. - \frac{b_k}{\Gamma(k)} \sqrt{\frac{\alpha\beta}{(g\beta+\Omega)}} x^{\frac{\alpha+k}{2}-\frac{3}{2}} K_{\alpha-k-1}\left(2\sqrt{\frac{\alpha\beta x}{(g\beta+\Omega)}} \right) \right),
\end{aligned} \tag{4.22}$$

and (b) follows from several mathematical manipulations. Accordingly, I_m belongs to the maximum domain of attraction $\mathcal{MDA}$ of Gumbel distribution. As a result, for a massive apertures selection at th source, the CDF of the FSO link can be written as

$$\lim_{M\to\infty} F_{\gamma^{FSO}}(x) = \exp\left[-\exp\left(-\frac{x - \bar{\gamma}_1 b_M}{\bar{\gamma}_1 c_M} \right) \right]. \tag{4.23}$$

Note that b_M and c_M are easily numerically evaluated.
The Laplace transform of the CCDF of γ^{FSO} yields its CMGF given by

$$\begin{aligned}
M_{\gamma^{FSO}}^{(c)}(s) &= \int_0^{\infty} e^{-sx} \left(1 - e^{-e^{-\frac{x-\bar{\gamma}_1 b_M}{\bar{\gamma}_1 c_M}}} \right) dx, \\
&\overset{(a)}{=} c_M \bar{\gamma}_1 \left[\int_0^{\frac{4}{\zeta}} t^{sc_M\bar{\gamma}_1 - 1} \left(1 - e^{-\zeta t} \right) dt + \int_{\frac{4}{\zeta}}^{1} t^{sc_M\bar{\gamma}_1 - 1} dt \right],
\end{aligned} \tag{4.24}$$

where (a) follows from letting $t = e^{-\frac{x}{c_M \bar{\gamma}_1}}$ and defining $\zeta = e^{\frac{b_M}{c_M}}$. We can easily see that the limit of the first term on (4.24) becomes vanishingly small as $\lim_{M\to\infty} \frac{4}{\zeta} \approx 0$. As a result, the integral of the second term can be evaluated easily as shown in (4.19). □

Lemma 4. As the number of users K at the RF link grows large, the CMGF of $\gamma^{RF} = \bar{\gamma}_2 \max_{k=1,\ldots,K}(r_k)$ is obtained as

$$M^{(c)}_{\gamma^{RF}}(s) = \frac{1}{s}\left(1 - e^{-\bar{\gamma}_2\left(\frac{m_2}{m_1}\left(\frac{K}{B(Lm_2,m_1)Lm_2}\right)^{\frac{1}{Lm_2}}-1\right)s}\right) \tag{4.25}$$

Proof. From (4.14), applying the transformation ${}_2F_1(a,b;b+1;x) = bx^{-b}B_x(b,1-a)$ and the Hospitals' rule yield

$$\lim_{x\to\infty}\frac{1-F_{r_n}(x)}{1-F_{r_n}(tx)} = \frac{t^{-m_1}(1+tx)^{Lm_2+m_1}}{(1+x)^{Lm_2+m_1}} = t^{Lm_2}, \tag{4.26}$$

which implies that $F_{\gamma^{RF}}(x)$ lies in the $\mathcal{MDA}$ of the Fréchet distribution [47, Theorem 11.5.2]. As a result, the CDF of the RF link can be written as

$$\lim_{K\to\infty} F_{\gamma^{RF}}(x) = \exp\left[-\left(\frac{x}{\bar{\gamma}_2 a_K}\right)^{-Lm_2}\right], \quad x \geqslant 0, \tag{4.27}$$

where $F^{(c)}_{r_k}(a_K) = \frac{1}{K} = \frac{m_2}{m_1}\left(\frac{K}{B(Lm_2,m_1)Lm_2}\right)^{\frac{1}{Lm_2}} - 1$, obtained after applying ${}_2F_1\left(a,b,c,x\right) = (1-x)^{c-a-b}{}_2F_1\left(c-a,c-b,c,x\right)$ to (4.14) and resorting to the Gauss hypergeometric asymptotic expansion.

Finally, applying the Laplace transform to (4.27) and following the same steps as in (4.24), we obtain the CMGF expression of the RF link as the number of user K grows without bound as shown in (4.25). □

Proposition 7 (Capacity for large M and K)**.** For massive FSO apertures selection and user scheduling, the ergodic capacity of mixed FSO/RF AF system with interference is given by

$$C = \frac{1}{2\ln(2)}\ln\left[\frac{(1+\bar{\gamma}_1(b_M-c_M))\left(1+\bar{\gamma}_2\left(\frac{m_2}{m_1}\left(\frac{K}{B(Lm_2,m_1)Lm_2}\right)^{\frac{1}{Lm_2}}-1\right)\right)}{1+\bar{\gamma}_1(b_M-c_M)+\bar{\gamma}_2\left(\frac{m_2}{m_1}\left(\frac{K}{B(Lm_2,m_1)Lm_2}\right)^{\frac{1}{Lm_2}}-1\right)}\right]. \tag{4.28}$$

Proof. The result follows after plugging (4.19) and (4.25) into (4.7) and resorting to [30, Eq 3.421.4]. □

Proposition 8 (Capacity for fixed M and large K)**.** The ergodic capacity for finite-count apertures and a massive user scheduling in mixed FSO/RF AF relay system with interference is obtained as in (4.29).

$$\begin{aligned} C &= \frac{1}{2\ln(2)} \sum_{t=1}^{M} \sum_{\Upsilon} \Theta_t \Bigg(G_{3,1}^{1,3}\left[\frac{\bar{\gamma}_1(\mu\beta+\Omega)}{t^2\alpha\beta} \;\middle|\; \begin{matrix} \frac{\delta_t}{2}+1, 1, \frac{1}{2} \\ \frac{\delta_t}{2}+1 \end{matrix} \right] \\ &\quad - (1+a_K\bar{\gamma}_2)^{\frac{\delta_t}{2}} G_{3,1}^{1,3}\left[\frac{\bar{\gamma}_1(\mu\beta+\Omega)}{t^2\alpha\beta\,(1+a_K\bar{\gamma}_2)} \;\middle|\; \begin{matrix} \frac{\delta_t}{2}+1, 1, \frac{1}{2} \\ \frac{\delta_t}{2}+1 \end{matrix} \right] \Bigg). \end{aligned} \tag{4.29}$$

Proof. The result follows after plugging (4.8) and (4.25) into (4.7) and resorting to [30, Eq.7.813.1]. □

4.5 Average Bit-Error Rate Analysis

The average BER $\overline{P_b}$ of a variety of binary modulations can be written in terms of the end-to-end SINR's CDF as [24, Eq.(21)]

$$\overline{P_b} = \frac{b^a}{2\Gamma(a)} \int_0^\infty x^{a-1} e^{-bx} F_{\gamma^{FSO,RF}}(x) dx, \tag{4.30}$$

where a and b are parameters that change for different modulation schemes (Refer to Table 4.1). The CDF of the end-to-end SINR is computed using the upper bound $\min(\gamma^{FSO}, \gamma^{RF}) > \gamma^{FSO}\gamma^{RF}/(\gamma^{FSO}+\gamma^{RF}+1)$ and the independence between γ^{FSO} and γ^{RF} as [24, Eq.(31)]

$$F_{\gamma^{FSO,RF}}(x) = 1 - F_{\gamma^{FSO}}^{(c)}(x) F_{\gamma^{RF}}^{(c)}(x) \tag{4.31}$$

Proposition 9. (Exact Analysis of the Average BER)The average BER for arbitrary M and K in mixed FSO/RF AF relay system with interference is obtained as in (4.32).

Proof. Substituting (4.12) and (4.15) into (4.30) and applying the multinomial expansion [30, Eq.(1.111.1)] and [30, Eq.(3.462.1)] yields the closed-form expression of the average BER in (4.32) after some manipulations. □

Tab. 4.1: BER Parameters for Binary Modulations

Modulation	a	b
Coherent Binary Pase Shift Keying (CBPSK)	0.5	1
Coherent Binary Frequency Shift Keying (CBFSK)	0.5	0.5
Differential Binary Phase Shift Keying (DBPSK)	1	1
Non-Coherent Binary Frequency Shift Keying (NCFSK)	1	0.5

$$\begin{aligned}\overline{P}_b &= \frac{1}{2}-\frac{1}{2\Gamma(a)}\sum_{t=1}^{M}\sum_{\Upsilon}\Theta_t\left(\sum_{q=0}^{\Delta-1}\sum_{m=0}^{\Delta}\frac{\binom{\Delta}{q}}{\binom{\Delta}{m}}\left(\frac{m_1}{m_2\bar{\gamma}_2}\right)^{q-m} b^{m-q-\frac{\delta_t}{2}}\right.\\
&\quad G_{1,2}^{2,1}\left[\frac{t^2\alpha\beta}{b\bar{\gamma}_1(\mu\beta+\Omega)}\left|\begin{matrix}1-a & -q+m-\frac{\delta_t}{2}\\ 0, \frac{1}{2}\end{matrix}\right.\right]\\
&\quad -\sum_{r=1}^{K}\sum_{\Upsilon_{r,Lm_2-1}}\sum_{n=0}^{\Delta}\frac{\varphi_r m_1\left(\frac{m_1}{m_2\bar{\gamma}_2}\right)^{\delta_r+\Delta+r(1-Lm_2)-n} b^{n-\delta_r-\Delta-r(1-Lm_2)}}{\binom{\Delta}{n}m_2\bar{\gamma}_2\Gamma\left(\delta_r+\Delta+1\right)}\\
&\quad \left.G_{1,2}^{2,1}\left[\frac{t^2\alpha\beta}{b\bar{\gamma}_1(\mu\beta+\Omega)}\left|\begin{matrix}1-a-\delta_r-\Delta-r(1-Lm_2+n)\\ 0, \frac{1}{2}\end{matrix}\right.\right]\right)\end{aligned} \tag{4.32}$$

Proposition 10 (The average BER for large M and K)**.** The average BER for massive FSO apertures selection and user scheduling of mixed FSO/RF AF system with interference for $a = 1$ is obtained as

$$\overline{P_b} = \frac{1}{2}-\frac{1}{2}\left(1-e^{-4^{-1/Lm_2}b\bar{\gamma}_2 aK}\right) + \frac{b}{2}c_M\bar{\gamma}_1\left(e^{\frac{b_M}{c_M}}\right)^{-c_M\bar{\gamma}_1 b}\Gamma\left(c_M\bar{\gamma}_1 b, e^{\frac{b_M}{c_M}}\right) \tag{4.33}$$

Proof. See Appendix E. □

Proposition 11 (The average BER for fixed M and large K)**.** The average BER for finite-count apertures and large-scale users is given by (4.34).

Proof. By plugging (4.12) and (4.27) into (4.30), we obtain

$$\begin{aligned}\overline{P}_b &= \frac{1}{2}-\frac{b^a}{2\Gamma(a)}\int_0^\infty x^{a-1}e^{-bx}F_{\gamma^{FSO}}^{(c)}(x)F_{\gamma^{RF}}^{(c)}(x)dx,\\
&= \frac{1}{2}-\frac{b^a}{2\Gamma(a)}\left(\int_0^\infty x^{a-1}e^{-bx}F_{\gamma^{FSO}}^{(c)}(x)dx - \int_0^\infty x^{a-1}e^{-bx}F_{\gamma^{FSO}}^{(c)}(x)e^{-\left(\frac{a_K\bar{\gamma}_2}{x}\right)^{Lm_2}}dx\right),\end{aligned} \tag{4.35}$$

$$\overline{P}_b = \frac{1}{2} - \frac{1}{2\Gamma(a)} \sum_{t=1}^{M} \sum_{\Upsilon} \Theta_t b^{-\frac{\delta_t}{2}} \left(G_{1,2}^{2,1} \left[\frac{t^2 \alpha\beta}{b\bar{\gamma}_1(\mu\beta+\Omega)} \middle| \begin{matrix} 1-a-\frac{\delta_t}{2} \\ 0, \frac{1}{2} \end{matrix} \right] \right.$$
$$\left. - \frac{2\sqrt{\pi}}{Lm_2} \mathrm{H}_{1,0:0,1:1,0}^{0,1:1,0:0,1} \left[\frac{4t^2\alpha\beta}{b\bar{\gamma}_1(\mu\beta+\Omega)}, \frac{1}{b\bar{\gamma}_2 a_K} \middle| \begin{matrix} (1-a-\frac{\delta_t}{2}, 1, 1) \\ - \end{matrix} \middle| \begin{matrix} - \\ (0,2) \end{matrix} \middle| \begin{matrix} (1, \frac{1}{Lm_2}) \\ - \end{matrix} \right] \right). \quad (4.34)$$

---

where, the first integral on the R.H.S of (4.35) is solved by resorting to [30, Eq.(3.462.1)], however, the second integral on the R.H.S can be derived by means of using [36, Eqs.(2.1.3) and (2.1.4)] and [32, Eq.(2.2)] with some additional algebraic manipulations. □

4.6 Performance Analysis in the Presence of Pointing Errors

In this section, we investigate the effect of pointing error due to source-relay misalignment. Therefore, the resulted received irradiance is a product of two independent random variables, i.e., $I_r = I_m I_p$, where I_m is the atmospheric-turbulence induced fading and I_p is the pointing errors impairments characterized by the following PDF

$$f_{I_p}(x) = \frac{\xi^2}{A_0^{\xi^2}} x^{\xi^2-1}, \quad 0 \leqslant x \leqslant A_0, \quad (4.36)$$

where ξ is the ratio between the equivalent beam radius at the relay and the pointing error displacement standard deviation (jitter) and A_0 is the fraction of the collected power at radial distance equal to 0.

4.6.1 Ergodic capacity

Capitalizing on the ergodic capacity framework presented in the previous section, we investigate the effect of pointing errors on the system performance.

To this end, conditioned on I_p, the ergodic capacity in the presence of pointing errors can be written as

$$C^P = \frac{I_p}{2\ln(2)} \int_0^\infty s e^{-s} M_{\gamma^{FSO}}^{(c)}(I_p s) M_{\gamma^{RF}}^{(c)}(s) ds. \quad (4.37)$$

$$C = \frac{1}{2\ln(2)} \sum_{t=1}^{M} \sum_{\Upsilon} \Theta_t \xi^2 A_0^{-\frac{\delta_t}{2}} \left(G_{4,2}^{1,4}\left[\frac{\bar{\gamma}_1 A_0 (g\beta+\Omega)}{t^2 \alpha\beta} \,\middle|\, \begin{matrix} \frac{\delta_t}{2}+1-\xi^2, \frac{\delta_t}{2}+1, 1, \frac{1}{2} \\ \frac{\delta_t}{2}+1, \frac{\delta_t}{2}-\xi^2 \end{matrix} \right] \right.$$
$$\left. - (1+a_K\bar{\gamma}_2)^{\frac{\delta_t}{2}} G_{4,2}^{1,4}\left[\frac{\bar{\gamma}_1 A_0 (g\beta+\Omega)}{t^2 \alpha\beta(1+a_K\bar{\gamma}_2)} \,\middle|\, \begin{matrix} \frac{\delta_t}{2}+1-\xi^2, \frac{\delta_t}{2}+1, 1, \frac{1}{2} \\ \frac{\delta_t}{2}+1, \frac{\delta_t}{2}-\xi^2 \end{matrix} \right] \right). \quad (4.39)$$

Corollary 9 (Capacity for large M and K with pointing errors)**.** In the presence of pointing errors, the ergodic capacity when M and K grow large is given by

$$C = \frac{A_0\xi^2}{2\ln(2)} \left(G_{3,3}^{1,3}\left[\bar{\gamma}_1 (b_M - c_M) A_0 \,\middle|\, \begin{matrix} -\xi^2, 1, 1 \\ 1, 0, -\xi^2-1 \end{matrix} \right] \right.$$
$$\left. - G_{3,3}^{1,3}\left[\frac{\bar{\gamma}_1 (b_M - c_M) A_0}{1+\bar{\gamma}_2 a_K} \,\middle|\, \begin{matrix} -\xi^2, 1, 1 \\ 1, 0, -\xi^2-1 \end{matrix} \right] \right). \quad (4.38)$$

Proof. Recall that $C = \mathbb{E}_{I_p}[C^P]$, then substituting (4.19) and (4.25) into (4.37) yields the ergodic capacity expression in (4.38) obtained after resorting to $\ln(1+x) = G_{2,2}^{1,2}[x \mid \begin{smallmatrix} 1,1 \\ 1,0 \end{smallmatrix}]$, and applying [30, 7.811.2]. □

Corollary 10 (Capacity for arbitrary M and large K with pointing errors)**.** In the presence of pointing errors, the ergodic capacity for finite-count FSO apertures and large K is given by (4.39).

Proof. The result follows from substituting (4.12) and (4.25) into (4.37) and averaging over the pointing errors distribution in (4.36) using [30, Eq.7.811.2]. □

In the special case where the FSO link is a single-aperture Gamma-Gamma distributed channel (i.e., $\rho = 1$ and $\Omega = 1$), the capacity of the mixed FSO/RF AF system with interference and pointing errors is reduced to

$$C = \frac{\xi^2}{2\ln(2)} \sum_{k=0}^{\alpha-\beta-\frac{1}{2}} \sum_{p=0}^{\alpha+\beta-k-\frac{3}{2}} \Theta_{k,p} \left(G_{2,4}^{4,1}\left[\frac{\alpha\beta}{\bar{\gamma}_1 A_0} \middle| \begin{matrix} 0, \xi^2+1 \\ \xi^2, 0, \frac{p}{2}, \frac{p}{2}+\frac{1}{2} \end{matrix} \right] \right.$$
$$\left. - G_{2,4}^{4,1}\left[\frac{\alpha\beta\,(1+a_K\bar{\gamma}_2)}{\bar{\gamma}_1 A_0} \middle| \begin{matrix} 0, \xi^2+1 \\ \xi^2, 0, \frac{p}{2}, \frac{p}{2}+\frac{1}{2} \end{matrix} \right] \right), \quad (4.40)$$

where $\Theta_{k,p} = \frac{(\alpha-\beta-\frac{1}{2}+k)!(\alpha+\beta-k-\frac{3}{2})! 2^{\frac{3}{2}-\alpha-\beta-k+p}}{\Gamma(\alpha)\Gamma(\beta)(\alpha-\beta-\frac{1}{2}-k)!k!p!}$.

$$\overline{P}_b = \frac{1}{2}-\frac{\xi^2}{2\Gamma(a)}\sum_{t=1}^{M}\sum_{\Upsilon}\Theta_t A_0^{\frac{-\delta_t}{2}}\Bigg(\sum_{q=0}^{\Delta-1}\sum_{m=0}^{\Delta}\frac{\binom{\Delta}{q}}{\binom{\Delta}{m}}\left(\frac{m_1}{m_2\bar{\gamma}_2}\right)^{q-m} b^{m-q-\frac{\delta_t}{2}}$$
$$G_{3,2}^{1,3}\left[\frac{A_0 b\bar{\gamma}_1(\mu\beta+\Omega)}{t^2\alpha\beta}\,\middle|\,\begin{matrix}\frac{\delta_t}{2}+1-\xi^2, 1, \frac{1}{2}\\ a+q-m+\frac{\delta_t}{2}, \frac{\delta_t}{2}-\xi^2\end{matrix}\right]$$
$$+\sum_{r=1}^{K}\sum_{\Upsilon_{r,Lm_2-1}}\sum_{n=0}^{\Delta}\frac{\varphi_r m_1\left(\frac{m_1}{m_2\bar{\gamma}_2}\right)^{\delta_r+\Delta+r(1-Lm_2)-n} b^{n-a-\delta_r-\Delta-r(1-Lm_2)}}{\binom{\Delta}{n} m_2\bar{\gamma}_2\Gamma\left(\delta_r+\Delta+1\right)}$$
$$G_{3,2}^{1,3}\left[\frac{A_0 b\bar{\gamma}_1(\mu\beta+\Omega)}{t^2\alpha\beta}\,\middle|\,\begin{matrix}\frac{\delta_t}{2}+1-\xi^2, 1, \frac{1}{2}\\ a+\delta_r+\Delta+r(1-Lm_2+n), \frac{\delta_t}{2}-\xi^2\end{matrix}\right]\Bigg) \tag{4.42}$$

4.6.2 Average BER

By exploiting the expressions of the average BER in the previous section, this latter can be written in the presence of pointing errors as

$$\overline{P_b}^{P}=\frac{1}{2}-\frac{b^a}{2\Gamma(a)}\int_0^{\infty}x^{a-1}e^{-bx}F_{\gamma^{FSO}}^{(c)}\left(\frac{x}{I_p}\right)F_{\gamma^{RF}}^{(c)}(x)dx. \tag{4.41}$$

Corollary 11 (Average BER for arbitrary M and K with pointing errors)**.** In the presence of pointing errors, the average BER for finite-count FSO apertures and arbitrary number of users K is given by (4.42).

Proof. Recall that $\overline{P}_b = \mathbb{E}_{I_p}\left[\overline{P}_b^{P}\right]$, then plugging (4.12) and (4.15) into (4.41) and averaging over the pointing errors distribution in (4.36) yields the expression in (4.42) after applying [30, Eq.(7.811.2)] along some manipulations. □

Corollary 12 (Average BER for arbitrary M and large K with pointing errors)**.** In the presence of pointing errors, the average BER for finite-count FSO apertures and large K is given by (4.43).

Proof. See Appendix F. □

4.7 Numerical Results

Here, we provide some numerical examples to illustrate the tightness of the closed-form expression of the ergodic capacity and average BER for the mixed FSO/RF AF

$$\overline{P}_b = \frac{1}{2} - \frac{\xi^2}{2\Gamma(a)} \sum_{t=1}^{M} \sum_{\Upsilon} \Theta_t b^{-\frac{\delta_t}{2}} A_0^{-\frac{\delta_t}{2}} \left(G_{3,2}^{1,3} \left[\frac{A_0 b \bar{\gamma}_1 (\mu\beta + \Omega)}{t^2 \alpha\beta} \;\middle|\; \begin{matrix} \frac{\delta_t}{2} + 1 - \xi^2, 1, \frac{1}{2} \\ \frac{\delta_t}{2} + a, \frac{\delta_t}{2} - \xi^2 \end{matrix} \right] \right.$$
$$\left. - \frac{2\sqrt{\pi}}{Lm_2} \mathrm{H}_{10,12,10}^{01,11,01} \left[\frac{4t^2\alpha\beta}{A_0 b \bar{\gamma}_1 (\mu\beta+\Omega)}, \frac{1}{b\bar{\gamma}_2 a_K} \;\middle|\; \begin{matrix} (1 - a - \frac{\delta_t}{2}, 1, 1) \\ - \end{matrix} \middle| \begin{matrix} (1 + \xi^2 - \frac{\delta_t}{2}, 1) \\ (\xi^2 - \frac{\delta_t}{2}, 1)(0, 2) \end{matrix} \middle| \begin{matrix} (1, \frac{1}{Lm_2}) \\ - \end{matrix} \right] \right). \tag{4.43}$$

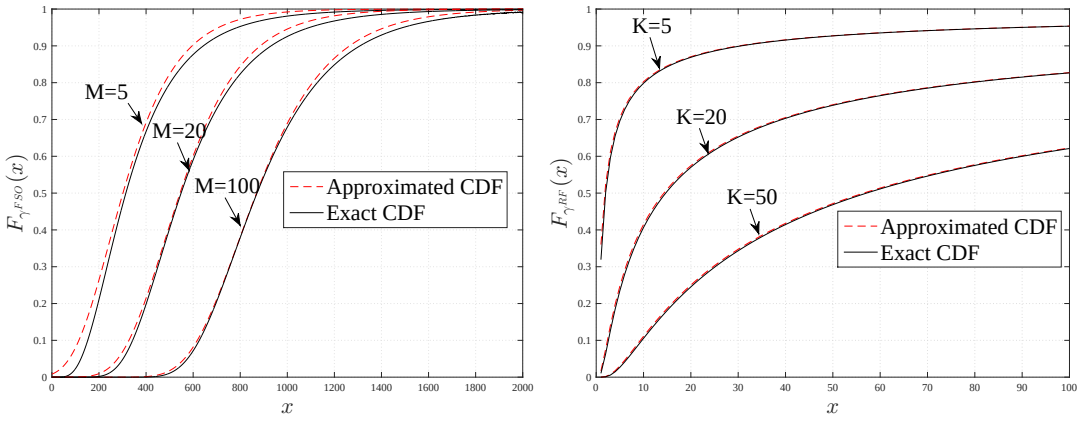

(a) (b)

Fig. 4.2: The exact and approximated CDF of (a): γ^{FSO} for different values of M, and (b): γ^{RF} for different values of K.

relay system. The simulation setup is summarized in the caption of each figure.

Fig. 4.2 shows the exact and asymptotic CDFs of the two hops, γ^{FSO} and γ^{RF} for different values of M and K, respectively. We observe that the asymptotic distributions in (4.23) and (4.27) are a good approximations even for small values of M and K, respectively.

Fig. 4.3(a) depicts the ergodic capacity for large K with fixed and large M using (4.29) and (4.28), respectively. We observe that the analytical curves approach the simulated curves for small to moderate values of K, thereby providing an attractive alternative to the cumbersome expression of the average capacity shown for any K in (4.16).

When M and K grow large, the obtained curves are in very good match with their stimulated counterparts showing the accuracy and effectiveness of the new approximation proposed in (4.28).

Fig. 4.3(b) investigates the effect of the atmospheric turbulence severity ρ on the system performance. As ρ increases, the atmospheric-turbulence over the FSO link

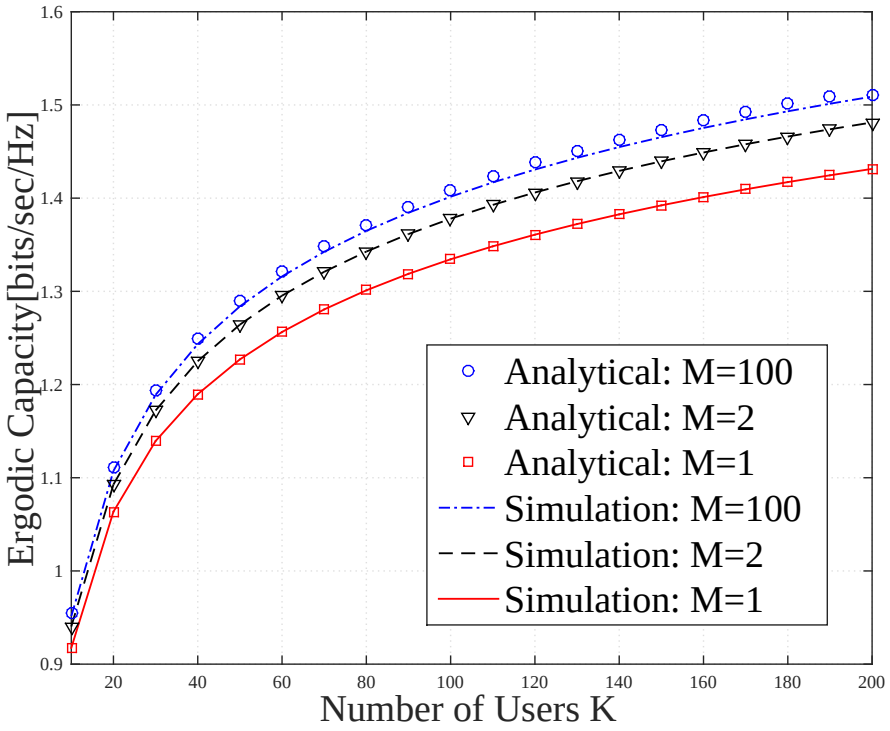

(a) Setup: $\alpha = 3.5$,$\beta = 2$,$\rho = 0.7, \bar{\gamma}_1 = 20$ dB, $m_1 = 3, m_2 = 2, L = 5, \bar{\gamma}_2 =$ 10 dB.

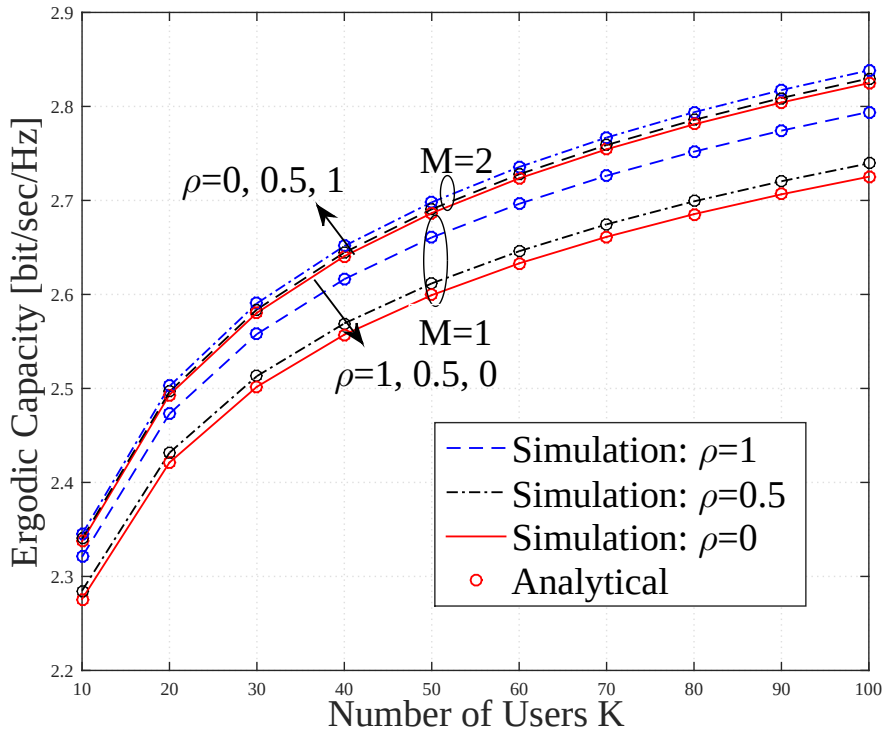

(b) Setup: $\alpha = 3.5, \beta = 2, \bar{\gamma}_1 = 30$ dB, $m_1 = 1, m_2 = 2, L = 2, \bar{\gamma}_2 = 10$ dB.

Fig. 4.3: Ergodic capacity of mixed FSO/RF systems for different values of (a): M, and (b): ρ.

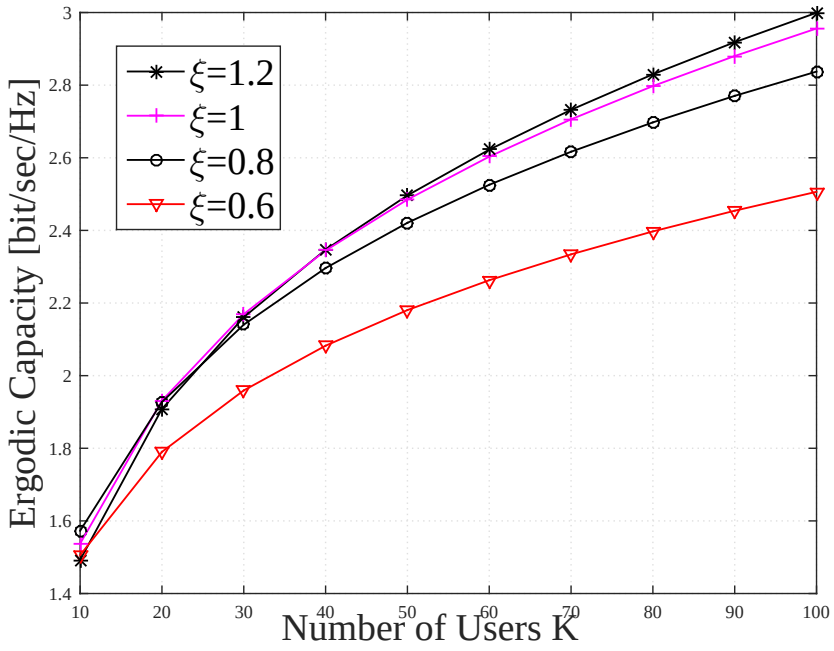

Fig. 4.4: Ergodic Capacity of mixed FSO/RF system with pointing errors for $M = 2$ apertures and different values of ξ. Setup: $\alpha = 3.5, \beta = 2, \rho = 0.5, \bar{\gamma}_1 = 30$ dB, $m_1 = 1, m_2 = 2, \bar{\gamma}_2 = 10$ dB, and $L = 5$.

is reduced thereby leading to better performance.

Fig. 4.4 depicts the ergodic capacity of the mixed FSO/RF AF relay system in the presence of pointing errors using Eq. (4.39) with $M = 2$. The curves are plotted for several values of ξ. As expected, increasing ξ, induces better performance, a behavior also observed in [27] and [38].

Fig.4.5 demonstrates the special case study with single-aperture Gamma-Gamma distributed FSO link with pointing errors. The same behavior is observed as Fig. 4.4 for different pointing errors severity. Furthermore, as the average SNR of the FSO link increases enough, the ergodic capacity of the system seems saturated which can be explained by the fact that the performance is depending on the weaker link (in this case is RF link) in relaying systems.

The average BER performance for NCFSK and CBPSK modulations with different turbulence severity ρ is presented in Fig. 4.6. It is evidently noticed that the analytical curves match perfectly their simulated counterparts. Moreover, it can be implied that as the average SNR of the FSO link increases, the performance of the system in terms of average BER remains the same since it follows the dominant link performance which is the weaker link (RF link) in the case of dual-hop AF relay

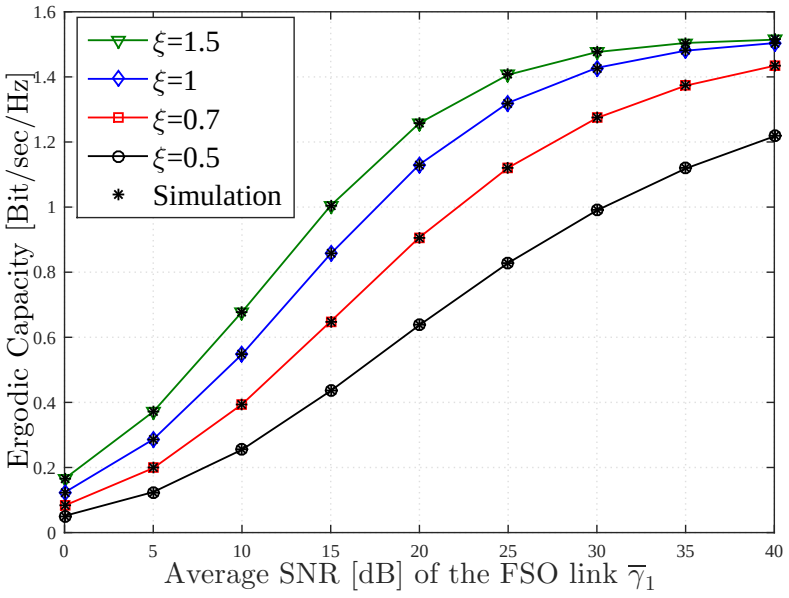

Fig. 4.5: Ergodic Capacity of mixed FSO/RF relay system with single-aperture Gamma-Gamma distributed FSO link (Eq.(4.40)). Setup: $\alpha = 3.5, \beta = 2, m_1 = 3, m_2 = 2, \bar{\gamma}_2 = 10$ dB, $M = 1, K = 200$ and $L = 5$.

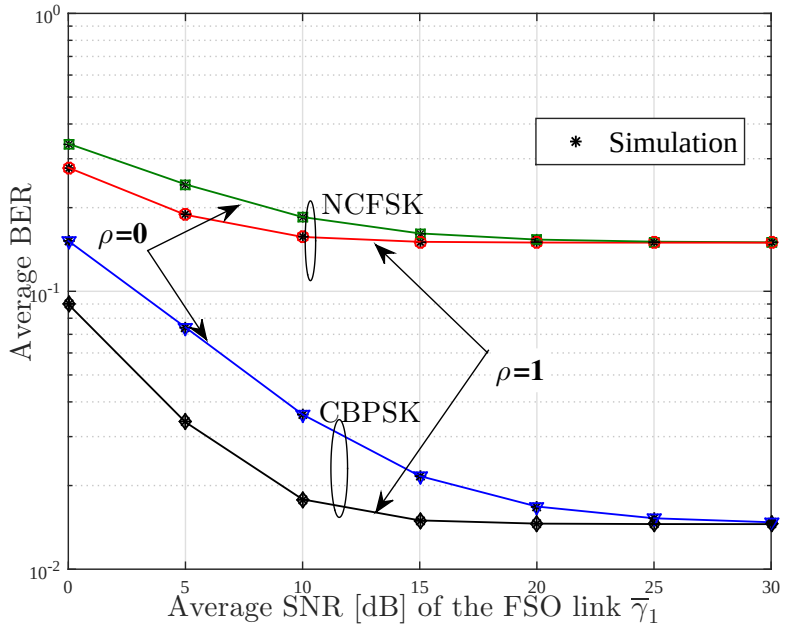

Fig. 4.6: Average BER of mixed FSO/RF relay system with different binary modulations (Eq.(4.34)). Setup: $\alpha = 3.5, \beta = 2, m_1 = 3, m_2 = 2, \bar{\gamma}_2 = 10$ dB, $M = 1, K = 200$ and $L = 5$.

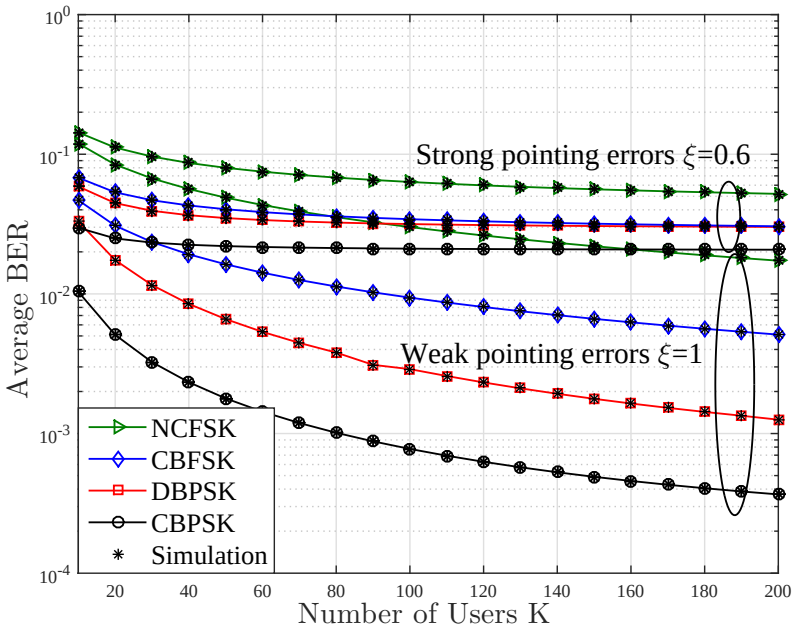

Fig. 4.7: Average BER of mixed FSO/RF relay system with pointing errors for different binary modulation and ξ (Eq.(4.43)). Setup: $M = 2, \alpha = 3.5, \beta = 2, \rho = 0.5, m_1 = 1, m_2 = 2, \bar{\gamma}_1 = 30$ dB, $\bar{\gamma}_2 = 0$ dB and $L = 2$.

system. Furthermore, weaker atmospheric turbulence (higher ρ) guarantee a better overall system's performance.

In Fig. 4.7, the average BER versus the users number K for different binary modulations as well as pointing error's severity is depicted. As conventional, the weaker the pointing errors effect is, the better is the performance of mixed FSO/RF AF relay system. Furthermore, the CBPSK presents the best performance comparing to other modulations independently of the pointing errors' severity.

4.8 Summary

In this chapter, we derived closed-form expressions of the ergodic capacity and the average BER of interference-limited mixed FSO/RF AF relay systems under the assumption of transmit aperture selection at the source and opportunistic scheduling at the destination. The system operates over mixed Málaga/Nakagami-m distributions. The large scale analysis reveals simpler and very accurate results thereby providing an attractive alternative to the cumbersome expression obtained in the case of finite aperture and user counts. The impact of pointing errors was also investigated. The accuracy of the derived expressions were unambiguously illustrated numerically.

Chapter 5

Conclusion

In this work, we introduced a new mathematical framework for the computation of some performance metrics of AF mixed FSO/RF systems. Throughout this thesis, the FSO link is assumed to operate under the generalized statistical model, i.e., the Málaga-$\mathcal{M}$ distribution, that includes the majority of atmospheric turbulence-induced fading channels. Furthermore, our study accounts for both detection techniques, i.e., heterodyne and IM/DD. We assumed also a generalized channel model at the RF link, the κ-μ shadowed fading, that encompasses the most common RF models such as Nakagami-m and Rice. We were able to derive the exact end-to-end outage probability and expressions, both in terms of FHF and bivariate FHF, respectively. Then, we emphasize these performance metrics in addition to average BER in interference-limited AF mixed FSO/RF experiencing Málaga/generalized-$\mathcal{K}$ channels while investigating both fixed and variable-gain relaying schemes. Some interesting and attractive asymptotic results were provided at high SNR regime as an alternative of the cumbersome exact close-form expressions. Finally, we examined the MIMO technology in the context of AF mixed FSO/RF systems. More interestingly, large-scale analysis, when the number of users and/or apertures goes large, were provided as an alternative to the finite-counts heavy capacity's and average BER's closed-form expressions.

In this work, due to the complexity of the PDF of the Málaga-$\mathcal{M}$ and shadowed κ-μ fading distributions, some difficulties have been faced during the computation of some of the key performances measures. For instance, the H-function and the bivariate FHF are not a built-in functions in Mathematica® and they are not integrated in any other software, thus, we were aware of the adjustment of the integration range to ensure that these functions will converge properly to the exact and accurate results.

Future work will investigate the possibility of including maximum ratio transmit

(MRT) and user scheduling in mixed multi aperture/multiuser FSO/RF operating over Málaga-$\mathcal{M}$ and shadowed κ-μ fading while assuming co-channel interference at each user. These advanced system setting incorporates almost the most innovative features investigated in mixed FSO/RF system so far, namely, multi aperture at the FSO link, multi user at the RF link, existence of the co-channel interference at the RF user while accounting for the most generalized distributions discovered for both FSO and RF links.

APPENDICES

A Ergodic Capacity at high SNR

Recall the closed-form expression of the capacity for $\mu \leqslant m$ that is given by

$$C = \frac{\xi^2 A r \mu_r B^{-r}}{2\ln(2)\Gamma(\alpha)} \sum_{k=1}^{\beta} \frac{b_k}{\Gamma(k)} \sum_{l=1}^{m} \frac{\chi_l}{\Gamma(m)} T(\theta_2, l, m), \tag{A.1}$$

where $T(\theta_2, l, m)$ can be rewritten as

$$\begin{aligned}
T(\theta_2, l, m) &= \mathrm{H}_{10:43:11}^{01:14:11}\left[\begin{array}{c|c} \frac{\mu_r}{B^r} & (-l,1,1) \\ & - \\ \theta_2 & (1-r,r),(1-\xi^2-r,r),(1-\alpha-r,r),(1-k-r,r) \\ & (0,1),(-\xi^2-r,r),(-r,r) \\ & (1-m,1) \\ & (0,1) \end{array}\right] \\
&\overset{(a)}{=} \frac{1}{4\pi^2 i^2} \int_{\mathcal{C}_1}\int_{\mathcal{C}_2} \frac{\Gamma(r+rs)\Gamma(\xi^2+r+rs)\Gamma(\alpha+r+rs)\Gamma(-s)}{\Gamma(1+\xi^2+r+rs)\Gamma(1+r+rs)} \\
&\quad \Gamma(k+r+rs)\Gamma(m+t)\Gamma(-t)\Gamma(1+l+s+t)\left(\frac{\mu_r}{B^r}\right)^s \theta_2^t \mathrm{d}s\mathrm{d}t \\
&\overset{(b)}{=} \frac{1}{2\pi i} \int_{\mathcal{C}_1} \frac{\Gamma(r+rs)\Gamma(\xi^2+r+rs)\Gamma(\alpha+r+rs)\Gamma(k+r+rs)\Gamma(-s)}{\Gamma(1+\xi^2+r+rs)\Gamma(1+r+rs)} \\
&\quad \mathrm{G}_{1,2}^{2,1}\left[\theta_2^{-1}\middle| \begin{array}{c} 1 \\ 1+l+s, m \end{array}\right] \left(\frac{\mu_r}{B^r}\right)^s \mathrm{d}s,
\end{aligned} \tag{A.2}$$

where (a) follows from explicitly expressing the bivariate FHF in its Mellin-Barnes integral form using [34, Eq.(2.56)] and (b) follows from rewriting all the terms in t as a Meijer-G function by means of [34, Eq.(1.112)]. Moreover in (A.2), $i^2 = -1$, and $\mathcal{C}_1$ and $\mathcal{C}_2$ denote the s and t-planes counters, respectively.

Since $\bar{\gamma}_2 \to +\infty$, it follows that $\theta_2^{-1} \to 0$. the Meijer-G function has an asymptotic series expansion at zero equal to

$$\mathrm{G}_{p,q}^{m,n}\left[z\middle| \begin{array}{c} a_1,\ldots,a_n,\ldots,a_p \\ b_1,\ldots,b_m,\ldots,b_q \end{array}\right] \to \sum_{k=1}^{m} \frac{\prod_{j=1,j\neq k}^{m}\Gamma(b_j-b_k)\prod_{j=1}^{n}\Gamma(1-a_j+b_k)}{\prod_{j=n+1}^{p}\Gamma(a_j-b_k)\prod_{j=m+1}^{q}\Gamma(1-b_j+b_k)} z^{b_k}, \tag{A.3}$$

with the assumption of $p \leqslant q$ and $z \to 0$. Applying (A.3) to the Meijer-G in (A.2)

yields

$$\mathrm{G}_{1,2}^{2,1}\left[\theta_2^{-1}\middle|\begin{matrix}1\\1+l+s,m\end{matrix}\right] \tag{A.4}$$
$$\underset{\theta_2^{-1}\to 0}{=} \Gamma(m-1-l-s)\Gamma(1+l+s)\theta_2^{-1-l-s}+\Gamma(1+l+s-m)\Gamma(m)\theta_2^{-m}.$$

Finally, plugging (A.4) into (A.2) and resorting to [34, Eq.(1.2)] complete the proof.

B End-to-End SNR's CDF

The CDF of the end-to-end SINR γ with fixed-gain relaying scheme can be derived, using [42, Eq.(8)], as

$$F_{\gamma}(x) = \int_0^{\infty} F_{\gamma_1}\left(x\left(\frac{\mathrm{C}}{y}+1\right)\right) f_{\gamma_2}(y)\mathrm{d}y, \tag{B.1}$$

where F_{γ_1} and f_{γ_2} are the FSO link's CDF and the PDF of RF link, respectively. More specifically, F_{γ_1} can be obtained similarly to (2.8) as

$$F_{\gamma_1}(x) = \frac{\xi^2 A r}{\Gamma(\alpha)} \sum_{k=1}^{\beta} \frac{b_k}{\Gamma(k)} \mathrm{H}_{2,4}^{3,1}\left[\frac{B^r x}{\mu_r}\middle| \begin{matrix}(1,r),(\xi^2+1,r)\\(\xi^2,r),(\alpha,r),(k,r),(0,r)\end{matrix}\right], \tag{B.2}$$

and f_{γ_2} is derived by differentiation over x as

$$f_{\gamma_2}(x) = \frac{-\kappa m}{\Gamma(Nm)\Gamma(\kappa)\Gamma(Lm_I)\Gamma(\kappa_I)\kappa_I m_I \bar{\gamma}_2} \mathrm{G}_{4,4}^{3,3}\left[\frac{\kappa m x}{\kappa_I m_I \bar{\gamma}_2}\middle| \begin{matrix}-1,-\kappa_I,-Lm_I,0\\-1,\kappa-1,Nm-1,0\end{matrix}\right]. \tag{B.3}$$

Substituting (B.2) and (B.3) into (B.1) while resorting to the integral representation of the Fox-H [34, Eq.(1.2)] and Meijer-G [30, Eq.(9.301)]functions yields

$$\begin{aligned} F_{\gamma}(x) \;=\; & \frac{-\xi^2 A r \kappa m}{\Gamma(\alpha)\Gamma(Nm)\Gamma(\kappa)\Gamma(Lm_I)\Gamma(\kappa_I)\kappa_I m_I \bar{\gamma}_2} \sum_{k=1}^{\beta} \frac{b_k}{\Gamma(k)} \frac{1}{4\pi^2 i^2} \int_{\mathcal{C}_1}\int_{\mathcal{C}_2} \\ & \frac{\Gamma(\xi^2+rs)\Gamma(k+rs)\Gamma(\alpha+rs)\Gamma(-rs)}{\Gamma(\xi^2+1+rs)\Gamma(1-rs)} \frac{\Gamma(-1-t)}{\Gamma(1+t)} \\ & \times \frac{\Gamma(\kappa-1-t)\Gamma(Nm-1-t)\Gamma(1+\kappa_I+t)\Gamma(1+Lm_I+t)\Gamma(2+t)}{\Gamma(-t)} \\ & \times \left(\frac{B^r x}{\mu_r}\right)^{-s} \left(\frac{\kappa m}{\kappa_I m_I \bar{\gamma}_2}\right)^{t} \int_0^{\infty} \left(1+\frac{\mathrm{C}}{y}\right)^{-s} y^t \mathrm{d}y \; \mathrm{d}s \; \mathrm{d}t. \end{aligned} \tag{B.4}$$

Finally, simplifying $\int_0^{\infty}\left(1+\frac{\mathrm{C}}{y}\right)^{-s} y^t \mathrm{d}y$ to $\frac{\mathrm{C}^{1+t}\Gamma(-1-t)\Gamma(1+t+s)}{\Gamma(s)}$ by means of [30, Eqs(8.380.3) and (8.384.1)] while utilizing the relations $\Gamma(1-rs) = -rs\Gamma(-rs)$ and $s\Gamma(s) = \Gamma(1+s)$ then [32, Eq.(1.1)], yield directly (3.6).

C Average BER for Fixed-Gain Relaying

The average BER can be rewritten as

$$\begin{aligned}\overline{P}_e &\overset{(a)}{=} \frac{\delta}{2\Gamma(p)}\frac{-\xi^2 A\kappa m\mathrm{C}}{\Gamma(\alpha)\Gamma(Nm)\Gamma(\kappa)\Gamma(Lm_I)\Gamma(\kappa_I)\kappa_I m_I\bar{\gamma}_2}\frac{1}{4\pi^2 i^2}\sum_{j=1}^{n}\sum_{k=1}^{\beta}\\ &\times\int_{\mathcal{C}_1}\int_{\mathcal{C}_2}\frac{b_k}{\Gamma(k)}\frac{\Gamma(\xi^2+rs)\Gamma(k+rs)\Gamma(\alpha+rs)}{\Gamma(\xi^2+1+rs)\Gamma(s)}\frac{\Gamma^2(-1-t)}{\Gamma(1+t)}\\ &\times\frac{\Gamma(\kappa-1-t)\Gamma(Nm-1-t)\Gamma(1+\kappa_I+t)\Gamma(1+Lm_I+t)\Gamma(2+t)}{\Gamma(-t)}\Gamma(1+t+s)\\ &\times\left(\frac{\mu_r}{B^r}\right)^s\left(\frac{\kappa m\mathrm{C}}{\kappa_I m_I\bar{\gamma}_2}\right)^t\int_0^\infty x^{-s-1}\Gamma(p,q_j x)\mathrm{d}x\ \mathrm{d}s\ \mathrm{d}t,\end{aligned} \tag{C.1}$$

where (a) follows after substituting (3.7) into (3.12) by means of [34, Eq.(2.56)]. Using the identity $\Gamma(a,bx)=\mathrm{G}_{1,2}^{2,0}[bx|\ {}^{1}_{0,a}]$ and [30, Eq.(7.811.4)], we obtain

$$\int_0^\infty x^{-s-1}\mathrm{G}_{1,2}^{2,0}\left[q_j x\middle|\begin{matrix}1\\0,p\end{matrix}\right]\mathrm{d}x=\frac{\Gamma(-s)\Gamma(p-s)}{\Gamma(1-s)}q_j^s. \tag{C.2}$$

Inserting (C.2) into (C.1) along some algebraic manipulations yields (3.13).

D Ergodic Capacity under CSI-assisted Relaying Scheme

Form [31], the ergodic capacity can be computed as

$$C = \frac{1}{2\ln(2)} \int_0^\infty s e^{-s} M_{\gamma_1}^{(c)}(s) M_{\gamma_2}^{(c)}(s) ds, \tag{D.1}$$

where $M_X^{(c)}(s) = \int_0^\infty e^{-sx} F_X^{(c)}(x) dx$ stands for the complementary MGF (CMGF).

The unified CMGF of the first hop's SNR γ_1 under Málaga-$\mathcal{M}$ distribution with pointing errors was shown in (2.9) to be equal to

$$M_{\gamma_1}^{(c)}(s) = \frac{\xi^2 A r \mu_r}{\Gamma(\alpha) B^r} \sum_{k=1}^{\beta} \frac{b_k}{\Gamma(k)} \mathrm{H}_{4,3}^{1,4} \left[\frac{\mu_r}{B^r} s \middle| \begin{matrix} (1-r,r), (1-\xi^2-r,r), (1-\alpha-r,r), (1-k-r,r) \\ (0,1), (-\xi^2-r,r), (-r,r) \end{matrix} \right]. \tag{D.2}$$

Moreover, the Laplace transform of the RF link's CCDF is derived after resorting to [30, Eq.(7.813.1)] and [34, Eq.(1.111)] as

$$M_{\gamma_2}^{(c)}(x) = \frac{s^{-1}}{\Gamma(Nm)\Gamma(\kappa)\Gamma(Lm_I)\Gamma(\kappa_I)} \mathrm{H}_{3,4}^{3,3} \left[\frac{\kappa_I m_I \bar{\gamma}_2}{\kappa m} s \middle| \begin{matrix} (1,1), (1-\kappa,1), (1-Nm,1) \\ (1,1), (\kappa_I,1), (Lm_I,1), (0,1) \end{matrix} \right]. \tag{D.3}$$

Finally, the ergodic capacity expression in (3.25) follows after plugging (D.2) and (D.3) into (D.1) and applying [32, Eq.(2.2)].

E Average BER for large M and K

Substituting (4.23) and (4.27) into (4.30) with the assumption of $a = 1$, we obtain

$$\begin{aligned}
\overline{P_b} &= \frac{1}{2} - \frac{b}{2}\int_0^\infty e^{-bx}\left(1 - e^{-e^{-\frac{x-\bar{\gamma}_1 b_M}{\bar{\gamma}_1 c_M}}}\right)\left(1 - e^{-\left(\frac{x}{\bar{\gamma}_2 a_K}\right)^{-Lm_2}}\right)dx \\
&\overset{(a)}{=} \frac{1}{2} - \frac{b}{2Lm_2} \\
&\times\Bigg[\underbrace{\int_0^{\frac{4}{\epsilon}} y^{-1-\frac{1}{Lm_2}} e^{-by^{-1/Lm_2}}\left(1 - e^{-e^{-\frac{y^{-1/Lm_2}-\bar{\gamma}_1 b_M}{\bar{\gamma}_1 c_M}}}\right)\left(1 - e^{-\epsilon y}\right)dy}_{\text{goes to 0 when } \epsilon \text{ goes large (i.e., } K \text{ goes large)}} \\
&\quad + \int_{\frac{4}{\epsilon}}^\infty y^{-1-\frac{1}{Lm_2}} e^{-by^{-1/Lm_2}}\left(1 - e^{-e^{-\frac{y^{-1/Lm_2}-\bar{\gamma}_1 b_M}{\bar{\gamma}_1 c_M}}}\right)dy\Bigg] \\
&\overset{(b)}{=} \frac{1}{2} - \frac{b}{2}\left[\int_0^{\frac{a_K\bar{\gamma}_2}{4^{1/Lm_2}}} e^{-bz}dz - \int_0^{\frac{a_K\bar{\gamma}_2}{4^{1/Lm_2}}} e^{-bz}e^{-e^{-\frac{z-\bar{\gamma}_1 b_M}{\bar{\gamma}_1 c_M}}}dz\right],
\end{aligned} \tag{E.1}$$

where (a) follows from letting $y = x^{-Lm_2}$ and defining $\epsilon = (\bar{\gamma}_2 a_K)^{Lm_2}$, and (b) follows from letting $z = y^{-1/Lm_2}$. The second integral on the R.H.S of (b) is obtained by approximating $a_K\bar{\gamma}_2/4^{1/Lm_2} \sim \infty$ when $K \to \infty$. The result in (4.33) follows after applying [30, Eq.(3.333.2)] with some additional manipulations.

F Average BER for Fixed M and Large K with Pointing Errors

The average BER conditioned on I_p for arbitrary M and large K in mixed FSO/RF AF relay system with interference is written as

$$\begin{aligned}\overline{P}_b^P =& \frac{1}{2} - \frac{1}{2\Gamma(a)} \sum_{t=1}^{M} \sum_{\Upsilon_{t\beta}} \sum_{\Upsilon_{t_p,\alpha-t_p+\frac{1}{2}}} \sum_{\Upsilon_{t_{pq}\alpha+t_p-t_{pq}-\frac{1}{2}}} \Theta_t b^{-\frac{\delta_t}{2}} I_p^{-\frac{\delta_t}{2}} \\ &\times \Bigg(G_{1,2}^{2,1}\left[\frac{t^2\alpha\beta}{I_p b\bar{\gamma}_1(\mu\beta+\Omega')} \middle| \begin{matrix} 1-a-\frac{\delta_t}{2} \\ 0, \frac{1}{2} \end{matrix} \right] - \frac{2\sqrt{\pi}}{Lm_2} H_{10,01,10}^{01,10,01} \\ &\left[\frac{4t^2\alpha\beta}{I_p b\bar{\gamma}_1(\mu\beta+\Omega')}, \frac{1}{b\bar{\gamma}_2 a_K} \middle| \begin{matrix} (1-a-\frac{\delta_t}{2}, 1, 1) \\ - \end{matrix} \middle| \begin{matrix} - \\ (0,2) \end{matrix} \middle| \begin{matrix} (1, \frac{1}{Lm_2}) \\ - \end{matrix} \right] \Bigg).\end{aligned} \tag{F.1}$$

Furthermore, based on the representation of the bivariate H-Fox function in [32, Eq.(1.1)] in terms of integrals, we can rewrite the bivariate H-Fox in the R.H.S of (F.1) as

$$\begin{aligned} I_p^{-\frac{\delta_t}{2}} H_{10,01,01}^{01,10,10}&\left[\frac{4t^2\alpha\beta}{I_p b\bar{\gamma}_1(\mu\beta+\Omega')}, \frac{1}{b\bar{\gamma}_2 a_K} \middle| \begin{matrix} (1-a-\frac{\delta_t}{2}, 1, 1) \\ - \end{matrix} \middle| \begin{matrix} - \\ (0,2) \end{matrix} \middle| \begin{matrix} (1, \frac{1}{Lm_2}) \\ - \end{matrix} \right] = \frac{I_p^{-\frac{\delta_t}{2}}}{(2\pi i)^2} \int_{\mathcal{C}_1}\int_{\mathcal{C}_2} \Gamma\left(a+\frac{\delta_t}{2}+s+t\right)\Gamma(-2s)\Gamma\left(\frac{t}{Lm_2}\right) \\ &\times \left(\frac{4t^2\alpha\beta}{I_p b\bar{\gamma}_1(\mu\beta+\Omega')}\right)^s \left(\frac{1}{b\bar{\gamma}_2 a_K}\right)^t ds\ dt, \end{aligned} \tag{F.2}$$

where $\mathcal{C}_1$ and $\mathcal{C}_2$ are the s-plane and the t-plane contours, respectively. Averaging (F.2) over pointing errors, the integral may be written as

$$\begin{aligned} &\frac{\xi^2}{A_0^{\xi^2}(2\pi i)^2} \int_{\mathcal{C}_1}\int_{\mathcal{C}_2} \Gamma\left(a+\frac{\delta_t}{2}+s+t\right)\Gamma(-2s)\Gamma\left(\frac{t}{Lm_2}\right)\left(\frac{1}{b\bar{\gamma}_2 a_K}\right)^t \\ &\times \left(\frac{4t^2\alpha\beta}{b\bar{\gamma}_1(\mu\beta+\Omega')}\right)^s \int_0^{A_0} x^{-\frac{\delta_t}{2}+\xi^2-1-s} dx\ ds\ dt. \end{aligned} \tag{F.3}$$

$\int_0^{A_0} x^{-\frac{\delta_t}{2}+\xi^2-1-s} dx$ simplifies to $\frac{A_0^{\xi^2-s-\frac{\delta_t}{2}}}{\xi^2-\frac{\delta_t}{2}-s}$, and by utilizing the relation $(\xi^2-\frac{\delta_t}{2}-s)\Gamma(\xi^2-\frac{\delta_t}{2}-s) = \Gamma(1+\xi^2-\frac{\delta_t}{2}-s)$ then [32, Eq.(1.1)], we obtain the desired BER in (4.43) after applying [30, Eq.(7.811.2)] to the first term of the R.H.S of (F.1) with some additional algebraic manipulations.

G Annexe: Récapitulatif des Travaux de mémoire

Résumé

Conduit par la forte demande des hauts débits de données et la croissance exponentielle des dispositifs sans fil, la technologie de la transmission du laser dans l'espace libre connu sous le nom 'free-space optics' (FSO) est présentée comme un candidat fort et fiable pour les réseaux cellulaires mobiles de la prochaine génération. En plus de sécuriser un débit très élevé et des services de données à grande vitesse, la technologie FSO est une approche rentable, facile à déployer, et qui offre une forte immunité aux interférences. En dépit de ces avantages, la transmission du FSO est entravée par des défaillances et des erreurs de pointage induites par la turbulence atmosphérique. Ces contraintes ont limité la transmission FSO à des petites distances. Pour élargir la couverture et assurer la fiabilité du lien FSO pour les réseaux backhaul cellulaires de nouvelle génération, les systèmes mixtes FSO/RF (radio-fréquence) assistés par un relais ont suscité un très grand intérêt durant les dernières années. L'objectif principal de ce travail est d'étudier les performances de bout-en-bout du système mixte FSO/RF assisté par un relais. Dans ce but, nous avons dérivé des expressions exactes, pour la capacité ergodique et la probabilité de coupure, qui unifient presque toutes les distributions linéaires du turbulence/évanouissement découvertes

jusqu'au présent tout en tenant compte des techniques de détection hétérodyne et modulation d'intensité/détection directe (IM/DD). L'originalité de ce travail repose sur la consolidation de deux modèles généralisées de canaux sans fil pour les liens FSO et RF. En outre, les expressions dérivées, en fonction de la fonction Fox-H de deux variable, sont exactes et précises puisque aucune approximation n'a été utilisée. En outre, nous présumons l'existence de l'interférence co-canal dans chaque utilisateur RF dans le système mixte FSO/RF . Dans ce modèle de système, nous avons dérivé des expressions exactes des métriques de performance de bout-en-bout, c'est-à-dire la probabilité de coupure, le taux d'erreur binaire moyen (BER) et la capacité ergodique, en termes de FHF de deux variables. L'exhaustivité de notre travail est soulignée grâce à la considération des mécanismes de relais à gain fixe et à gain variable et à l'association des techniques de détection hétérodyne et IM/DD. Motivé par les résultats obtenus, nous menons une autre étude pour étudier l'effet de la diversité spatiale sur la performance du système en considérant un système mixtes FSO/RF multi-ouverture/multi-utilisateur. En outre, nous avons étudié les performances à grande échelle d'un tel système. La diversité spatiale résultant de l'utilisation de la transmission du ratio maximal (MRT) lors de la liaison FSO multi-ouverture et la planification opportuniste des utilisateurs pour la liaison RF multi-utilisateurs a en-

core amélioré la performance en atténuant les effets de la turbulence, des erreurs de pointage et de l'évanouissement dans le systèmes mixtes FSO/RF.

Contexte du travail

La prolifération des services et des dispositifs sans fil marque le phénomènes le plus bouleversant dans la vie contemporaine. La croissance exponentielle des utilisateurs mobiles au cours des dernières années conjointement avec la forte demande des hauts débits de données présentent une tâche difficile pour l'architecture existante de la communication sans fil où le backhaul cellulaire est requis de fournir un lien fiable avec des services de données à haute vitesse [1]. Plus précisément, le lien de backhaul cellulaire se compose de stations de base, de contrôleur de réseau radio et de contrôleurs de stations de base [1], [2]. En outre, le backhaul cellulaire est le composant le plus coûteux de l'architecture d'un réseau sans fil avec plus de trois quart du coût de déploiement total du réseau [1]. Ainsi, c'est un besoin urgent et un facteur clé pour la prochaine génération de communication sans fil de réduire le coût de déploiement du backhaul cellulaire tout en proposant des services de données à haut débit et de haute vitesse [2].

La majorité des réseaux backhaul cellulaire traditionnels comptent aujourd'hui

sur des supports de cuivre qui s'expliquent par le fait que les opérateurs tentent de maintenir l'architecture existante pour économiser le coût du déploiement d'une nouvelle architecture [2]. Le backhaul cellulaire à fibre optique a été rarement utilisé dans l'architecture actuelle du réseau en raison du coût élevé de l'investissement initial pour remplacer les liaisons de cuivre par ses homologues de fibres optiques, en particulier dans les océans profonds et sur les terrains difficiles [2]. Le point commun entre le backhaul cellulaire à base cuivre ou de fibres optiques est son caractère câblé. Récemment, un nouveau système de backhaul cellulaire sans fil, FSO, a été introduit comme un candidat intéressant pour les réseaux cellulaires de la prochaine génération afin de fournir un débit de données élevé tout en étant une architecture rentable [3–9].

Le FSO fait référence à la transmission de faisceaux laser à travers des supports optiques, c'est-à-dire des bandes infrarouges (IR) et ultraviolets (UV) [10]. Étant donné que la transmission FSO nécessite une ligne de vision directe entre l'émetteur optique et le récepteur optique, elle garantie une haute sécurité et une grande immunité aux interférences dans le spectre non-régularisé (au-delà de 300 Ghz) par rapport à la transmission par radio fréquence traditionnelle (RF) [10]. Basé sur la transmission des faisceaux laser étroits, la technologie FSO permet des vitesses élevées dans le le spectre non-régularisé. Une autre caractéristique attrayante de la technologie FSO

est sa rentabilité du fait que son déploiement ne nécessite aucune réglementation ou licenciement auprès des organismes gouvernementaux [10]. En outre, la propriété sans fil du lien FSO rend son déploiement facile à l'inverse aux liaisons à base de fibres optiques ou de cuivre qui nécessitent plus de temps pour leur implémentation [4]. Le FSO est considéré comme une technologie révolutionnaire car elle permet une transmission cellulaire sans fil de bout-en-bout [5].

Contrairement à la transmission RF, le lien FSO fournit des débits de données très élevés et une forte immunité aux interférences dans la bande passante Terahertz entre autres [7], [8], [11]. Cependant, bien que tous les avantages que la technologie FSO présente, la transmission FSO est inhibée par la faiblesse de la fiabilité de son lien, en particulier dans des longues distances en raison dela turbulence atmosphérique et de sa grande sensibilité aux conditions météorologiques [12–15]. Plus précisément, les fluctuations de la pluie, du brouillard et de la température affectent directement la transmission FSO et entraînent un lien moins fiable et, par conséquent, une grave dégradation des performances. En outre, l'écart du faisceau par rapport à son chemin d'origine provoqué par des catastrophes naturelles entraîne une nouvelle détérioration de la performance du lien FSO [16]. Ce désalignement est largement référencé dans la littérature comme des erreurs de pointage [16]. Ces principales faiblesses de la

liaison FSO, à savoir les erreurs de pointage et la turbulence atmosphérique, affectent gravement la qualité du lien du FSO [10].

La modélisation des canaux de la turbulence atmosphérique a été largement étudiée dans la littérature [15], [17], où les distributions lognormal et Gamma-Gamma sont les plus répandues pour caractériser le lien FSO [15]. La distribution lognormal est un modèle de canal efficace uniquement dans des conditions de turbulence faibles. Cependant, le modèle Gamma-Gamma convient aux fluctuations atmosphériques à petite et grande échelle. Récemment, Navas et al [18] ont dérivé un nouveau modèle statistique généralisé pour les communications optiques sans fil, connu sous le nom de la distribution Málaga-$\mathcal{M}$, unifie presque tous les modèles de canaux FSO existants dans la littérature découverte jusqu'au présent. La distribution statistique Málaga-$\mathcal{M}$ est un modèle polyvalent avec sa capacité à refléter une large gamme de fluctuations optiques et offre une traçabilité mathématique attrayante pour l'analyse de performance [18], [19].

Les systèmes mixtes FSO/RF dans la littérature

La couverture à courte distance, les erreurs induites par la turbulence et les erreurs de pointage peuvent causer sérieusement la panne et l'échec du lien FSO. Dans une

tentative de dépassement de toutes les contraintes listées, le système mixte de communication FSO/RF assisté par un relais, où un lien fonctionne avec la technologie FSO, et l'autre lien de transmission est RF, a suscité un vif intérêt pendant les très récentes années [20–23]. Le système mixte de relais FSO/RF est une solution efficace pour étendre la couverture du FSO, pour améliorer les performances du système lorsque le lien FSO devient inopérant [24], [25] et pour combler la connectivité entre le backhaul cellulaire (FSO) Et le réseau d'accès RF. De nombreuses tentatives ont été faites pour étudier la performance de bout-en-bout des systèmes mixtes FSO/RF en supposant une variété de distributions de canaux FSO et RF et en utilisant des techniques de détection hétérodyne et IM/DD [24], [25]. Il est intéressant de noter que les schémas de relais de gain fixe et variable ont été largement pris en compte dans la ligne de recherche sur les systèmes mixte FSO/RF. Tout le travail qui a été réalisé dans ce domaine suppose toujours des modèles restrictifs de turbulences et de fading [20–25]. Par exemple, Gamma-Gamma et Nakagami- m sont les distributions les plus considérées pour les liaisons FSO et RF, respectivement, dans les systèmes mixtes FSO/RF assistés par relais [24], [25].

Principales Contributions dans cette Mémoire

Les principales contributions de ce travail par rapport aux efforts existants dans la littérature peuvent être résumées dans les points suivants:

- Nous avons pu fournir une expression mathématique exacte de certaines métriques de performance (probabilité de coupure et capacité ergodique) du système mixte FSO/RF dont les modèles des canaux FSO et RF sont les plus généralisés, c'est-à-dire Málaga-$\mathcal{M}$ et shadowed κ-μ fading, respectivement, sous les deux techniques de détection hétérodyne et IM/DD. L'analyse de performance est valable pour toutes les distributions linéaires de turbulence/évanouissement dérivées jusqu'au présent. Aucun des travaux existants n'a supposé une telle distribution généralisée pour étudier les performances de bout-en-bout de ce système. La majorité des tentatives de cette ligne de recherche ont examiné Gamma-Gamma pour le lien FSO et les distributions Nakagami-m ou Rayleigh pour le lien RF.

- En supposant un scénario pratique de communication sans fil, où l'interférence est présumée chez l'utilisateur RF et le canal RF est gêné non seulement par des variations à petite échelle, c'est-à-dire par un évanouissement, mais aussi par

des variations à grande échelle, c'est-à-dire , L'ombrage, nous avons élaboré une formulation mathématique complète et unifiée de la probabilité de coupure, taux moyen d'erreur binaire et capacité ergodique pour les systèmes mixtes FSO/RF avec interférence opérant sous les distributions Málaga-$\mathcal{M}$ et generalized-K en assumant les techniques de détection hétérodyne et IM/DD et en supposant des schémas de relais à gain fixe et variable, tous en termes de FHF à deux variables.

- Motivé par les promesses des systèmes MIMO dans les réseaux de communication sans fil RF traditionnels, nous soulignons l'utilité de la diversité spatiale résultant des configurations MIMO pour réduire la dégradation de performance du au turbulence et améliorer la fiabilité du lien FSO. Tout d'abord, nous avons fourni des résultats intéressants de la capacité ergodique et le taux moyen d'erreu binaire dans le réseau multi-ouverture/multi-utilisateur. Conduite par les résultats obtenus, nous analysons la performance du système dont le nombre des ouvertures et des utilisateurs est à grand échelle.

References

[1] S. Chia, M. Gasparroni, and P. Brick, "The next challenge for cellular networks: Backhaul," *IEEE Microwave Magazine*, vol. 10, no. 5, 2009.

[2] R. Ford, C. Kim, and S. Rangan, "Opportunistic third-party backhaul for cellular wireless networks," in *Signals, Systems and Computers, 2013 Asilomar Conference on*. IEEE, 2013, pp. 1594–1600.

[3] W. Rabinovich, C. Moore, H. Burris, J. Murphy, R. Mahon, M. Ferraro, P. Goetz, L. Thomas, C. Font, G. Gilbreath *et al.*, "Free space optical communications research at the us naval research laboratory," in *SPIE LASE*. International Society for Optics and Photonics, 2010, pp. 758 702–758 702.

[4] D. L. Begley, "Free-space laser communications: a historical perspective," in *Lasers and Electro-Optics Society, 2002. LEOS 2002. The 15th Annual Meeting of the IEEE*, vol. 2. IEEE, 2002, pp. 391–392.

[5] D. Killinger, "Free space optics for laser communication through the air," *Optics and Photonics News*, vol. 13, no. 10, pp. 36–42, 2002.

[6] V. W. Chan, "Free-space optical communications," *Journal of Lightwave Technology*, vol. 24, no. 12, pp. 4750–4762, 2006.

[7] E. Leitgeb, M. Awan, P. Brandl, T. Plank, C. Capsoni, R. Nebuloni, T. Javornik, G. Kandus, S. S. Muhammad, F. Ghassemlooy *et al.*, "Current optical technologies for wireless access," in *10th International Conference on Telecommunications, ConTEL*. IEEE, 2009, pp. 7–17.

[8] A. K. Majumdar and J. C. Ricklin, *Free-space laser communications: principles and advances*. Springer Science & Business Media, 2010, vol. 2.

[9] H. Willebrand and B. S. Ghuman, *Free space optics: enabling optical connectivity in today's networks*. SAMS publishing, 2002.

[10] M. A. Khalighi and M. Uysal, "Survey on free space optical communication: A communication theory perspective," *IEEE Communications Surveys & Tutorials*, vol. 16, no. 4, pp. 2231–2258, 2014.

[11] D.-Y. Song, Y.-S. Hurh, J.-W. Cho, J.-H. Lim, D.-W. Lee, J.-S. Lee, and Y. Chung, "4 × 10 Gb/s terrestrial optical free space transmission over 1.2 km using an edfa preamplifier with 100 GHz channel spacing," *Optics express*, vol. 7, no. 8, pp. 280–284, 2000.

[12] L. C. Andrews, R. L. Phillips, C. Y. Hopen, and M. Al-Habash, "Theory of optical scintillation," *JOSA A*, vol. 16, no. 6, pp. 1417–1429, 1999.

[13] V. Tatarskii and V. Zavorotnyi, "Wave propagation in random media with fluctuating turbulent parameters," *JOSA A*, vol. 2, no. 12, pp. 2069–2076, 1985.

[14] X. Zhu and J. M. Kahn, "Free-space optical communication through atmospheric turbulence channels," *IEEE Transactions on communications*, vol. 50, no. 8, pp. 1293–1300, 2002.

[15] M. Al-Habash, L. C. Andrews, and R. L. Phillips, "Mathematical model for the irradiance probability density function of a laser beam propagating through turbulent media," *Optical Engineering*, vol. 40, no. 8, pp. 1554–1562, 2001.

[16] F. Yang, J. Cheng, and T. A. Tsiftsis, "Free-space optical communication with nonzero boresight pointing errors," *IEEE Transactions on Communications*, vol. 62, no. 2, pp. 713–725, 2014.

[17] N. D. Chatzidiamantis, H. G. Sandalidis, G. K. Karagiannidis, S. A. Kotsopoulos, and M. Matthaiou, "New results on turbulence modeling for free-space optical systems," in *IEEE 17th International Conference on Telecommunications (ICT)*. IEEE, 2010, pp. 487–492.

[18] A. Jurado-Navas, J. M. Garrido-Balsells, J. F. Paris, and A. Puerta-Notario, "A unifying statistical model for atmospheric optical scintillation," *Numerical Simulations of Physical and Engineering Processes*, 2011.

[19] J. M. Garrido-Balsells, A. Jurado-Navas, J. F. Paris, M. Castillo-Vazquez, and A. Puerta-Notario, "Novel formulation of the m model through the Generalized-K distribution for atmospheric optical channels," *Optics express*, vol. 23, no. 5, pp. 6345–6358, 2015.

[20] E. Lee, J. Park, D. Han, and G. Yoon, "Performance analysis of the asymmetric dual-hop relay transmission with mixed rf/fso links," *IEEE Photonics Technology Letters*, vol. 23, no. 21, pp. 1642–1644, 2011.

[21] I. S. Ansari, F. Yilmaz, and M.-S. Alouini, "Impact of pointing errors on the performance of mixed rf/fso dual-hop transmission systems," *IEEE Wireless Communications Letters*, vol. 2, no. 3, pp. 351–354, 2013.

[22] H. Samimi and M. Uysal, "End-to-end performance of mixed rf/fso transmission systems," *Journal of Optical Communications and Networking*, vol. 5, no. 11, pp. 1139–1144, 2013.

[23] J. Zhang, L. Dai, Y. Zhang, and Z. Wang, "Unified performance analysis of mixed radio frequency/free-space optical dual-hop transmission systems," *Journal of Lightwave Technology*, vol. 33, no. 11, pp. 2286–2293, 2015.

[24] E. Zedini, I. S. Ansari, and M.-S. Alouini, "Performance analysis of mixed Nakagami-m and gamma–gamma dual-hop fso transmission systems," *IEEE Photonics Journal*, vol. 7, no. 1, pp. 1–20, 2015.

[25] E. Zedini, H. Soury, and M.-S. Alouini, "On the performance analysis of dual-hop mixed FSO/RF systems," *IEEE Transactions on Wireless Communications*, vol. 15, no. 5, pp. 3679–3689, 2016.

[26] S. Arnon, J. Barry, G. Karagiannidis, R. Schober, and M. Uysal, *Advanced optical wireless communication systems*. Cambridge university press, 2012.

[27] I. S. Ansari, F. Yilmaz, and M.-S. Alouini, "Performance analysis of free-space optical links over málaga-$\mathcal{M}$ turbulence channels with pointing errors," *IEEE Transactions on Wireless Communications*, vol. 15, no. 1, pp. 91–102, 2016.

[28] J. F. Paris, "Statistical characterization of κ-μ shadowed fading," *IEEE Transactions on Vehicular Technology*, vol. 63, no. 2, pp. 518–526, 2014.

[29] S. L. Cotton, "Human body shadowing in cellular device-to-device communications: Channel modeling using the shadowed κ-μ fading model," *IEEE Journal on Selected areas in Communications*, vol. 33, no. 1, pp. 111–119, 2015.

[30] I. Gradshteyn and I. Ryzhik, "Table of integrals, series, and products," 1994.

[31] I. Trigui, S. Affes, and A. Stéphenne, "Capacity scaling laws in interference-limited multiple-antenna AF relay networks with user scheduling," *IEEE Transactions on Communications*, vol. 64, no. 8, pp. 3284–3295, 2016.

[32] P. Mittal and K. Gupta, "An integral involving generalized function of two variables," in *Proceedings of the Indian Academy of Sciences-Section A*, vol. 75, no. 3. Springer, 1972, pp. 117–123.

[33] H. Lei, I. S. Ansari, G. Pan, B. Alomair, and M.-S. Alouini, "Secrecy capacity analysis over α-μ fading channels," *IEEE Communications Letters*, 2017.

[34] A. M. Mathai, R. K. Saxena, and H. J. Haubold, *The H-function: theory and applications*. Springer Science & Business Media, 2009.

[35] F. J. Lopez-Martinez, J. F. Paris, and J. M. Romero-Jerez, "The κ-μ shadowed fading model with integer fading parameters," *IEEE Transactions on Vehicular Technology*, vol. PP, no. 99, pp. 1–1, 2017.

[36] A. A. Kilbas, *H-transforms: Theory and Applications*. CRC Press, 2004.

[37] I. S. Ansari, F. Yilmaz, and M.-S. Alouini, "Impact of pointing errors on the performance of mixed RF/FSO dual-hop transmission systems," *IEEE Wireless Communications Letters*, vol. 2, no. 3, pp. 351–354, 2013.

[38] L. Yang, M. O. Hasna, and X. Gao, "Performance of mixed RF/FSO with variable gain over generalized atmospheric turbulence channels," *IEEE Journal on Selected Areas in Communications*, vol. 33, no. 9, pp. 1913–1924, 2015.

[39] I. Trigui, A. Laourine, S. Affes, and A. Stéphenne, "Performance analysis of mobile radio systems over composite fading/shadowing channels with co-located interference," *IEEE Transactions on Wireless Communications*, vol. 8, no. 7, pp. 3448–3453, 2009.

[40] N. I. Miridakis, "On the ergodic capacity of underlay cognitive dual-hop af relayed systems under non-identical Generalized-K fading channels," *IEEE Communications Letters*, vol. 19, no. 11, pp. 1965–1968, 2015.

[41] A. H. A. El-Malek, A. M. Salhab, S. A. Zummo, and M. S. Alouini, "Effect of RF interference on the security-reliability tradeoff analysis of multiuser mixed rf/fso relay networks with power allocation," *Journal of Lightwave Technology*, vol. 35, no. 9, pp. 1490–1505, May 2017.

[42] I. Trigui, S. Affes, and A. Stephenne, "On the performance of dual-hop fixed gain relaying systems over composite multipath/shadowing channels," in *Vehicular Technology Conference Fall (VTC 2010-Fall), 2010 IEEE 72nd.* IEEE, 2010, pp. 1–5.

[43] E. Zedini, H. Soury, and M. S. Alouini, "Dual-hop FSO transmission systems over Gamma-Gamma turbulence with pointing errors," *IEEE Transactions on Wireless Communications*, vol. 16, no. 2, pp. 784–796, Feb 2017.

[44] S. Enayati and H. Saeedi, "Deployment of hybrid FSO/RF links in backhaul of relay-based rural area cellular networks: Advantages and performance analysis," *IEEE Communications Letters*, vol. 20, no. 9, pp. 1824–1827, 2016.

[45] R. Verma, "On some integrals involving Meijer's G-fucntion of two variables," in *Proc. Nat. Inst. Sci. India*, vol. 39, no. 5/6, 1966, pp. 509–515.

[46] M. Shah, "On generalizations of some results and their applications," *Collectanea Mathematica*, vol. 24, no. 3, pp. 249–266, 1973.

[47] H. David and H. Nagaraja, "Order statistics, john wiley & sons," *Inc., New York*, 2003.